Uniwersytet Jagielloński
Collegium Medicum
Wydział Lekarski

Krzysztof A. Tomaszewski

Wapnienie płytki granicznej, okluzja naczyń odżywczych oraz rola białek odpowiedzialnych za przetwarzanie nieorganicznego pirofosforanu w chorobie degeneracyjnej szyjnych dysków międzykręgowych

Praca doktorska

Promotor:
prof. dr hab. med. Jerzy A. Walocha

Pracę wykonano w Katedrze Anatomii
Uniwersytetu Jagiellońskiego Collegium Medicum
Kierownik jednostki: prof. dr hab. med. Jerzy A. Walocha

oraz

Katedrze Patomorfologii
Uniwersytetu Jagiellońskiego Collegium Medicum
Kierownik jednostki: prof. dr hab. med. Dariusz Adamek

Kraków, 2014

Panu Profesorowi Jerzemu Walosze – za ciągłe wsparcie we wszystkich moich działaniach oraz całą okazaną życzliwość

Rodzicom i najbliższym – za wszystko, ale przede wszystkim za to, że zawsze mogę na nich liczyć

Mojej Iwonie – za to, że zawsze przy mnie jest i nieustannie okazuje mi anielską cierpliwość

Dziękuję!

Spis treści

1. Nota informacyjna

Niniejsza rozprawa doktorska pt. „Wapnienie płytki granicznej, okluzja naczyń odżywczych oraz rola białek odpowiedzialnych za przetwarzanie nieorganicznego pirofosforanu w chorobie degeneracyjnej szyjnych dysków międzykręgowych", oparta jest o monotematyczny cykl artykułów (3 artykuły oryginalne i 1 artykuł poglądowy) opublikowanych lub przyjętych do druku w międzynarodowych czasopismach naukowych indeksowanych w bazie PubMed oraz znajdujących się na liście Journal Citation Reports (Thomson Reuters).

Łączna wartość „Impact Factor" dla cyklu wymienionych prac (według Thomson Reuters Journal Citation Reports 2013) wynosi 2,712 oraz 60 punktów Ministerstwa Nauki i Szkolnictwa Wyższego (według „listy A").

Część wyników z niniejszej pracy doktorskiej została zaprezentowana, w postaci doniesień zjazdowych, na:

1. 15th EFORT Congress (London, 4-6.06.2014) - Krzysztof A. Tomaszewski, Jerzy A. Walocha: „Pathogenesis of cervical disc degenerative disease - the role of ankyrin, ectoenzyme PC-1, osteopontin, vertebral endplate calcification and microvessel occlusion".
2. XL Zjeździe Naukowym Polskiego Towarzystwa Ortopedycznego i Traumatologicznego (Wrocław, 17-21.09.2014) - Krzysztof A. Tomaszewski, Ewa Mizia, Jan Paradowski, Waldemar Wrażeń, Bartosz Stasiak, Edward B. Golec, Jerzy A. Walocha: „Płytka graniczna – wapnienie czy kostnienie? Rola ankiryny, osteoprotegeryny i osteokalcyny w patogenezie choroby degeneracyjnej szyjnych dysków międzykręgowych".

Praca zaprezentowana na 15th EFORT Congress w Londynie została wyróżniona Best „Basic Science" Poster Session Award. Była to jedyna wyróżniona praca na ponad 50 zaprezentowanych w tej sesji.

W cykl artykułów, o które oparta jest rozprawa doktorska, wchodzą:

1. Tomaszewski KA, Saganiak K, Gładysz T, Walocha JA. The biology behind the human intervertebral disc and its endplates. Folia Morphologica 2014 (*IF 0,524; MNiSW 15 punktów*)
2. Tomaszewski KA, Walocha JA, Mizia E, Gładysz T, Głowacki R, Tomaszewska R. Age- and degeneration-related variations in cell density and glycosaminoglycan content in the human cervical intervertebral disc and its endplates. Polish Journal of Pathology 2014 (*IF 0,832; MNiSW 15 punktów*)
3. Tomaszewski KA, Adamek D, Pasternak A, Głowacki R, Tomaszewska R, Walocha JA. Degeneration and calcification of the cervical endplate is connected with a decreased expression of ANK, ENPP-1, OPN and TGF-β1 in the intervertebral disc. Polish Journal of Pathology 2014;65(3):204-211 (*IF 0,832; MNiSW 15 punktów*)
4. Tomaszewski KA, Adamek D, Konopka T, Tomaszewska R, Walocha JA. Endplate calcification and cervical intervertebral disc degeneration – the role of endplate marrow contact channel occlusion. Folia Morphologica 2014 (*IF 0,524; MNiSW 15 punktów*)

Listy od redakcji potwierdzające przyjęcie do publikacji prac niewydanych jeszcze drukiem znajdują się na końcu pracy doktorskiej.

Prace opublikowane, są zamieszczone w rozprawie w wersji autorskiej (format Word), będącej w pełni zgodną z wersją ostateczną, która ukazała się drukiem w danym czasopiśmie.

Źródła finansowania

Autor uzyskał środki finansowe na przygotowanie rozprawy doktorskiej z Narodowego Centrum Nauki w ramach finansowania stypendium doktorskiego Etiuda na podstawie decyzji numer DEC-2013/08/T/NZ5/00020. Opisywany projekt badawczy został sfinansowany ze środków Narodowego Centrum Nauki (Preludium) przyznanych na podstawie decyzji numer DEC-2012/07/N/NZ5/00078 oraz ze środków pochodzących z dotacji celowej dla młodych naukowców (nr K/DSC/002093; Uniwersytet Jagielloński Collegium Medicum).

2. Podsumowanie pracy doktorskiej w języku polskim

Wstęp

W badaniu Global Burden of Disease z 2010 roku ból szyi znalazł się na 4-tym miejscu pod względem lat przeżytych w niepełnosprawności (spośród 291 ocenionych problemów zdrowotnych) oraz na 21-szym miejscu pod względem całościowego obciążenia osoby chorej. Całkowita częstość występowania bólu szyi w populacji światowej waha się od 0,4% do 86,8%, przy średniej wartości 23,1%.

Ból szyi jest silnie związany z chorobą degeneracyjną dysków międzykręgowych (intervertebral disc – IVD). Dyski międzykręgowe ulegają degeneracji znacznie wcześniej niż inne tkanki mięśniowo-szkieletowe. Pierwsze oznaki zwyrodnienia w lędźwiowych IVD są widoczne już między 11, a 16 rokiem życia. Krzywa postępowania degeneracji, szczególnie u mężczyzn, silnie zwiększa nachylenie z wiekiem – około 10% 50-latków i 60% 70-latków ma IVD ze znacznego stopnia zmianami zwyrodnieniowymi.

Dyski międzykręgowe są strukturami o cylindrycznym kształcie, składającymi się głównie z chrząstki włóknistej i stanowiącymi centralny element stawów międzykręgowych, które umożliwiają wykonywanie ruchów w sztywnej, przedniej kolumnie kręgosłupa. Dyski międzykręgowe mają około 7 do 10 mm grubości i 2,5 cm średnicy w szyjnej części kręgosłupa i stanowią około 1/3 wysokości kolumny kręgosłupa. Umożliwiają one równe rozkładanie się obciążeń na trzonach kręgów niezależnie od pozycji w jakiej znajduje się kręgosłup. Makroskopowo IVD można podzielić na znajdujący się na zewnątrz pierścień włóknisty (annulus fibrosus – AF), który otacza leżące w środku jądro miażdżyste (nucleus pulposus – NP). Płytki graniczne mają mniej niż 1 mm grubości, składają się zarówno z chrząstki szklistej jak i komponenty kostnej oraz otaczają IVD zarówno od strony głowowej jak i ogonowej, oddzielając je w ten sposób od trzonów kręgów i zapobiegając by bogato

uwodnione NP nie przebiło się do trzonu sąsiadującego kręgu. Płytki graniczne pochłaniają również znacznego stopnia ciśnienie hydrostatyczne, które generowane jest w wyniku przenoszonych prze kolumnę kręgosłupa obciążeń.

Płytki graniczne, w trakcie rozwoju rosnącego kręgosłupa, przenikane są przez sieć mikroskopijnych naczyń krwionośnych, których zadaniem jest zapewnić dowóz substancji odżywczych do IVD. Zanikają one w okresie gdy proces kostnienia w organizmie dobiega końca. Od tego momentu kostną część płytki granicznej przenikają już tylko szpikowe otwory odżywcze (marrow contac channels – MCC), przez które przechodzą naczynia kapilarne transportujące substancje odżywcze do IVD. Naczynia te łączą przestrzenie międzybeleczkowe z chrzęstną częścią płytki granicznej, ale nie wnikają w nią. Poza rzadkim unaczynieniem w zewnętrznych warstwach AF, dojrzałe IVD prawie w całości otrzymują niezbędne substancje odżywcze i pozbywają się produktów przemiany materii na zasadzie dyfuzji poprzez płytkę graniczną. Uprzednie badania wykazały, że to centralna część płytki granicznej odpowiada za dyfuzję większości substancji odżywczych.

Pomimo że złożone i dynamiczne zależności pomiędzy degeneracją IVD i kostnieniem/wapnieniem płytki granicznej są dobrze poznane, to jednak jesteśmy dalecy od ich pełnego zrozumienia. Do powstania i rozwoju choroby degeneracyjnej IVD może prowadzić szereg czynników takich jak starzenie się organizmu, zmiany biochemiczne (utrata zawartości proteoglikanów i włókien kolagenowych, zwiększona aktywność enzymatyczna metaloproteinaz macierzowych), genetyczne, przeciążenia mechaniczne i urazy, jak również upośledzenie dowozu substancji odżywczych.

Jak napisano powyżej, jednym z głównych powodów prowadzących do rozwinięcia się choroby degeneracyjnej IVD może być zaburzenie w transporcie substancji odżywczych do komórek IVD. *In vitro* aktywność komórek IVD jest bardzo wrażliwa na zmiany w pozakomórkowym stężeniu tlenu oraz na wahania pH. Komórki IVD szybko obumierają

kiedy zostaną wystawione na działanie niskiego pH lub niskiego stężenia glukozy. W konsekwencji spadek w dowozie substancji odżywczych, który prowadzi od obniżenia prężności tlenu lub wartości pH (w wyniku wzrostu stężenia mleczanów) może wpływać na zdolność komórek IVD do syntezowania i utrzymywania macierzy zewnątrzkomórkowej, co w konsekwencji może doprowadzić do degeneracji IVD. Nawet jeśli przepływ krwi nie zostanie zaburzony, to substancje odżywcze mogę nie dotrzeć do IVD w wyniku zwapnienia płytki granicznej.

Gen ANKH jest ludzkim homologiem genu odpowiedzialnego za postępującą ankylozę w naturalnie żyjących myszach. Odpowiada on za produkcję przezbłonowego białka ANK, które reguluje transport wewnątrzkomórkowy nieorganicznego pirofosforanu (PPi) z cytoplazmy do przestrzeni pozakomórkowej. W ten sposób ANK utrzymuje stężenie PPi na jednorodnym poziomie, prawdopodobnie zapobiegając nadmiernemu wapnieniu tkanek.

Transformujący czynnik wzrostu β1 (TGF-β1) odgrywa znaczącą rolę w regulacji odkładania się kryształów wapnia w chrzęstnej części płytki granicznej. Posiada on możliwość indukcji przetwarzania PPi poprzez zwiększania ekspresji genu ANKH, przez co staje się istotnym elementem w regulacji procesów wapnienia. Fosfataza alkaliczna (alkaline phosphatease – ALP) odgrywa aktywną rolę w inicjowaniu odkładania kryształów fosforanu wapnia – bardzo istotnego elementu w procesie wapnienia. Fosfataza alkaliczna hydrolizuje organiczne fosforany i PPi, prowadząc do powstania jonów monofosforanowych (Pi), które w obecności jonów wapnia tworzą kryształy hydroksyapatytu. Jednakże proces ten jest dużo bardziej skomplikowany niż jesteśmy w stanie obecnie stwierdzić. Wiemy, że zaburzenia w ekspresji ANKH (wspólnie z ektoenzymem PC-1 – ENPP1) powodują istotne spadki w poziomach PPi i osteopontyny (OPN).

Cytując badania odnośnie choroby degeneracyjnej IVD można być więcej niż pewnym, że dotyczą one eksperymentów przeprowadzonych na ludzkich lędźwiowych IVD lub

zwierzęcych IVD. Ilość informacji dostępnych na temat degeneracji szyjnych IVD jest bardzo ograniczona lub praktycznie nie istnieje w przypadku procesów zwyrodnieniowych przebiegających w płytce granicznej szyjnych IVD.

Zakres artykułów wchodzących w skład rozprawy doktorskiej

W skład niniejszej pracy doktorskiej wchodzą cztery artykuły opublikowane w uznanych, międzynarodowych czasopismach naukowych z dziedziny anatomii i patologii.

Artykuł numer 1 opublikowany w *Folia Morphologica* jest opisowym przeglądem piśmiennictwa i podsumowuje oraz uaktualnia obecny stan wiedzy na temat embriologii, struktury i biomechaniki IVD oraz płytek granicznych. Aby zaprezentować całość przedstawionej wiedzy w bardziej kliniczny świetle, artykuł opisuje wpływ starzenia się i degeneracji na wymienione wyżej właściwości IVD i płytek granicznych. Artykuł ten ma za zadanie wprowadzić Czytelnika w problematykę niniejszej rozprawy doktorskiej.

Artykuł numer 2 opublikowany w *Polish Journal of Pathology* skupia się na kwantyfikacji gęstości komórkowej i zawartości glikozaminoglikanów w całej objętości szyjnego IVD i jego płytek granicznych. Wyniki tejże analizy zostały następnie odniesione do wieku, jak również do histologicznego stopnia zwyrodnienia tkanki IVD i płytki granicznej.

Artykuł numer 3 opublikowany w *Polish Journal of Pathology* bada i wyjaśnia zależności występujące między ekspresją białek odpowiedzialnych za przetwarzanie i transport nieorganicznego pirofosforanu w szyjnych IVD, a wapnieniem i degeneracją szyjnych płytek granicznych.

Artykuł numer 4 opublikowany w *Folia Morphologica* opisuje i bada problematykę degeneracji szyjnych IVD oraz wapnienie szyjnych płytek granicznych w aspekcie drożności szpikowych otworów odżywczych.

Cele

Niniejsza praca miała na celu:

1. Podsumowanie i uaktualnienie obecnego stanu wiedzy na temat embriologii, struktury i biomechaniki IVD i płytek granicznych.
2. Przedstawienie wpływu starzenia się i degeneracji na powyższe właściwości (*cel 1*) zarówno IVD jak i płytek granicznych.
3. Kwantyfikację gęstości komórkowej w szyjnych IVD i płytkach granicznych o różnym wieku i stopniu zaawansowania zmian zwyrodnieniowych, tak aby możliwym stało się przygotowanie trójwymiarowych map gęstości komórkowej, które mogłyby stanowić podstawę teoretyczną do przyszłego stosowania komórek macierzystych w leczeniu choroby zwyrodnieniowej szyjnych dysków międzykręgowych.
4. Analizę zawartości glikozaminoglikanów w szyjnych IVD i płytkach granicznych, tak aby dostarczyć danych niezbędnych komputerowego modelowania zachowania tkanki ludzkich IVD.
5. Wyjaśnienie zależności występujących pomiędzy ekspresją białek odpowiedzialnych za przetwarzanie nieorganicznego pirofosforanu w IVD, a wapnieniem i degeneracją szyjnych płytek granicznych.
6. Ustalenie podstawowych zależności pomiędzy degeneracją szyjnych IVD, wapnieniem płytki granicznej oraz drożnością szpikowych otworów odżywczych.

Materiały i metody

Pobieranie materiału do badań

Do badania pobrano 60 szyjnych IVD ze zwłok ludzkich (Katedra Medycyny Sądowej Uniwersytetu Jagiellońskiego Collegium Medicum). Materiał wypreparowano używając dostępu przedniego, a samo pobranie wykonano nie później niż 24 godziny od zgonu.

Materiał wycięto w jednym bloku składającym się z trzonów kręgów, IVD, płytek granicznych i naczyń zaopatrujących te struktury. Po wypreparowaniu materiał zawinięto w nasączoną solą fizjologiczną gazę, zapakowano próżniowo w celu zapobiegnięcia odwodnieniu tkanki i przechowywano w temperaturze 4° Celsjusza przez okres transportu oraz do czasu dalszych badań. Materiał preparowano od poziomu dolnej połowy kręgu C4 do górnej połowy kręgu C6.

Kryterium włączenia do badania była możliwość wypreparowania wskazanego powyżej odcinka przedniej kolumny kręgosłupa wraz z przednim i tylnym więzadłem podłużnym oraz naczyniami krwionośnymi zaopatrującymi kręgi.

Kryteria wyłączenia z badania uwzględniały (1) przebyty uraz szyjnego odcinka kręgosłupa, który uniemożliwiałby wykonanie zaplanowanych czynności preparacyjnych; (2) przebyte zabiegi operacyjne w zakresie szyjnego odcinka kręgosłupa; (3) przebyta chemioterapia w okresie ostatnich 12 miesięcy; (4) przebyta radioterapia w zakresie kręgosłupa; (5) całkowity paraliż o okresie trwania dłuższym niż 6 miesięcy; (6) zesztywniające zapalenie stawów kręgosłupa.

Przetwarzanie materiału do badań

Rycina zamieszczona na kolejnej stronie w sposób schematyczny przedstawia jak przetwarzany był materiał do badań. W celu zapoznania się ze szczegółową metodyką poszczególnych badań autor odsyła Czytelnika do poszczególnych artykułów.

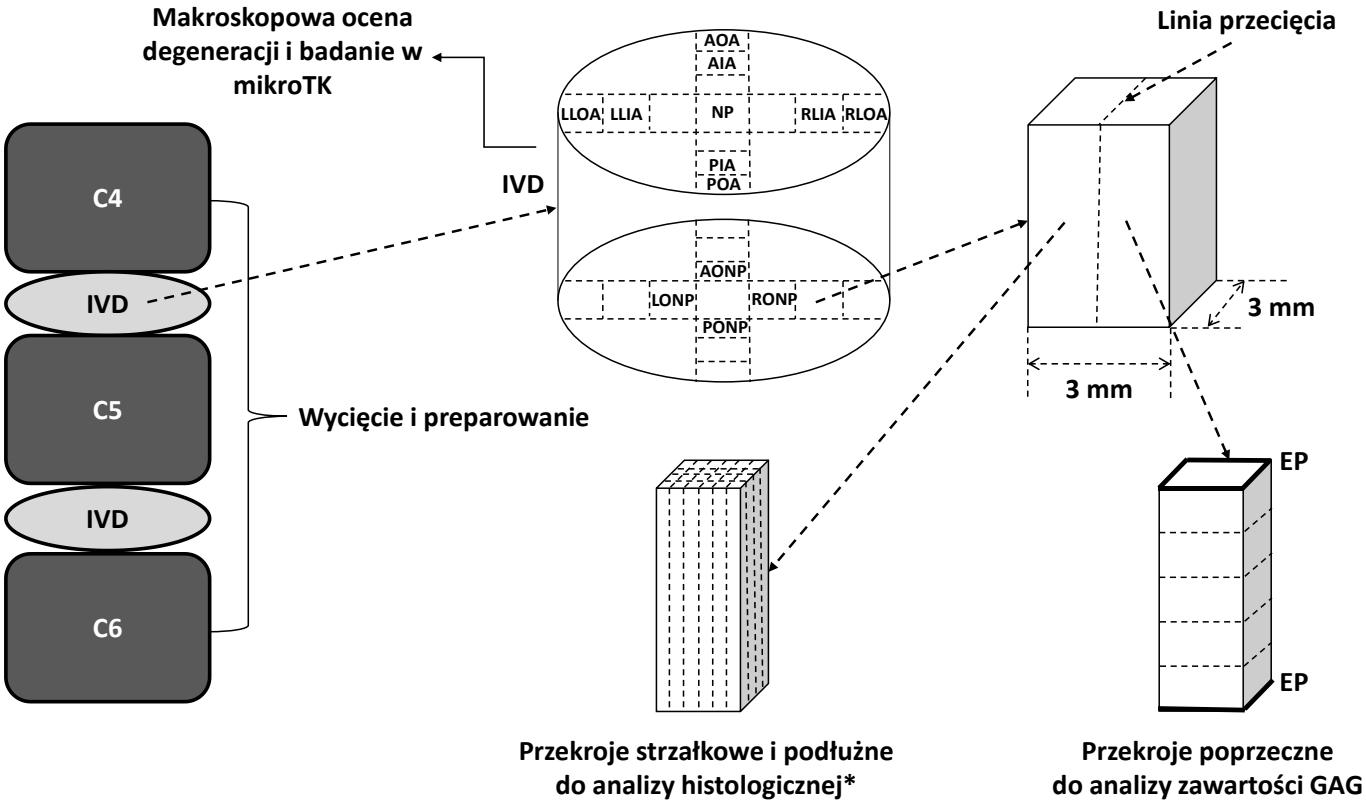

Zarówno IVD jak i płytki graniczne przeszły pełną analizę histologiczną. Uwzględniała ona barwienie preparatów hematoksyliną i eozyną oraz trichromem Masona, histologiczną ocenę stopnia zaawansowania zamian zwyrodnieniowych, ocenę stopnia zwapnienia płytki granicznej, kwantyfikację gęstości komórkowej w IVD i w płytce granicznej oraz immunohistochemię (w kierunku ANK, OPN, ALP, ENPP1 i TGF- β1).

Etyka

Badanie uzyskało pozytywną opinię Komisji Bioetycznej UJ CM (numer KBET/319/B/2012) i zostało przeprowadzone zgodnie z wytycznymi Deklaracji Helsińskiej (1964) i jej późniejszymi poprawkami. Pobrania materiału dokonano w taki sposób by nie zdestabilizować kolumny kręgosłupa zwłok.

Główne wyniki, wnioski i implikacje praktyczne badania

Artykuł numer 1 opublikowany w Folia Morphologica

Opisywana praca poglądowa podsumowuje i uaktualnia obecny stan wiedzy na temat embriologii, struktury i biomechaniki IVD i płytek granicznych. Aby zaprezentować przedstawione dane w bardziej klinicznym kontekście, artykuł opisuje wpływ starzenia się i degeneracji na wymienione wyżej właściwości IVD i płytek granicznych.

Dysk międzykręgowy razem z płytkami granicznymi jest z pozoru strukturą prostą, która przy bliższej analizie okazuje w pełni swój poziom skomplikowania, uświadamiając badaczowi, że do tej pory nie poznaliśmy jej w pełni. Dyski międzykręgowe powstają z mezodermalnej notochordy i otrzymują substancje odżywcze w wyniku dyfuzji zachodzącej poprzez płytki graniczne. W warunkach fizjologicznych IVD unerwione są wyłącznie w zakresie zewnętrznego AF poprzez czuciowe i sympatyczne włókna nerwowe okołonaczyniowe. Są to gałęzie od nerwu zatokowo-kręgowego, brzusznych gałęzi nerwów rdzeniowych oraz od gałęzi łączących szarych. Wraz z wiekiem i degeneracją w IVD zachodzą znaczące zmiany. Te powstałe na tle zwyrodnieniowym możemy podzieli na dwa typy tj. „zależne od płytki granicznej" w skład których wchodzą defekty samej płytki granicznej i zapadanie się do wewnątrz AF oraz „zależne od pierścienia włóknistego" w skład których wchodzi powstawanie promienistych pęknięć IVD lub powstawanie przepuklin IVD.

Artykuł numer 2 opublikowany w Polish Journal of Pathology

Badanie to miało na celu kwantyfikację gęstości komórkowej w szyjnych IVD oraz płytkach granicznych o zróżnicowanym wieku i stopniu zaawansowania zmian zwyrodnieniowych. Autor badania chciał aby możliwym stało się stworzenie trójwymiarowych map gęstości komórkowej, które mogłyby stanowić podstawę teoretyczną do przyszłego stosowania komórek macierzystych w leczeniu choroby zwyrodnieniowej szyjnych dysków

międzykręgowych. Aby przystąpić do stosowania takiego leczenia niezbędna jest znajomość podstawowej liczby komórek znajdujących się w IVD.

Jako że komórki IVD są bezpośrednio odpowiedzialne za produkcję proteoglikanów, drugim celem opisywanego badania była analiza zawartości glikozaminoglikanów (GAG) w szyjnych IVD i płytkach granicznych. Ta część badania miała dostarczyć danych na temat zmian w zawartości GAG w IVD i płytkach granicznych w warunkach fizjologicznych i patologicznych. Dane w ten sposób uzyskane miałyby posłużyć do komputerowego modelowania zachowania tkanki ludzkiego IVD w różnych warunkach.

Po przeprowadzeniu dokładnej analizy histologicznej i biochemicznej autorowi badania udało się stworzyć trójwymiarowe mapy gęstości komórkowej oraz zawartości GAG w całej objętości szyjnego IVD oraz jego płytek granicznych. Analizując cały IVD gęstość komórkowa była najwyższa w rejonie NP (4218±417 komórek/mm^3) i stopniowo obniżała się w kierunku do przodu i na zewnątrz (przednia część AF: 3283±438 komórek/mm^3), a wzrastała w kierunku do tyłu i na zewnątrz (tylna część AF: 4464±551 komórek/mm3). Wraz ze wzrostem stopnia degeneracji IVD gęstość komórkowa zmniejszała się. Co ciekawe podobny efekt nie występował wraz ze starzeniem się – w różnych grupach wiekowych próbek gęstość komórkowa pozostawała na zbliżonym poziomie. Gęstość komórkowa i zawartość GAG była bardzo zbliżona w głowowych i ogonowych płytkach granicznych. Płytka graniczna wykazywała podobną gęstość komórkową w całej swojej objętości, w niektórych przypadkach „uzupełniając" rejony IVD o niskiej gęstości komórkowej, „własnymi" rejonami o wysokiej gęstości komórkowej. Jednak w przeciwieństwie do IVD, w przypadku płytek granicznych wiek istotnie negatywnie korelował z ich gęstością komórkową. Fakt ten może wynikać z samego wapnienia płytki granicznej (które wyraźnie postępowało z wiekiem) i prostego obumierania komórek lub może sugerować, że komórki

IVD są bardziej odporne ze względu na „trudniejsze” warunku w jakich przyszło im funkcjonować.

Analizując zawartość GAG, zarówno w IVD jak i płytkach granicznych, widocznym staje się, że wartości gęstości komórkowej blisko korelują z zawartością GAG. Interesujący jest fakt, że zmienność zawartości GAG w strzałkowych i czołowych przekrojach była znacząco wyższa niż w badaniach dotychczas opublikowanych. Tak było jednak tylko w przypadku IVD, gdyż w przypadku płytki granicznej zawartość GAG była homogenna w całej jej objętość – niezależnie od wieku preparatu lub stopnia degeneracji IVD/płytki granicznej. Zmienności w osiowej zawartości GAG w IVD były niewielkie i podobne do tych znalezionych w lędźwiowych IVD.

Podsumowując, wyniki badania pozwoliły na przygotowanie serii trójwymiarowych map gęstości komórkowej i zawartości GAG w szyjnych IVD i ich płytkach granicznych. Jednym z najważniejszych elementów przygotowujących do przeprowadzenia poprawnej technicznie i skutecznej klinicznie implantacji komórek macierzystych w IVD jest znajomość liczby i rozłożenia komórek w danym rejonie IVD, niezależnie od stopnia jego zwyrodnienia. Wiedza zdobyta poprzez to badanie stworzyła teoretyczne podstawy do przygotowywania zawiesin/żelów zawierających odpowiednią biologicznie liczbę komórek macierzystych.

Dodatkowo, badanie to wykazało, że szyjne IVD i ich płytki graniczne różnią się tylko nieznacznie, pod względem gęstości komórkowej i zawartości GAG, od ich odpowiedników w lędźwiowym odcinku kręgosłupa. Co więcej, badanie to dostarczyło nowych informacji na temat rozkładu zawartości GAG we wszystkich trzech płaszczyznach IVD. Wiedza ta może okazać się przydatna w komputerowym modelowaniu zachowania ludzkiego IVD. Przedstawione dane wskazują również na występowanie związanego z wiekiem trendu, sugerującego, że spadek aktywności metabolicznej komórek IVD może być wyrażony przez zmniejszone stężenie GAG.

Artykuł numer 3 opublikowany w Polish Journal of Pathology

Według najlepszej wiedzy autora, opisywane badanie jest pierwszą próbą we współczesnej literaturze mającą na celu analizę zależności pomiędzy ekspresją ANK, ALP, ENPP-1, OPN oraz TGF-β1, a wapnieniem i degeneracją szyjnych płytek granicznych.

Badanie to wykazało, że stopień zwapnienia płytki granicznej silnie koreluje ze stopniem zaawansowania zwyrodnienia samej płytki granicznej jak i IVD (w obu przypadkach $r=0.91$; $p<0.0001$). Zarówno liczba jak i intensywność wybarwionych komórek przypadających na analizowane pole widzenia znacząco zmniejszała się w przypadku ANK, ENPP-1 oraz TGF-β1 w odniesieniu do stopnia degeneracji IVD, niezależnie od analizowanego rejonu IVD. Jedynie liczba komórek wybarwiona pod kątem ekspresji ALP wzrastała wraz z narastaniem zwyrodnienia IVD.

Najważniejszym wynikiem badania jest fakt, że po raz pierwszy udało potwierdzić się, na dużej grupie szyjnych IVD, że spadek ekspresji ANK, ENPP-1 i TGF-β1 w IVD połączony jest z nasilającą się degeneracją IVD jak i degeneracją i wapnieniem płytki granicznej. Zależność ta była najbardziej widoczna w przypadku ANK i TGF-β1, jako że obydwa białka są ze sobą ściśle połączone w procesach powodujących wapnienie. Tak jak oczekiwano, ekspresja ALP wzrastała wraz z postępującym wapnieniem płytki granicznej – widomo, że ALP jest markerem zachodzącej mineralizacji.

Badanie to potwierdziło również, że wapnienie płytki granicznej może zostać wykryte w materiale histologicznym już w trzeciej dekadzie życia.

Modulowanie ekspresji wymienionych powyżej białek, szczególnie ANK i TGF-β1, może okazać się nowym sposobem zapobiegania degeneracji i wapnienia IVD.

Artykuł numer 4 opublikowany w Folia Morphologica

Celem opisywanego badania było ustalenie podstawowych zależności pomiędzy degeneracją szyjnych IVD, wapnieniem płytki granicznej oraz drożnością szpikowych otworów odżywczych (MCC).

Badania przeprowadzone na lędźwiowych IVD sugerowały, że wapnienie płytki granicznej może zaburzać transport substancji odżywczych do IVD. Jednakże odkrycia te nie zostały nigdy bezpośrednio odniesione do degeneracji płytki granicznej, ani zbadane szerzej w kontekście IVD pochodzących z innych poziomów niż lędźwiowy.

W badaniu tym, dzięki zastosowaniu mikrotomografii komputerowej (mikroTK) stwierdzono, że liczba otworów w płytce granicznej o średnicy 300 μm koreluje negatywnie z liczbami otworów o mniejszej średnicy ($r=-0.62-(-0.82)$; $p<0.0001$). Korelacja ta była najsilniejsza w przypadku MCC o średnicy 10 – 50 μm. Podobna zależność została zaobserwowana pomiędzy liczbą MCC, a degeneracją IVD i degeneracją oraz wapnieniem płytki granicznej, gdzie liczba otworów o średnicy 300 μm korelowała pozytywnie, a liczba MCC o mniejszych rozmiarach korelowała negatywnie z nasileniem zmian degeneracyjnych oraz rozległością wapnienia.

Opierając się na uzyskanych wynikach, jak również na danych pochodzących z badań przeprowadzonych z użyciem skaningowej mikroskopii elektronowej stwierdzono, że pozytywna zależność pomiędzy otworami w płytce granicznej o średnicy 300 μm, a degeneracją IVD i płytki granicznej sugeruje, że otwory te nie mogą zostać uznane jako MCC, a wyłącznie jako pęknięcia płytki granicznej wynikające z jej degeneracji. Otwory te nie zawierają zakończeń naczyń kapilarnych i są pochodną ścieńczenia płytki granicznej i jej zmian powstających z wiekiem.

Dodatkowo stopień degeneracji IVD, oceniany za pomocą makroskopowej klasyfikacji Thompsona korelował pozytywnie ze stopniem degeneracji wyznaczonym przy użyciu histologicznej klasyfikacji Boos'a ($r=0.77$; $p<0.0001$).

Jest to pierwsze badanie, które wykorzystało mikroTK w połączeniu z analizą histologiczną w celu lokalizacji, kwantyfikacji i scharakteryzowania MCC w szyjnych płytkach granicznych. Do tej pory tylko jedno podobne badanie zostało przeprowadzone, jednak autorzy wykorzystali w nim skaningową mikroskopię elektronową i oceniali występowanie MCC w lędźwiowych płytkach granicznych. Inne badania oceniające współwystępowania zmian zwyrodnieniowych i zmian w charakterystyce MCC bazowały wyłącznie na analizie histologicznej, która umożliwia zobrazowanie wyłącznie części płytki granicznej, nie zaś jej całej struktury.

Nadal nie jest jasnym czy wapnienie płytki granicznej jest przyczyną czy efektem degeneracji zachodzącej w IVD lub płytce granicznej. Niektórzy autorzy odpowiadają w sposób wymijający, że oba procesy zachodzą równocześnie i są mocno ze sobą związane. Jednak wyniki niniejszego badania zasygnalizowały, że wapnienie płytki granicznej jest raczej przyczyną, niż efektem spadku w dowozie substancji odżywczych, jako, że rozpoczyna się w dobrze unaczynionym centrum płytki granicznej, a nie na jej brzegach gdzie liczba MCC jest znacząco niższa. Niestety autorzy muszą się wstrzymać ze stawianiem definitywnych stwierdzeń dopóki nie zostaną przeprowadzone badania wyraźnie wskazujące na istnienie ciągu przyczynowo-skutkowego.

Podsumowując, jest to pierwsze tego typu badanie, które zostało przeprowadzone na szyjnych IVD. Wykazało ono, że podobnie do lędźwiowych IVD, występuje silna negatywna korelacja pomiędzy liczbą MCC w płytce granicznej, a makroskopowo i mikroskopowo ocenianą degeneracją IVD i płytki granicznej. Stanowi to dodatkowy argument przemawiający za tym, że wapnienie płytki granicznej, przez okluzję MCC, prowadzi do spadku transportu substancji

odżywczych do IVD, co powoduje jego degenerację. Dodatkowo, wykorzystana w tym artykule metoda badania płytki granicznej (mikroTK) pozawala na wykonywanie dokładnych i powtarzalnych pomiarów liczby, wielkości i kształtu MCC płytki granicznej. Co więcej, wykazano, że makroskopowa klasyfikacja Thompsona dobrze koreluje z histologiczną klasyfikacją Boos'a w przypadku oceny degeneracji IVD i płytki granicznej. Czyni to klasyfikację Thompsona dobrym surogatem mikroskopowej degeneracji, do czasu kiedy dostępne są wyniki analizy histologicznej.

Aspekty praktyczne pracy

Obok walorów czysto naukowych, praca ta niesie ze sobą również istotne aspekty praktyczne, zarówno dla obecnej jak i przyszłej działalności naukowo-lekarskiej. Wartym wspomnienia jest również fakt, że według najlepszej wiedzy autora, jest to pierwsze tego typu badanie przeprowadzone na szyjnych IVD.

Badanie to przedstawia szereg trójwymiarowych map gęstości komórkowej i zawartości GAG w szyjnych IVD i ich płytkach granicznych. Wiedza zdobyta poprzez to badanie stworzyła teoretyczne podstawy do przygotowywania zawiesin/żelów zawierających dostosowaną biologicznie liczbę komórek macierzystych. Przedstawiony rozkład GAG w całej objętości IVD (we wszystkich trzech płaszczyznach) i płytkach granicznych może być pomocny w modelowaniu tkanki ludzkiego IVD za pomocą metody elementów skończonych.

Przedstawione wyniki sugerują, że modulowanie ekspresji wybranych białek, szczególnie ANK i TGF-β1, może okazać się nowym sposobem zapobiegania degeneracji i wapnienia IVD.

Dodatkowo, wykorzystana metoda badania płytki granicznej (mikroTK) pozwala na wykonywanie dokładnych i powtarzalnych pomiarów liczby, wielkości i kształtu MCC płytki granicznej. Co więcej, wykazano, że makroskopowa klasyfikacja Thompsona dobrze koreluje

z histologiczną klasyfikacją Boos'a w przypadku oceny degeneracji IVD i płytki granicznej. Czyni to klasyfikację Thompsona dobrym surogatem mikroskopowej degeneracji, do czasu kiedy dostępne są wyniki analizy histologicznej.

3. Podsumowanie pracy doktorskiej w języku angielskim

Introduction

In the 2010 Global Burden of Disease Study neck pain was found to be the 4th biggest contributor to Years Lived with Disability (out of 291 conditions assessed), and 21st in terms of overall burden. The overall prevalence of neck pain in the general population ranges between 0.4% and 86.8%, with a mean value of 23.1%.

Neck pain has a strong association with intervertebral disc (IVD) degeneration. Discs degenerate far earlier than other musculoskeletal tissues, and the first findings of degeneration in the lumbar discs are seen between 11-16 years of age. The process of degeneration increases steeply with age, especially in males – around 10% of 50-year-olds and 60% of 70-year-olds have severely degenerate IVDs.

The IVDs are roughly cylindrical, fibrocartilaginous, articulating structures connecting the vertebral bodies, and allowing movement in the otherwise rigid anterior portion of the vertebral column. They are approximately 7 to 10 mm thick and 2.5 cm in diameter in the cervical region of the spine, and constitute 1/3 of the vertebral column's height. The IVDs spread loading evenly on the vertebral bodies, regardless of the position of the spine. Macroscopically the IVD can be divided into an outer annulus fibrosus (AF) surrounding a centrally located nucleus pulposus (NP). The endplates (which are less than 1 mm thick and composed of both hyaline cartilage and bone) surround the IVDs from both the cranial and caudal ends, separate them from the vertebral bodies and prevent the highly hydrated NP from bulging into the adjacent vertebrae. The endplates also absorb the considerable hydrostatic pressure that results from mechanical loading of the spine.

A network of microscopic blood vessels penetrates the endplates during development of the growing spine, principally to provide nutrition for the disc, before disappearing around the

time of skeletal maturity. After this point in development the mineralized portion of the endplate is penetrated only by marrow contact channels (MCC), through which capillary buds emerge. These capillary buds connect the trabecular spaces to the cartilaginous endplate, but do not penetrate into it. Apart from a sparse vascular supply in the outer lamellae of the annulus, mature discs are almost totally dependent on diffusion of essential solutes across the endplates for nutrition and metabolic exchange. In addition, several studies have shown that it is the central portion of the endplate that is responsible for the diffusion of the majority of nutritional substances.

Although the complex and dynamic relationships between IVD degeneration and sclerosis of the vertebral endplate are well recognized, they are poorly understood. IVD degenerative disease is known to be caused by a series of factors including ageing, biochemical changes (loss of proteoglycan, collagen fibers and increased enzymatic activity), genetics, mechanical loading and injury, as well as impaired disc nutrition.

As it was stated above, one of the primary causes of disc degeneration is thought to be failure of nutrient supply to the disc cells. In vitro, the activity of disc cells is very sensitive to changes in extracellular oxygen and pH levels. Disc cells do not survive prolonged exposure to low pH or glucose concentrations. A fall in nutrient supply that leads to a lowering of oxygen tension or of pH (a result of raised lactic acid concentrations) could thus affect the ability of IVD cells to synthesize and maintain the IVD extracellular matrix and could ultimately lead to IVD degeneration. Even if the blood supply remains undisturbed, nutrients may not reach the disc cells if the cartilaginous endplate calcifies.

The ANKH gene is the human homologue of the gene responsible for progressive ankylosis in a naturally occurring mutant mouse. It produces a multiple-pass transmembrane protein (ANK) which regulates intracellular inorganic pyrophosphate (PPi) transportation from the

cytoplasm to the extracellular space, thereby maintaining the PPi steady-state concentration, and thus possibly preventing increased calcification of the tissue.

Transforming growth factor β1 (TGF-β1) plays a significant role in regulating calcium crystal deposition in endplate cartilage, and is able to induce PPi elaboration via TGF-β1-induced ANKH gene expression, thus being an important factor in the regulation of the calcification process. Calcification involves the deposition of calcium phosphates, with alkaline phosphatase (ALP) playing an active role in initiating this process. It hydrolyzes organic phosphates and PPi, yielding monophosphate ions (Pi), which, in the presence of calcium ions, form hydroxyapatite crystals. This process is however far more complicated with ANKH (conjointly with ectoenzyme PC-1 – ENPP1) deficiencies causing a possible decrease in PPi and osteopontin (OPN) levels.

When one cites research regarding IVD degeneration it is more than sure to be based on lumbar IVD material, most often of animal origin. The amount of information available regarding cervical IVD degeneration is very limited, and almost non-existent when it comes to degenerative processes occurring in cervical endplates.

Scope of the manuscripts constituting the PhD thesis

This PhD thesis consists of 4 manuscripts published in renowned international journals.

Manuscript number 1 published in *Folia Morphologica* is a narrative review which summarizes and updates the current state of knowledge on the embryology, structure, and biomechanics of the IVD and its endplates. To further translate this into a more clinical context this review demonstrates the impact of ageing and degeneration on the above properties of both the IVD and its endplates. It is meant to introduce the Reader to the subjects with which this thesis deals further on.

Manuscript number 2 published in the *Polish Journal of Pathology* focuses on quantifying cell density and glycosaminoglycan content throughout different regions of cervical IVDs and their endplates. These results are later related to age as well as IVD and endplate histological degeneration.

Manuscript number 3 published in the *Polish Journal of Pathology* explores and clarifies the relationships between the expression of inorganic pyrophosphate elaborating proteins in cervical IVDs, and cervical vertebral endplate calcification and degeneration.

Manuscript number 4 published in *Folia Morphologica* describes and studies the problems of cervical IVD degeneration and endplate calcification in the aspect of endplate marrow contact channels patency.

Aims

This study had the following aims:

1. To summarize and update the current state of knowledge on the embryology, structure, and biomechanics of the IVD and its endplates.
2. To demonstrates the impact of ageing and degeneration on the above properties (*aim 1*) of both the IVD and its endplates.
3. To quantify cell density in cervical IVDs and endplates of varying age and degeneration grade to produce cell density maps, which would provide a knowledge base for future cell based therapies for cervical disc degenerative disease.
4. To analyze glycosaminoglycan content in cervical IVDs and their endplates to supply data for future computer modelling of IVD behavior.
5. To clarify the relationship between the expression of inorganic pyrophosphate elaborating proteins in the IVD, and cervical vertebral endplate calcification and degeneration.

6. To determine the fundamental relationships between cervical IVD degeneration, endplate calcification, and the patency of endplate marrow contact channels.

Materials and Methods

Material acquisition

Sixty cervical IVDs were excised from 30 human cadavers (at the Department of Forensic Medicine, Jagiellonian University Medical College), using the anterior approach, not later than 24 hours post-mortem. The material was excised in one block comprising vertebral bodies, IVDs, endplates and blood vessels supplying these structure, wrapped in saline soaked gauze, vacuum-sealed to prevent dehydration, and kept at 4° Celsius for transport, and until further processing. Excision started at the level of the lower half of the C4 vertebra and ended at the level of the upper half of the C6.

The study inclusion criterion was the ability to excise a section of the anterior spinal column (from the lower half of the C4 vertebra to the upper half of the C6), with the anterior and posterior longitudinal ligaments and blood vessels supplying the vertebrae.

Study exclusion criteria were: (1) injury to the cervical spine, preventing from excising the required section; (2) previous cervical spine surgery; (3) receiving chemotherapy in the last 12 months; (4) previous radiation therapy to the perispinal region; (5) long-standing paralysis (6 or more months); (6) ankylosing spondylitis.

Material processing

An overview of how the study material was processed is depicted in the figure below. For detailed material processing methods please refer to specific manuscripts.

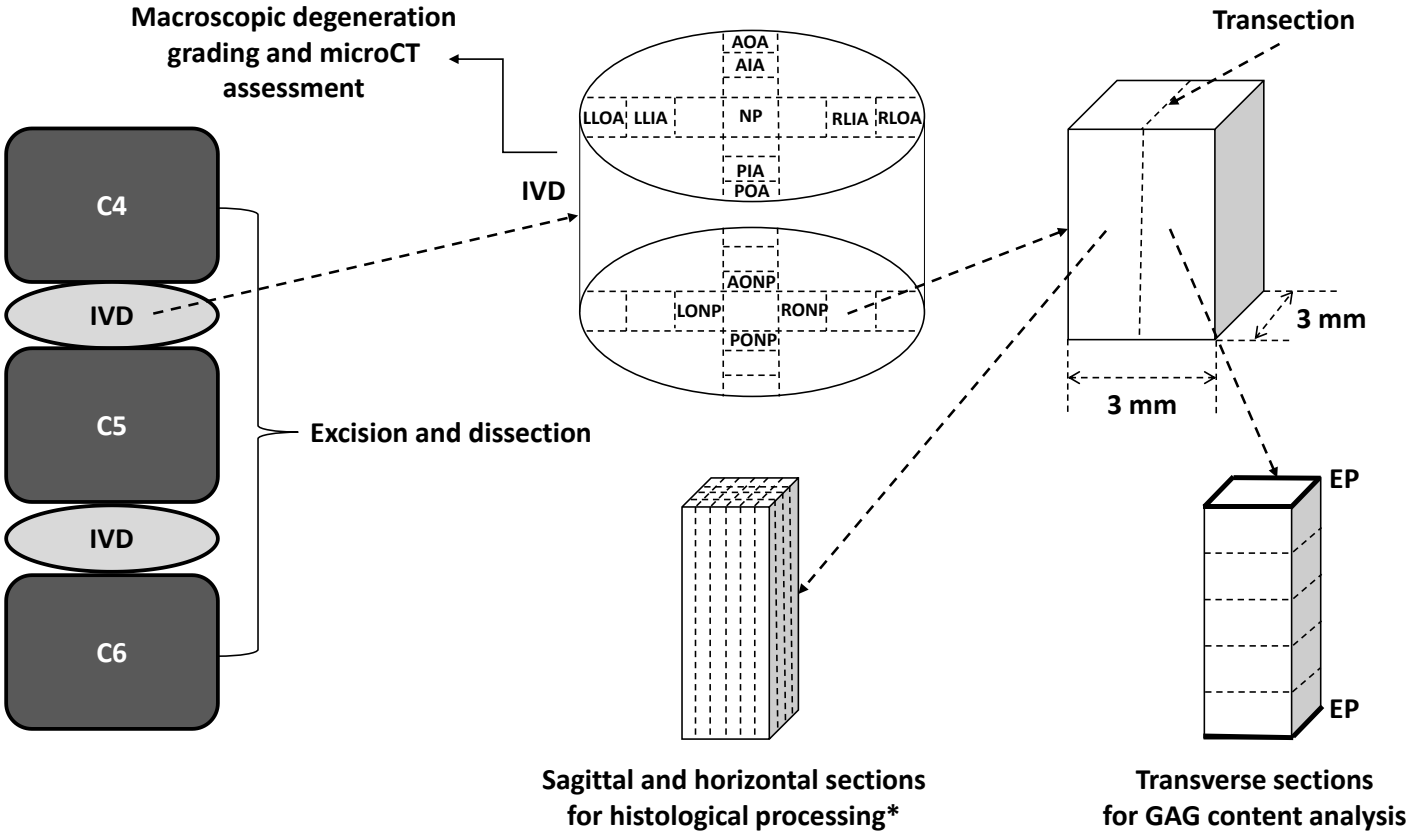

*****_Both IVD and endplate samples were processed. This included H&E and Masson trichrome staining, histological degeneration assessment, endplate calcification assessment, IVD and endplate cell density counting and immunohistochemistry (ANK, OPN, ALP, ENPP1, and TGF-_ β_1)._

Ethics

The research protocol was approved by the Jagiellonian University Medical College Ethics Committee (registry number KBET/319/B/2012). The study has been performed in accordance with the ethical standards laid down in the 1964 Declaration of Helsinki and its later amendments. The specimen excision method was chosen so as not to destabilize the cadaver's spinal column.

Main results, conclusions, and importance of the study

Manuscript number 1 published in Folia Morphologica

This review summarizes and updates the current state of knowledge on the embryology, structure, and biomechanics of the intervertebral disc and its endplates. To further translate this into a more clinical context this review also demonstrates the impact of ageing and degeneration on the above properties of both the intervertebral disc and its endplates.

The IVD together with its endplates forms an apparently simple structure, which at a closer look reveals its complexity – largely still unknown to us. The IVDs develop from the mesodermal notochord and receive nutrients mostly through the cartilaginous endplates. Physiologically they are innervated only in the outer AF by sensory and sympathetic perivascular nerve fibers, branches from the sinuvertebral nerve, the ventral rami of spinal nerves or from the gray rami communicantes. The IVDs undergo changes with ageing and degeneration, the latter having two types i.e. "endplate-driven" involving endplate defects and inward collapse of the AF and "annulus-driven" involving a radial fissure and/or an IVD prolapse.

Manuscript number 2 published in the Polish Journal of Pathology

This study aimed at quantifying cell density in cervical IVDs and endplates of varying age and degeneration grade to produce cell density maps, which would provide a knowledge base for future cell based therapies for cervical disc degenerative disease. As IVD cells are directly responsible for proteoglycan production, the second aim of the study was to analyze glycosaminoglycan (GAG) content in cervical IVDs and their endplates. This part of the study aimed at providing additional insight into IVD and endplate physiology and pathology, and was meant to supply data for future computer modelling of IVD behavior. To the authors best

knowledge this is the first study to analyze cell density and GAG content in cervical IVDs and their endplates.

After careful histological and biochemical analysis this study was able to produce maps of cell density and GAG content throughout the entire cervical IVD and its endplate. Overall, taking into account the IVD, cell density was highest in the NP (4218±417 cells/mm^3) and gradually decreased outwards and anteriorly (anterior AF: 3283±438 cells/mm^3), and increased outwards and posteriorly (posterior AF: 4464±551 cells/mm^3). With progressing degeneration cell density in the IVD decreased. Age did not have a similar effect, with cell density being alike in different age groups. Both cranial and caudal endplates exhibited similar cell density and GAG content. The endplate presented similar cell density throughout all of its structure, in some cases "matching" IVD regions of low cell density with endplate areas of high cell density. However, contrary to what we found in the IVD, in the endplate age significantly negatively correlated with endplate cell density. This finding might either stem from simple endplate calcification (which markedly progressed with age) and physical destruction of cells or suggest that IVD cells are more resistant in nature, due to the "harsher" environment that is present in the IVD when compared with the endplate.

Overall GAG content, both in the IVD and the endplates, followed cell density values. Interestingly sagittal and coronal variations in IVD GAG content were rather high when compared to previous studies. However, this was only true for the IVD, while the endplate, regardless of donor age or IVD/endplate degeneration, had similar GAG content throughout all of its regions. Axial variations in IVD GAG content were small, and resembled those from lumbar IVDs.

Concluding, this study introduced several detailed 3D maps of cervical IVD and cervical endplate cell density and GAG content. The most important prerequisite for successful IVD cell injection in cell-based tissue engineering approaches is a clear understanding of the actual

cell numbers in normal and degenerated IVDs. Knowledge from this study may partially bridge the gap on IVD cell numbers in normal and degenerated discs.

Furthermore, the results from this study show that cervical IVDs and their endplates only slightly differ, in terms of cell density and GAG content, from their lumbar counterparts.

Additionally this study provides new information characterizing GAG content distributions in the three primary directions in the IVD. This information may be helpful for future computer modelling of human IVD tissue. The data presented also points out an overall age-related trend towards decreased IVD cellular metabolic activity as manifested by decreasing concentrations of GAGs.

Manuscript number 3 published in the Polish Journal of Pathology

To the authors best knowledge, this study is the first attempt in current literature to analyze the relationship between the expression of ankiryn (ANK), alkaline phosphatase (ALP), ectoenzyme PC-1 (ENPP-1), osteopontin (OPN), and transforming growth factor β1 (TGF-β1) in the cervical IVD, and cervical vertebral endplate calcification and degeneration.

This study has shown that the percentage of endplate calcification significantly correlates with the degree of endplate and IVD histological degeneration (both $r=0.91$; $p<0.0001$). The intensity and number of stained cells per field of view markedly decreased, for ANK, ENPP-1, and TGF-β1, with the grade of IVD degeneration, regardless of the analyzed IVD region. This was not true only for ALP which demonstrated an increasing trend corresponding to the degree of IVD degeneration. The expression of OPN was low throughout all analyzed regions, regardless of the degree of degeneration.

The most significant finding of this study is the fact that, for the first time in a large group of cervical IVDs, it was possible to confirm that there exists a strong relationship between the decreased expression of ANK, ENPP-1, and TGF-β1 in the IVD and an increase in IVD

degeneration and endplate degeneration and calcification. This finding was probably most evident for ANK and TGF-β1 as both proteins are strongly intertwined with each other in the process of calcification. ALP, as expected, was expressed more intensively in IVDs with a higher degree of calcification, as ALP is a marker of ongoing mineral deposition.

This study also confirms that the first calcifications in the endplate can be seen as early as in the third decade of life.

Modulating the expression of the abovementioned proteins, especially ANK and TGF-β1, may be a new way to prevent the degeneration and calcification of the IVD.

Manuscript number 4 published in *Folia Morphologica*

The aim of this study was to determine the fundamental relationships between cervical IVD degeneration, endplate calcification, and the patency of endplate marrow contact channels (MCC).

Studies on lumbar IVDs have suggested that endplate calcification can impede nutrient transport to the IVD. However this finding was never directly related to endplate degeneration or explored further in IVDs other than lumbar.

This study, through the use of computed microtomography (microCT) has found that the number of 300 μm endplate openings negatively correlates with the number of all other openings ($r=-0.62-(-0.82)$; $p<0.0001$). This correlation was strongest for openings 10 – 50 μm in diameter. A similar relationship between the number of endplate openings and IVD and endplate degeneration/calcification was seen, with 300 μm opening correlating positively, while MCCs of smaller sizes correlated negatively.

Basing on our results and the scanning electron microscopy findings of previous studies we concur that the positive relationship between large (300 μm) endplate openings and IVD degeneration suggests that those in fact are not MCCs but are rather the effects of endplate

cracking during degeneration. These openings do not contain capillary buds, and are the offspring of age-associated endplate thinning, clefts and fissures.

Additionally IVD degeneration, graded using Thompson's classification (macroscopic assessment), significantly correlated with Boos'es IVD degeneration score (microscopic assessment) ($r=0.77$; $p<0.0001$).

This study is the first to use microCT together with histological analysis to allow for the localization, quantification, and characterization of MCCs in the cervical endplate. Up-to-date only one similar study explored such a relationship in lumbar IVDs, using scanning electron microscopy (SEM). Other studies assessing this relationship based solely on histological analysis, which allows only to visualize a certain portion of the endplate, and not its entire structure.

It is still not clear whether endplate calcification is the cause or the effect of IVD and/or endplate degeneration. Some authors safely reply that both processes exist simultaneously and are strongly associated with each other. However, the results of this study have signaled that endplate calcification is rather the cause, than the effect of a fall in nutrient transport, as it starts in the well-vascularized center of the endplate, and not in the outer regions where the number of MCCs is lower. Unfortunately, definitive sentences have to be withheld until "cause and effect" studies provide further data.

Concluding, this is the first study to perform such an investigation on human cervical spine samples. It has brought to light that, similarly to lumbar IVDs, there is a strong negative correlation between the number of endplate MCCs, and both macroscopic and microscopic cervical IVD and endplate degeneration. This could further support the idea that endplate calcification, through the occlusion of MCCs, leads to a fall in nutrient transport to the IVD, and subsequently causes its degeneration. Additionally, the sample examination method demonstrated in this study allows to perform accurate and easily reproducible measurements

of the number, size and shape of endplate MCCs. What is more, we have shown that Thompson's classification corresponds well to Boos'es histological classification of endplate and IVD degeneration, allowing to use Thompson's classification as a surrogate of microscopic degeneration, until the results of pathological analysis are known.

Practical application of presented results

Apart from pure scientific value, this study carries with it also important clinical implications – both for current and future practice. It is also worth mentioning that, to the authors best knowledge, this is the first such study to be performed on cervical IVDs.

This study introduces several detailed 3D maps of cervical IVD and cervical endplate cell density and GAG content. This knowledge will allow to properly estimate the number of cells that need to be injected into the IVD in order for the experimental stem cell treatments to effectively match the IVD and the endplate cell density. The provided GAG content distribution throughout the cervical IVD (in the three primary directions) and the endplates may be helpful for future finite element modelling of human IVD tissue.

The presented results also bring to light the fact that modulating the expression of selected proteins in the IVD, especially ANK and TGF-β1, may be a new way to prevent its degeneration and endplate calcification.

Additionally, the method used in this study (computed microtomography) allows to perform accurate and easily reproducible measurements of the number, size and shape of endplate MCCs. What is more, the obtained results show that, in cervical IVDs, Thompson's classification corresponds well to Boos'es histological classification of endplate and IVD degeneration. This allows to use Thompson's classification as a surrogate of microscopic degeneration, until the results of pathological analysis are known.

4. Artykuł numer 1

Tomaszewski KA, Saganiak K, Gładysz T, Walocha JA. The biology behind the human intervertebral disc and its endplates. Folia Morphologica 2014

Table of Contents

The biology behind the human intervertebral disc and its endplates

Krzysztof A. Tomaszewski[1], Karolina Saganiak[1], Tomasz Gładysz[1,2], Jerzy A. Walocha[1]

[1]Department of Anatomy, Jagiellonian University Medical College, Krakow, Poland

[2]Department of Oral Surgery, Jagiellonian University Medical College, Krakow, Poland

Running title: Biology of the human intervertebral disc

Corresponding author

Krzysztof A. Tomaszewski

Department of Anatomy

Jagiellonian University Medical College

12 Kopernika street, 31-034 Krakow, Poland

Tel./fax. +48-12-422-95-11

e-mail: krtomaszewski@gmail.com

Abstract

The intervertebral discs are roughly cylindrical, fibrocartilaginous, articulating structures connecting the vertebral bodies, and allowing movement in the otherwise rigid anterior portion of the vertebral column. They also transfer loads and dissipate energy. Macroscopically the intervertebral disc can be divided into an outer annulus fibrosus surrounding a centrally located nucleus pulposus. The endplates surround the intervertebral discs from both the cranial and caudal ends, and separate them from the vertebral bodies and prevent the highly hydrated nucleus pulposus from bulging into the adjacent vertebrae. The intervertebral discs develop from the mesodermal notochord and receive nutrients mostly through the cartilaginous endplates. Physiologically they are innervated only in the outer annulus fibrosus by sensory and sympathetic perivascular nerve fibers, branches from the sinuvertebral nerve, the ventral rami of spinal nerves or from the gray rami communicantes. The intervertebral discs undergo changes with ageing and degeneration, the latter having two types i.e. “endplate-driven” involving endplate defects and inward collapse of the annulus fibrosus and “annulus-driven” involving a radial fissure and/or an intervertebral disc prolapse. This review summarizes and updates the current state of knowledge on the embryology, structure, and biomechanics of the intervertebral disc and its endplates. To further translate this into a more clinical context this review also demonstrates the impact of ageing and degeneration on the above properties of both the intervertebral disc and its endplates.

Keywords: biomechanics; degeneration; disc degenerative disease; embryology; endplate; intervertebral disc.

Introduction

The intervertebral discs (IVD) are roughly cylindrical, fibrocartilaginous, articulating structures connecting the vertebral bodies, and allowing movement (flexion, extension, and rotation) in the otherwise rigid anterior portion of the vertebral column [63]. They are approximately 7 to 10 mm thick and 4 cm in diameter in the lumbar region of the spine [14], and constitute 1/3 of the vertebral column's height [60]. The IVDs spread loading evenly on the vertebral bodies, regardless of the position of the spine. Macroscopically the IVD can be divided into an outer annulus fibrosus (AF) surrounding a centrally located nucleus pulposus (NP) [Figure 1]. The endplates surround the IVDs from both the cranial and caudal ends, and separate them from the vertebral bodies and prevent the highly hydrated NP from bulging into the adjacent vertebrae. The endplates also absorb the considerable hydrostatic pressure that results from mechanical loading of the spine [64].

The aim of this review was to summarize and update the current state of knowledge on the embryology, structure, and biomechanics of the IVD and its endplates. To further translate this into a more clinical context this review demonstrates the impact of ageing and degeneration on the above properties of both the IVD and its endplates.

The development of the human intervertebral disc

The development of the vertebral column is centered around the mesodermal notochord [72, 75]. It both gives rise to the NP, as well as acts as a "signaling-center" for cell migration, differentiation and survival [18, 72]. The development of the IVD is depicted on Figure 2.

The two different parts of the IVD – the AF and the NP arise on two separate developmental pathways. At approximately 30 days human fetal gestation cells of the sclerotome migrate medially from pairs of paraxial somites to condense around the notochord [37] [Figure 2A

and 2B]. The metameric pattern of regions differing in the level of cell condensations gives rise to the AF (more condensed) and the vertebral bodies (less condensed) [72] [Figure 2C]. Concurrently with AF morphogenesis, the notochord contracts within the forming vertebral body rudiments while simultaneously expanding within the intervertebral regions to form the NP [9] [Figure 2D]. Simultaneously, cells in the future AF adopt a fibroblastic morphology, and mediated by cytoskeletal actin filaments align and orient to form the template for matrix deposition that later defines the AF angle-ply lamellar structure [Figure 2E] [34]. Vertebrae ossification commences at the end of the 10^{th} week of gestation [71].

The main players in the molecular signaling of IVD embryogenesis are Sonic hedgehog (Shh), Noggin, Pax, Sox and TGFβ. Shh is responsible for regulating skeletal morphogenesis by providing positional information and directing cell differentiation – leading to the definition of the sclerotome [24]. Noggin, expressed by notochordal cells [43], acts synergistically to Shh, and becomes localized to the developing AF where it remains until birth, potentially acting to block BMP signaling that originates from the vertebral bodies [22].

Pax genes encode transcription factors that regulate proliferation, differentiation, apoptosis, cell migration and stem cell maintenance [72]. In particular, Pax expression is important for specifying and maintaining tissue boundaries [28], and as such might be responsible for delineating the more and less condensed regions of cells that will give rise to the IVDs and vertebral bodies, respectively [73]. Pax1 and Pax9 genes were specifically implicated in the development of the IVD, as in their absence, both IVDs and vertebral bodies fail to develop, being substituted by an irregular cartilaginous rod [59].

Among the Sox gene family Sox5, Sox6 and Sox9 are specifically implicated in chondrogenesis [68], and thus are important for IVD development. Sox5 and Sox6 are expressed in both sclerotome-derived and notochordal cells [74]. Sox9 is expressed in all

primordial cartilage during embryogenesis, coincident with collagen II expression, including in the sclerotome and notochord [10].

TGFβ-3 signaling is important for regulating cell proliferation and differentiation, and extracellular matrix production during skeletal development, with different TGFβ-3 isoforms exhibiting tissue-specific expression profiles [46]. TGFβ-3 has been shown to be strongly localized to the perichordal condensations that give rise to the AF and vertebral bodies. As condensation advances, this expression pattern becomes localized to the IVD anlagen, showing clear demarcation with respect to the adjacent vertebral bodies [58].

Structure – anatomy, histology and biochemistry of the intervertebral disc and its endplates

Nucleus pulposus

The centrally located NP consists of randomly arranged type II collagen fibers, and radially placed elastin fibers which are embedded in a highly hydrated aggrecan-containing gel [38]. The proteoglycan to collagen ratio is approximately 27:1 [19]. These large quantities of aggrecan located along chains of hyaluronan carry a fixed negative charge and generate an osmotic swelling pressure within the irregular meshwork of collagen type II fibrils [72]. Dispersed, at a low density (approximately 3000-5000/mm^3) are chondrocyte-like cells [41, 60]. At least two distinct cell phenotypes can be identified in the NP – notochordal cells (which disappear after the 3rd year of life) [41], and chondrocyte-like cells – distinctly different from articular chondrocytes [47]. Recently Sakai et al. [67] described a third type of NP cells with properties similar to those of mesenchymal stem cells. However, due to their characteristics, these cells can be in fact notochordal cells [19].

Cells of the NP are highly specialized and survive in a very hypoxic environment (1% of O2). Hypoxia inducible transcription factors-1 and -2, which are key cellular regulators of the

hypoxic response, were found to be constitutively active in NP cells [61]. This activity might be partly responsible for the large production of aggrecan by NP-resident cells, independent of oxygen conditions [5].

Recent studies have pointed out the importance of notochordal cells in the survival of chondrocyte-like cells. Erwin et al. [26] have shown that the secretome of notochordal cells had an anti-apoptotic effect on chondrocyte-like cells, through inhibition of apoptotic caspases-3 and -9, and favored the expression of aggrecan and type II collagen. Thus, the gradual disappearance of notochordal cells during skeletal maturation and aging constitutes a primary event initiating NP degeneration.

Outside the NP is the AF – the boundary between these two regions being very distinct in individuals <10 years of age [60].

Annulus fibrosus

The AF can be divided into two distinct areas – the inner and the outer AF. The inner AF, which is also known as the transition zone, contains poorly organized extracellular matrix composed of type II collagen, proteoglycans, and water. In contrast, the outer AF is highly organized and is rich in type I collagen, with undetectable levels of type II collagen and proteoglycans, and higher resistance to tension [19].

A typical lumbar AF is made up of 15-25 concentric lamellae, with type I collagen fibers passing obliquely (at approximately 60° to the vertical axis) between vertebral bodies, with orientation of the fibers being reversed in successive lamellae [42] [Figure 1B] (however type II collagen can also be produced by AF cells) [17]. These lamellae originate as individual discrete bundles of collagen fibers, but their organization becomes increasingly complex with more bifurcation and interdigitations as the individual ages, and the lamellae increase in thickness [42]. Elastin fibers, constituting 2% of the AF dry weight, pass radially from one

lamella to the next, binding them together, and possibly helping the IVD return to its original arrangement following bending [89]. Additionally, the lamellae are interconnected by lubricin and type VI collagen [45, 70]. Lubricin, known for its lubricant role within diarthrodial joints, is probably involved in the reduction of friction between adjacent lamellae.

The morphology of AF cells (approximately 9000cells/mm^3) changes from the outer to the inner part, from thin, elongated (parallel to the collagen fibers) and fibroblast-like to more oval, respectively. AF cells, similar to NP cells, can have several long, thin cytoplasmic projections, which may be more than 30 mm long. The function of these projections remains unknown, but it is speculated that they act as sensors of mechanical strain within the tissue [25].

Endplates

Each IVD is bordered at the cranial and caudal ends by endplates which separate the vertebral bone from the IVD itself [Figure 3] and prevent the highly hydrated nucleus from bulging into the adjacent vertebrae. They are identifiable from an early embryological stage and possess an osseous as well as a hyaline cartilage component [78]. The endplates are usually less than 1 mm thick (thinner in the center than on the outside) and composed of hyaline cartilage [60]. Type II collagen fibers within the endplate run horizontal and parallel to the vertebral bodies, with the fibers continuing into the IVD [64] [Figure 3]. Additionally, type X collagen is thought to be the most important in the endplate since it is a marker of hypertrophic chondrocytes and is involved in calcification [6].

Proteoglycan molecules within the endplate matrix are necessary for the control of solute transport and maintenance of water content throughout the IVD. Depletion of proteoglycans from the endplate cartilage is associated with loss of proteoglycans from the NP [65]. This

translates further that proteoglycan loss would ultimately lead to degeneration of the IVD [56]. Alterations in IVD biochemistry, particularly in the endplate, during the skeletal growth may also be involved in the development of scoliosis [7].

In regards to cell type only chondrocytes constitute the endplates, and produce an extracellular matrix rich in type II collagen and proteoglycans (1:2 ratio – similar to articular cartilage), with water content of 50-60% [64].

The endplates also contain a network of microscopic blood vessels that are responsible for nutritional intake during development and growth of IVDs [Figure 4A]. Metabolites diffuse through pores present in the growth plates based on their size and charge. Only positive ions (e.g., sodium, calcium) or neutral molecules, such as glucose and oxygen, can diffuse [65]. The network mostly involutes around the time of skeletal maturity [31].

Vascular supply and nutrition of the intervertebral disc and its endplates

Blood with nutrients reaches the IVD through external (present around the outer AF) and endplate capillaries that are branches of segmental arteries, which in turn branch off the aorta [60]. The blood drains to the subchondral venous network or into the veins of the marrow spaces of the vertebral bodies [21]. Blood flow in the region of the endplates is not entirely passive - muscarinic receptors have been identified, and they can probably influence disc nutrition under altered physiological conditions [84].

The IVD is the largest avascular structure in the human body, with some cells being up to 8 mm from the nearest direct blood supply [80]. Essential nutrients (e.g. oxygen, glucose, amino acids etc.) are supplied to the IVD from its peripheries [Figure 5]. Metabolic waste products are removed from the IVD via a reverse route [35]. This causes variations in both oxygen concentration and pH throughout the different zones of the IVD [35]. Low oxygen tension in the center of the IVD leads to anaerobic metabolism, resulting in a high

concentration of lactic acid and low pH [80]. In vitro experiments show that a chronic lack of oxygen causes NP cells to become quiescent, while a chronic lack of glucose leads to their death [36].

In vitro studies using small dye molecules have demonstrated that the lateral margins of the endplate near the vertebral rim are relatively impermeable compared with the central portion or the entire AF [49]. It was shown that endplate permeability is caused by microscopic blood vessels, ending in capillary buds (loop-like structures), that penetrate the endplate via marrow contact channels [12, 49]. It is through this route that the majority (approximately 80%) of nutrients are transported to the IVD [43]. However, diffusion from the capillary buds to the IVD is purely dependent on the size and ionic charge of the molecules involved. The net negative charge of the NP conferred by the high concentration of proteoglycans permits passage of positive ions such as sodium and calcium and uncharged molecules such as glucose and oxygen, while impeding movement of negatively charged ions such as sulphate and chloride and macromolecules such as immunoglobulins and enzymes [35, 48].

In humans, during the early postnatal years, blood vessels that have penetrated the AF and cartilage endplates, from as early as 35 weeks gestation, begin to recede, eventually leaving the IVD as a completely avascular structure [50], with only a low number of vessels present in the endplate. Possible reasons for vascular regression include decreased nutrient requirements following the initial period of rapid growth or, more likely, the inability of the circulatory pressure to compete with large physiological stresses in the surrounding extracellular matrix [72]. What is more, the paths that the blood vessels followed never fully remodel and leave translamellar bridging elements [45], whose function is as of yet unknown. Probably they respond to radial and shear deformations [72]. However, it is unclear whether this influence would assist or impair the function of the IVD. In the fetus and in infants, the subchondral plate is also penetrated by regularly spaced nutrient canals similar to those seen in other

growth cartilages [87]. These disappear in childhood, leaving residual “weak spots” that may later lead to Schmorl node formation and even later, to sclerosis of the subchondral plate [16].

Innervation of the intervertebral disc

Under physiological conditions the human IVD is poorly innervated - only by sensory and sympathetic perivascular nerve fibers, found mostly in the outer zone of the AF, accompanying blood vessels or travelling independently [29, 60]. Most of the fibers innervating the IVD are nociceptive, and to a lesser extent proprioceptive. A small number of mechanoreceptors are also present in the IVD in its 2-3 outer AF lamellae, most commonly having the morphology of Golgi tendon organs, a few Ruffini receptors, and even fewer Pacinian corpuscles [62]. The adult vertebral endplate is fully aneural [57].

The IVD is innervated by branches of the sinuvertebral nerve, by nerves derived from the ventral rami of spinal nerves or by nerves derived from the gray rami communicantes [77]. IVDs also receive innervation from two dense nerve interconnected plexuses located in the anterior and posterior longitudinal ligaments [30, 76] [Figure 6]. It is agreed that lumbar IVDs are innervated segmentarily [8]. The innervating fibers arise primarily from small dorsal root ganglions which are classified based on their stimulus-response function and also based on their neurochemistry and connectivity [29].

Healthy IVDs are innervated only in the region of the external lamellae of the AF [29, 57, 77, 88] [Figure 7A]. The fibers responsible for this innervation pattern can be either associated with blood vessels or travel independently, and are positive for substances such as acetylcholinesterase, neurofilament protein, substance P, calcitonin gene-related peptide, vasoactive intestinal polypeptide, neuropeptide Y, C-flanking peptide and synaptophysin [20, 55].

With progressive IVD degeneration the nerves grow into the inner part of the AF, and sometimes even to the NP. These are mostly nociceptive fibers, that may accompany ingrowing blood vessels [Figure 7B]. The immunohistochemical profile of nerve fibers and neurons innervating pathological IVDs is identical to that reported in normal conditions. Thus, the differences in the pattern of IVD innervation in normal conditions in comparison with degenerated conditions are quantitative rather than qualitative [20, 44, 77]. Additionally, together with the hyperinnervation of the IVD, there is increased nerve growth factor expression [40], as well as an increase in the number of Golgi-tendon organ-like structures such as Ruffini's and Pacinian corpuscles [20, 62]. There is also evidence that sympathetic afferents are also increased in degenerating IVDs and that they play a significant role in lower back pain [29].

Biomechanics of the intervertebral disc and its endplate

The most important function of the IVD is mechanical – to transfer loads, dissipate energy, and allow movement in the vertebral column. Both the NP and AF act synergistically to distribute and transmit loads between the vertebral bodies [51]. During compression hydrostatic pressure is generated within the NP which is constrained peripherally by the AF. In turn in the lamellar structure of the AF circumferential tensile stresses are generated [51]. The NP has a high water content (because of aggrecan which has a high anionic glycosaminoglycan content and provides appropriate osmotic properties [85]), which makes it act almost like fluid. This entire "compression-coping" mechanism is additionally supported by the inner AF, which is rich in proteoglycans [83] [Figure 8]. The angle-ply structure and nonlinear properties of the AF facilitate joint mobility and stability in multiple modalities, including bending, rotation, and combinations of both [32, 69].

With increasing age, IVD water content decreases, especially in the NP. Most of the AF then acts like a fibrous solid band to resist compression directly. In physically disrupted discs, regions of fibrous tissue resist mechanical loading in a haphazard manner, and the hydrostatic balance of the NP is reduced or absent [4].

The endplates also have to be noted for their ability to absorb the considerable hydrostatic pressure that results from mechanical loading of the spine [48].

Intervertebral disc ageing and degeneration

To begin with, the most important thing is to distinguish between physiological ageing, healing and remodeling and pathological degeneration of the IVD and its endplate. Adams and Roughely [4] proposed a definition of IVD degeneration, based on IVD loss of structural integrity - "excessive mechanical loading causes an IVD to degenerate by disrupting its structure and precipitating a cascade of nonreversible cell-mediated responses leading to further disruption. A degenerated IVD is one with structural failure combined with accelerated or advanced signs of aging.".

The following sections will review the basic changes related to IVD and endplate ageing and degeneration.

Ageing of the intervertebral disc

During growth and skeletal maturation, the boundary between the AF and the NP becomes less obvious, and with increasing age the NP generally becomes more fibrotic and less gel-like [15]. The NP tends to condense into several fibrous lumps, separated from each other and from the cartilage endplate by softer material [4]. Proteoglycan fragmentation starts during childhood [15] and with increasing age, the overall proteoglycan and water content of the IVD decreases, especially in the NP [4]. In turn, the collagen content increases, with type I

collagen replacing type II, and the AF "engulfing" the NP, and making the IVD stiffer [4]. Interestingly, as long as the detached proteoglycans remain inside the IVD (encapsulated by the AF and the endplates), they still fulfill a functional role similar to that of the intact proteoglycans [2]. Reduced matrix turnover in older discs enables collagen molecules and fibrils to become increasingly cross-linked with each other, and existing cross-links become more stable [23].

Since early childhood, the blood supply to the IVD and the endplate decreases [13], together with cell density [41], leading to an increased incidence of structural defects – mostly in the AF [4]. Changes progress gradually, affecting first the endplates, then the NP, and finally the AF [13]. However, these changes might simply reflect the necessary adaptations to increased mechanical loading at the onset of ambulation, and reduced metabolite transport in a growing IVD.

The microstructural clefts and tears that appear increasingly during growth may possibly lead to more extensive disruption in later life, but so long as they remain small, they appear to have little effect on the internal mechanical function of the IVD [3].

As mentioned earlier, with increasing age, the hydrostatic NP becomes smaller and decompressed. Thus more of the compressive load-bearing is taken by the AF [4]. Disc height does not show a major decrease with age [27], although degenerative changes can cause the AF to collapse in older IVDs [4].

It is also important to distinguish simple injury from IVD degeneration. AF tears are not remodeled as in bone, presumably because the sparse cell population is unable to break down the large collagen fiber bundles of the AF and replace them with new ones [66]. Collagen turnover time in articular cartilage is approximately 100 years [81] and could be even longer in the IVD. Proteoglycan turnover is faster, possibly 20 years [66]. Injuries that affect the inner AF or the endplate decompress the NP [79] and healing processes are then overtaken by

severe degenerative changes [4]. It is important to note that age-related IVD changes are not associated with pain [11].

Degeneration of the intervertebral disc

Adams and Dolan [1] have brought to light that there exist two distinct types of IVD degeneration – "endplate-driven" involving endplate defects and inward collapse of the AF and "annulus-driven" involving a radial fissure and/or an IVD prolapse. The structural defects which initiate the two processes both act to decompress the NP, making it less likely that the other defect could occur subsequently. The first type of IVD degeneration is characterized by high heritability, mostly affects IVDs in the upper lumbar and thoracic spine, often starts to develop before 30 years of age, usually leads to moderate back pain, and is associated with compressive injuries. The second type has a low heritability, mostly affects IVDs in the lower lumbar spine, develops progressively after 30 years of age, usually leads to severe back pain and sciatica, and is associated with repetitive bending and lifting.

Individual genes associated with IVD degeneration include those for type IX collagen, aggrecan, vitamin D receptor, MMP-3, and cartilage intermediate layer protein [1, 4, 39, 54, 82]. The products of these genes probably affect the strength of skeletal tissues, and their systemic effects may explain why IVD degeneration is more prevalent in those with osteoarthritis [33].

Endplate changes with ageing and degeneration

With ageing the cartilaginous part of the endplate diminishes in thickness and undergoes remodeling, leading to cartilage calcification or formation of true bone [52]. Which of the two actually occur remains unresolved. This process impedes nutrient transport via the endplate contact channels [12], not only by physically obstructing them but also through blood vessel

occlusion [48] [Figure 4B]. It has been shown, both in vitro and in vivo, that calcification found in scoliotic IVDs can impede transport of even small molecules [65, 80].

In some cases the endplate undergoes revascularization – in response to both physiological [53] and pathological stimuli [48]. The creation of blood vessels in the endplate occurs by activation of MMPs which are normally maintained in latent form by tissue inhibitors [86].

Morphological changes are also present in the endplates in association with IVD degeneration, and include fissures and clefts along the length of the endplate in the horizontal plane with occasional chondrocyte death [48].

Conclusions

The IVD together with its endplates forms an apparently simple structure, which at a closer look reveals its complexity – largely still unknown to us. Though recent years have brought about considerable research advancements in the field of IVD degeneration, we are still not yet sure where ageing ends and degeneration begins. However, there are multiple reasons to be optimistic, as new insights into the process of IVD and endplate degeneration are made every day, and we are always ever closer to unravelling the mysteries of back pain.

Conflict of Interest Statement

All authors declare that they have no conflict of interest.

Acknowledgements

This study was funded by the National Science Center – Poland under grant number DEC-2012/07/N/NZ5/00078. Krzysztof A. Tomaszewski received a scholarship to prepare his PhD thesis from the National Science Center – Poland under award number DEC-2013/08/T/NZ5/00020.

Author contribution

Design and planning of the study – KAT, TG, JAW. Bibliographic search – KAT, KS, TG. Drafting and revising the manuscript – KAT. Preparing figures – KS. Obtaining funding – KAT. Critical revision of the manuscript – JAW. All authors have read and approved the final version of the manuscript.

All co-authors confirm the above-mentioned contributions and consent to the fact that this study is a part of Krzysztof A. Tomaszewski PhD thesis. The co-authors confirm that Krzysztof A. Tomaszewski has contributed significantly (80% in total) to every part of this study, as stated above.

References

1. Adams MA, Dolan P (2012) Intervertebral disc degeneration: evidence for two distinct phenotypes, J Anat, 221: 497-506.
2. Adams MA, Freeman BJ, Morrison HP, Nelson IW, Dolan P (2000) Mechanical initiation of intervertebral disc degeneration, Spine, 25: 1625-1636.
3. Adams MA, McNally DS, Dolan P (1996) 'Stress' distributions inside intervertebral discs. The effects of age and degeneration, J Bone Joint Surg Br, 78: 965-972.
4. Adams MA, Roughley PJ (2006) What is intervertebral disc degeneration, and what causes it? Spine (Phila Pa 1976), 31: 2151-2161.
5. Agrawal A, Guttapalli A, Narayan S, Albert TJ, Shapiro IM, Risbud MV (2007) Normoxic stabilization of HIF-1alpha drives glycolytic metabolism and regulates aggrecan gene expression in nucleus pulposus cells of the rat intervertebral disk, Am J Physiol Cell Physiol, 293: 621-631.
6. Aigner T, Gresk-otter KR, Fairbank JC, von der Mark K, Urban JP (1998) Variation with age in the pattern of type X collagen expression in normal and scoliotic human intervertebral discs, Calcif Tissue Int, 63: 263-268.
7. Antoniou J, Arlet V, Goswami T, Aebi M, Alini M (2001) Elevated synthetic activity in the convex side of scoliotic intervertebral discs and endplates compared with normal tissues, Spine 26: 198-206.
8. Aoki Y, Ohtori S, Takahashi K, Ino H, Takahashi Y, Chiba T, Moriya H (2004) Innervation of the lumbar intervertebral disc by nerve growth factor-dependent neurons related to inflammatory pain, Spine 29: 1077-1081.

9. Aszodi A, Chan D, Hunziker E, Bateman JF, Fassler R (1998) Collagen II is essential for the removal of the notochord and the formation of intervertebral discs, J, Cell Biol, 143, 1399-1412.
10. Barrionuevo F, Taketo MM, Scherer G, Kispert A (2006) Sox9 is required for notochord maintenance in mice. Dev Biol, 295: 128-140.
11. Battie MC, Videman T, Parent E (2004) Lumbar disc degeneration: Epidemiology and genetic influences, Spine, 29: 2679-2690.
12. Benneker LM, Heini PF, Alini M, Anderson SE, Ito K (2005) 2004 Young Investigator Award Winner: vertebral endplate marrow contact channel occlusions and intervertebral disc degeneration, Spine (Phila Pa 1976), 30: 167-173.
13. Boos N, Weissbach S, Rohrbach H, Weiler C, Spratt KF, Nerlich AG (2002) Classification of age-related changes in lumbar intervertebral discs: 2002 Volvo Award in basic science, Spine, 27: 2631-2644.
14. Broberg KB (1983) On the mechanical behaviour of intervertebral discs, Spine, 8: 151-165.
15. Buckwalter JA (1995) Aging and degeneration of the human intervertebral disc, Spine, 20: 1307-1314.
16. Chandraraj S, Briggs CA, Opeskin K (1998) Disc herniations in the young and end-plate vascularity, Clin Anat, 11: 171-176.
17. Chelberg MK, Banks GM, Geiger DF, Oegema TR Jr (1995) Identification of heterogeneous cell populations in normal human intervertebral disc, J Anat, 186: 43-53.
18. Choi KS, Cohn MJ, Harfe BD (2008) Identification of nucleus pulposus precursor cells and notochordal remnants in the mouse: implications for disk degeneration and chordoma formation, Dev Dyn, 237: 3953-3958.

19. Colombier P, Clouet J, Hamel O, Lescaudron L, Guicheux J (2014) The lumbar intervertebral disc: from embryonic development to degeneration, Joint Bone Spine, 81: 125-129.
20. Coppes MH, Marani E, Thomeer RT, Groen GJ (1997) Innervation of "painful" lumbar discs, Spine, 22: 2342-2349.
21. Crock HV, Goldwasser M (1984) Anatomic studies of the circulation in the region of the verterbal end-plate in adult greyhound dogs, Spine, 9: 702-706.
22. DiPaola CP, Farmer JC, Manova K, Niswander LA (2005) Molecular signaling in intervertebral disk development, J Orthop Res. 23: 1112-1119.
23. Duance VC, Crean JK, Sims TJ, Avery N, Smith S, Menage J, Eisenstein SM, Roberts S (1998) Changes in collagen cross-linking in degenerative disc disease and scoliosis, Spine 23: 2545-2551.
24. Ehlen HW, Buelens LA, Vortkamp A (2006). Hedgehog signaling in skeletal development, Birth Defects Res C Embryo Today, 78: 267-279.
25. Errington RJ, Puustjarvi K, White IR, Roberts S, Urban JP (1998) Characterisation of cytoplasm-filled processes in cells of the intervertebral disc, J Anat, 192: 369-378.
26. Erwin WM, Islam D, Inman RD, Fehlings MG, Tsui FW (2011) Notochordal cells protect nucleus pulposus cells from degradation and apoptosis: implications for the mechanisms of intervertebral disc degeneration, Arthritis Res Ther, 13: R215.
27. Frobin W, Brinckmann P, Biggemann M, Tillotson M, Burton K (1997) Precision measurement of disc height, vertebral height and sagittal plane displacement from lateral radiographic views of the lumbar spine, Clin Biomech (Bristol, Avon), 12:S1-S63.
28. Frost V, Grocott T, Eccles MR, Chantry A (2008) Self-regulated Pax gene expression and modulation by the TGFbeta superfamily. Crit Rev Biochem Mol Biol, 43: 371-391.

29. García-Cosamalón J, del Valle ME, Calavia MG, García-Suárez O, López-Muñiz A, Otero J, Vega JA (2010) Intervertebral disc, sensory nerves and neurotrophins: who is who in discogenic pain? J Anat, 217: 1-15.
30. Groen GJ, Baljet B, Drukker J (1990) Nerves and nerve plexuses of the human vertebral column, Am J Anat, 188: 282-296.
31. Grunhagen T, Wilde G, Soukane DM, Shirazi-Adl SA, Urban JP (2006) Nutrient supply and intervertebral disc metabolism, J Bone Joint Surg, 88: 30-35.
32. Guerin HL, Elliott DM (2007) Quantifying the contributions of structure to annulus fibrosus mechanical function using a nonlinear, anisotropic, hyperelastic model, J, Orthop Res, 25: 508-516.
33. Hassett G, Hart DJ, Manek NJ, Doyle DV, Spector TD (2003) Risk factors for progression of lumbar spine disc degeneration: The Chingford Study, Arthritis Rheum, 48: 3112-3117.
34. Hayes AJ, Benjamin M, Ralphs JR (1999) Role of actin stress fibres in the development of the intervertebral disc: cytoskeletal control of extracellular matrix assembly, Dev Dyn, 215: 179-189.
35. Holm S, Maroudas A, Urban JP, Selstam G, Nachemson A (1981) Nutrition of the intervertebral disc: solute transport and metabolism. Connect Tissue Res, 8: 101-119.
36. Horner HA, Urban JP (2001) 2001 Volvo Award Winner in Basic Science Studies: Effect of nutrient supply on the viability of cells from the nucleus pulposus of the intervertebral disc, Spine, 26: 2543-2549.
37. Hunter CJ, Matyas JR, Duncan NA (2003) The notochordal cell in the nucleus pulposus: a review in the context of tissue engineering. Tissue Eng, 9: 667-677.
38. Inoue H (1981) Three-dimensional architecture of lumbar intervertebral discs, Spine, 6: 139-146.

39. Kawaguchi Y, Osada R, Kanamori M, Ishihara H, Ohmori K, Matsui H, Kimura T (1999) Association between an aggrecan gene polymorphism and lumbar disc degeneration, Spine, 24, 2456-2460.
40. Kokubo Y, Uchida K, Kobayashi S, Yayama T, Sato R, Nakajima H, Takamura T, Mwaka E, Orwotho N, Bangirana A, Baba H (2008) Herniated and spondylotic intervertebral discs of the human cervical spine: histological and immunohistological findings in 500 en bloc surgical samples. Laboratory investigation, J Neurosurg Spine, 9: 285-295.
41. Liebscher T, Haefeli M, Wuertz K, Nerlich AG, Boos N (2011) Age-related variation in cell density of human lumbar intervertebral disc, Spine (Phila Pa 1976), 36: 153-159.
42. Marchand F, Ahmed AM (1990) Investigation of the laminate structure of lumbar disc annulus fibrosus, Spine, 15: 402-410.
43. McMahon JA, Takada S, Zimmerman LB, Fan CM, Harland RM, McMahon AP (1998) Noggin-mediated antagonism of BMP signaling is required for growth and patterning of the neural tube and somite, Genes Dev. 12: 1438-1452.
44. Melrose J, Roberts S, Smith S, Menage J, Ghosh P (2002) Increased nerve and blood vessel ingrowth associated with proteoglycan depletion in an ovine anular lesion model of experimental disc degeneration, Spine, 27: 1278-1285.
45. Melrose J, Smith SM, Appleyard RC, Little CB (2008) Aggrecan: versican and type VI collagen are components of annular translamellar crossbridges in the intervertebral disc, Eur Spine J, 17: 314-324.
46. Millan FA, Denhez F, Kondaiah P, Akhurst RJ (1991) Embryonic gene expression patterns of TGF beta 1, beta 2 and beta 3 suggest different developmental functions in vivo, Development, 111: 131-143.
47. Minogue BM, Richardson SM, Zeef LA, Freemont AJ, Hoyland JA (2010) Characterization of the human nucleus pulposus cell phenotype and evaluation of novel

marker gene expression to define adult stem cell differentiation, Arthritis Rheum, 62: 3695-3705.

48. Moore RJ (2006) The vertebral endplate: disc degeneration, disc regeneration, Eur Spine J, Suppl 3: S333-S337.
49. Nachemson A, Lewin T, Maroudas A, Freeman MAR (1970) In vitro diffusion of dye through the endplate and the annulus fibrosus of human intervertebral discs, Acta Orthop Scand, 41: 589-607.
50. Nerlich AG, Schaaf R, Walchli B, Boos N (2007) Temporo-spatial distribution of blood vessels in human lumbar intervertebral discs, Eur Spine J, 16: 547-555.
51. O'Connell GD, Johannessen W, Vresilovic EJ, Elliott DM (2007) Human internal disc strains in axial compression measured noninvasively using magnetic resonance imaging, Spine, 32: 2860-2868.
52. Oda J, Tanaka H, Tsuzuki N (1988) Intervertebral disc changes with aging of human cervical vertebra from the neonate to the eighties. Spine, 13: 1205-1211.
53. Oki S, Matsuda Y, Shibata T, Okumura H, Desaki J (1996) Morphologic differences of the vascular buds in the vertebral endplate-scanning electron microscopic study, Spine, 21: 174–177.
54. Paassilta P, Lohiniva J, Göring HH, Perälä M, Räinä SS, Karppinen J, Hakala M, Palm T, Kröger H, Kaitila I, Vanharanta H, Ott J, Ala-Kokko L (2001) Identification of a novel common genetic risk factor for lumbar disk disease, JAMA 285: 1843-1849.
55. Dimitroulias A, Tsonidis C, Natsis K, Venizelos I, Djau SN, Tsitsopoulos P, Tsitsopoulos P (1999) An immunohistochemical study of nerve structures in the annulus fibrosus of human normal lumbar intervertebral discs, Spine, 24: 2075-2079.
56. Pearce RH, Grimmer BJ, Adams ME (1987) Degeneration and the chemical composition of the human intervertebral disc, J Orthop Res, 5: 198-205.

57. Pederson HE, Blunck CFJ, Gardner E (1956) The anatomy of lumbosacral posterior rami and meningeal branches of spinal nerves (sinu-vertebral nerves): with an experimental study of their functions, J Bone Joint Surg Am 38-A: 377–391.
58. Pelton RW, Dickinson ME, Moses HL, Hogan BL (1990) In situ hybridization analysis of TGF beta 3 RNA expression during mouse development: comparative studies with TGF beta 1 and beta 2, Development, 110: 609-620.
59. Peters H, Wilm B, Sakai N, Imai K, Maas R, Balling R (1999) Pax1 and Pax9 synergistically regulate vertebral column development, Development, 126: 5399-5408.
60. Raj PP (2008) Intervertebral disc: anatomy-physiology-pathophysiology-treatment, Pain Pract, 8: 18-44.
61. Rajpurohit R, Risbud MV, Ducheyne P, Vresilovic EJ, Shapiro IM (2002) Phenotypic characteristics of the nucleus pulposus: expression of hypoxia inducing factor-1, glucose transporter-1 and MMP-2, Cell Tissue Res, 308: 401-407.
62. Roberts S, Eisenstein SM, Menage J, Evans EH, Ashton IK (1995) Mechanoreceptors in intervertebral discs, Spine, 20: 2645-2651.
63. Roberts S, Evans H, Trivedi J, Menage J (2006) Histology and pathology of the human intervertebral disc, J Bone Joint Surg Am, 88: 10-14.
64. Roberts S, Menage J, Urban JPG (1989) Biochemical and structural properties of the cartilage end-plate and its relation to the intervertebral disc, Spine, 14, 166-174.
65. Roberts S, Urban JP, Evans H, Eisenstein SM (1996) Transport properties of the human cartilage endplate in relation to its composition and calcification, Spine, 21: 415-420.
66. Roughley PJ (2004) Biology of intervertebral disc aging and degeneration: Involvement of the extracellular matrix, Spine, 29: 2691-2699.
67. Sakai D, Nakamura Y, Nakai T, Mishima T, Kato S, Grad S, Alini M, Risbud MV, Chan D, Cheah KS, Yamamura K, Masuda K, Okano H, Ando K, Mochida J (2012) Exhaustion

of nucleus pulposus progenitor cells with ageing and degeneration of the intervertebral disc, Nat Commun, 3: 1264.

68. Schepers GE, Teasdale RD, Koopman P (2002) Twenty pairs of sox: extent, homology, and nomenclature of the mouse and human sox transcription factor gene families, Dev Cell, 3: 167-170.
69. Schmidt H, Kettler A, Heuer F, Simon U, Claes L, Wilke HJ (2007) Intradiscal pressure, shear strain, and fiber strain in the intervertebral disc under combined loading, Spine, 32: 748-755.
70. Shine KM, Simson JA, Spector M (2009) Lubricin distribution in the human intervertebral disc, J Bone Joint Surg Am, 91: 2205-2212.
71. Skórzewska A, Grzymisławska M, Bruska M, Lupicka J, Woźniak W (2013) Ossification of the vertebral column in human foetuses: histological and computed tomography studies, Folia Morphol (Warsz), 72: 230-238.
72. Smith LJ, Nerurkar NL, Choi KS, Harfe BD, Elliott DM (2011) Degeneration and regeneration of the intervertebral disc: lessons from development. Dis Model Mech, 4: 31-41.
73. Smith CA, Tuan RS (1994) Human PAX gene expression and development of the vertebral column, Clin Orthop Relat Res, 302: 241-250.
74. Smits P, Lefebvre V (2003) Sox5 and Sox6 are required for notochord extracellular matrix sheath formation, notochord cell survival and development of the nucleus pulposus of intervertebral discs, Development, 130: 1135-1148.
75. Stemple DL (2005) Structure and function of the notochord: an essential organ for chordate development, Development, 132: 2503-2512.

76. Suseki K, Takahashi Y, Takahashi K, Chiba T, Yamagata M, Moriya H (1998) Sensory nerve fibers from lumbar intervertebral discs pass through rami communicantes, J Bone Joint Surg, 80-B: 737-742.
77. Takahasi Y, Ohtori S, Takahashi K (2009) Peripheral nerve pathways of afferent fibers innervating the lumbar spine in rats, J Pain, 10: 416-425.
78. Taylor JR, Twomey LT (1988) Growth of human intervertebral discs and vertebral bodies, J Anat, 120: 49-68.
79. Urban JP, Roberts S (2003) Degeneration of the intervertebral disc, Arthritis Res Ther, 5: 120-130.
80. Urban JP, Smith S, Fairbank JC (2004) Nutrition of the intervertebral disc, Spine (Phila Pa 1976), 29: 2700-2709.
81. Verzijl N, DeGroot J, Thorpe SR, Bank RA, Shaw JN, Lyons TJ, Bijlsma JW, Lafeber FP, Baynes JW, TeKoppele JM (2000) Effect of collagen turnover on the accumulation of advanced glycation end products, J Biol Chem, 275: 39027-39031.
82. Videman T, Gibbons LE, Battié MC, Maravilla K, Vanninen E, Leppävuori J, Kaprio J, Peltonen L (2001) The relative roles of intragenic polymorphisms of the vitamin d receptor gene in lumbar spine degeneration and bone density. Spine, 26: E7-12.
83. Vresilovic EJ, Johannessen W, Elliott DM (2006) Disc mechanics with transendplate partial nucleotomy are not fully restored following cyclic compressive loading and unloaded recovery, J Biomech Eng, 128: 823-829.
84. Wallace AL, Wyatt BC, McCarthy ID, Hughes SPF (1994) Humoral regulation of blood flow in the vertebral endplate, Spine, 19: 1324-1328.
85. Watanabe H, Yamada Y, Kimata K (1998) Roles of aggrecan, a large chondroitin sulfate proteoglycan, in cartilage structure and function, J Biochem (Tokyo), 124: 687-693.

86. Weiler C, Nerlich AG, Zipperer J, Bachmeier BE, Boos N (2002) SSE Award Competition in Basic Sciences: expression of major matrix metalloproteinases is associated with intervertebral disc degeneration and resorption, Eur Spine J, 11: 308-320.
87. Whalen JL, Parke WW, Mazur JM, Stauffer ES (1985) The intrinsic vasculature of developing vertebral end plates and its nutritive significance to the intervertebral discs. J Pediatr Orthop, 5: 403-410.
88. Wiberg G (1947) Back pain in relation to the nerve supply of the intervertebral discs, Acta Orthop Scand, 19: 211-221.
89. Yu J, Fairbank JC, Roberts S, Urban JP (2005) The elastic fibre network of the annulus fibrosus of the normal and scoliotic human intervertebral disc, Spine, 30: 1815-1820.

Figures

Figure 1. Location and structure of the human intervertebral disc on (A) an axial section of the spine and (B) on a cut out portion of the disc.

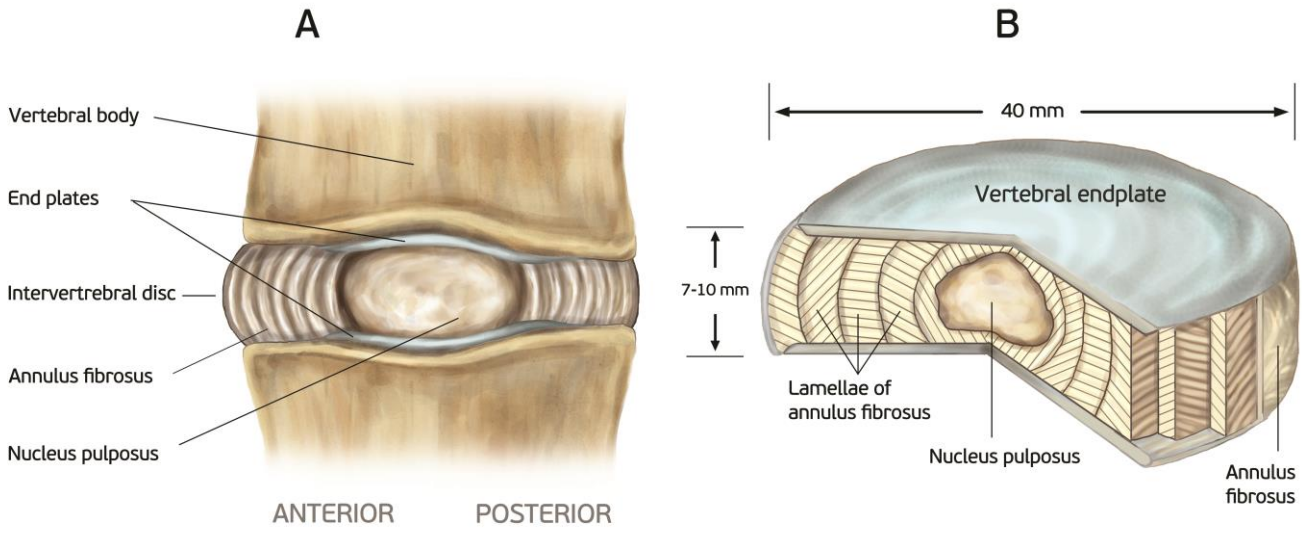

Note the organization of annulus fibrosus lamellae.

Figure 2. Schematic representation of embryonic morphogenesis of the mammalian intervertebral disc.

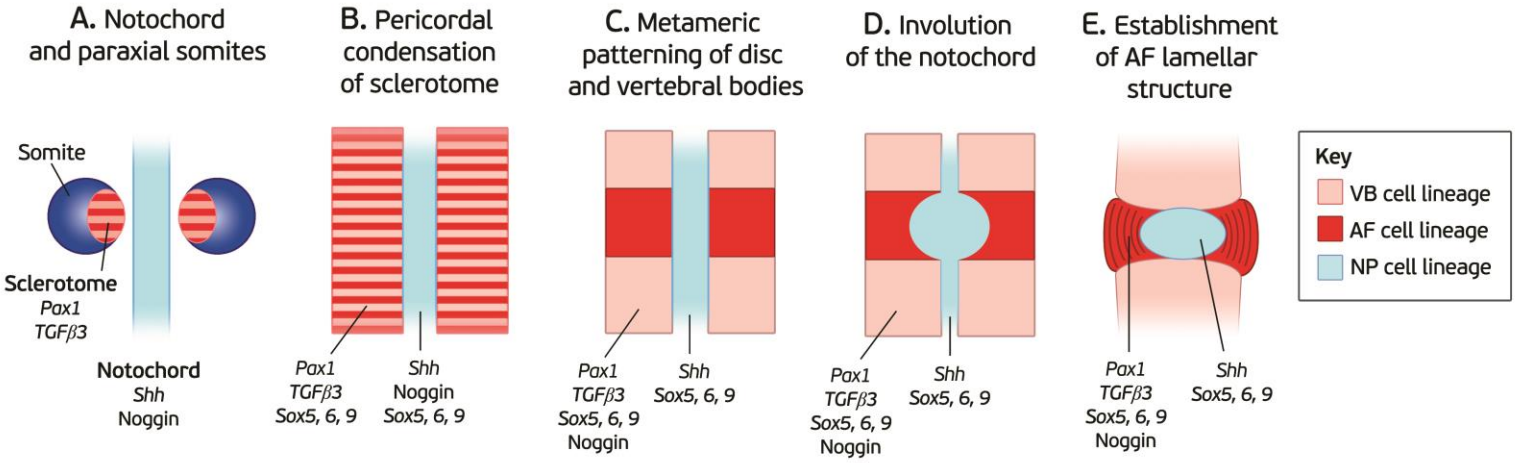

Colors represent origins and fates of cell populations. Also indicated are key morphogens and transcriptional regulators implicated in the growth and differentiation of the disc structures at each developmental stage.

(A) The notochord adjacent to pairs of paraxial somites, which contain sclerotome cells.

(B) Sclerotome cells condense around the notochord.

(C) Cells adopt a metameric pattern of more condensed (red) and less condensed (pink) regions that give rise to the disc and vertebral bodies, respectively.

(D) The notochord contracts within the vertebral body rudiments and expands within the future intervertebral disc to form the nucleus pulposus.

(E) Basic structures of the disc are established, and annulus fibrosus cells adopt orientations and alignments that form the template for the lamellar structure.

VB – vertebral body; AF – annulus fibrosus; NP – nucleus pulposus.

Figure adapted from Smith et al. [72].

Figure 3. Histological slide (midsagittal section at the level of the nucleus pulposus) showing (A) vertebral bone marrow, (B) cartilaginous endplate, (C) nucleus pulposus.

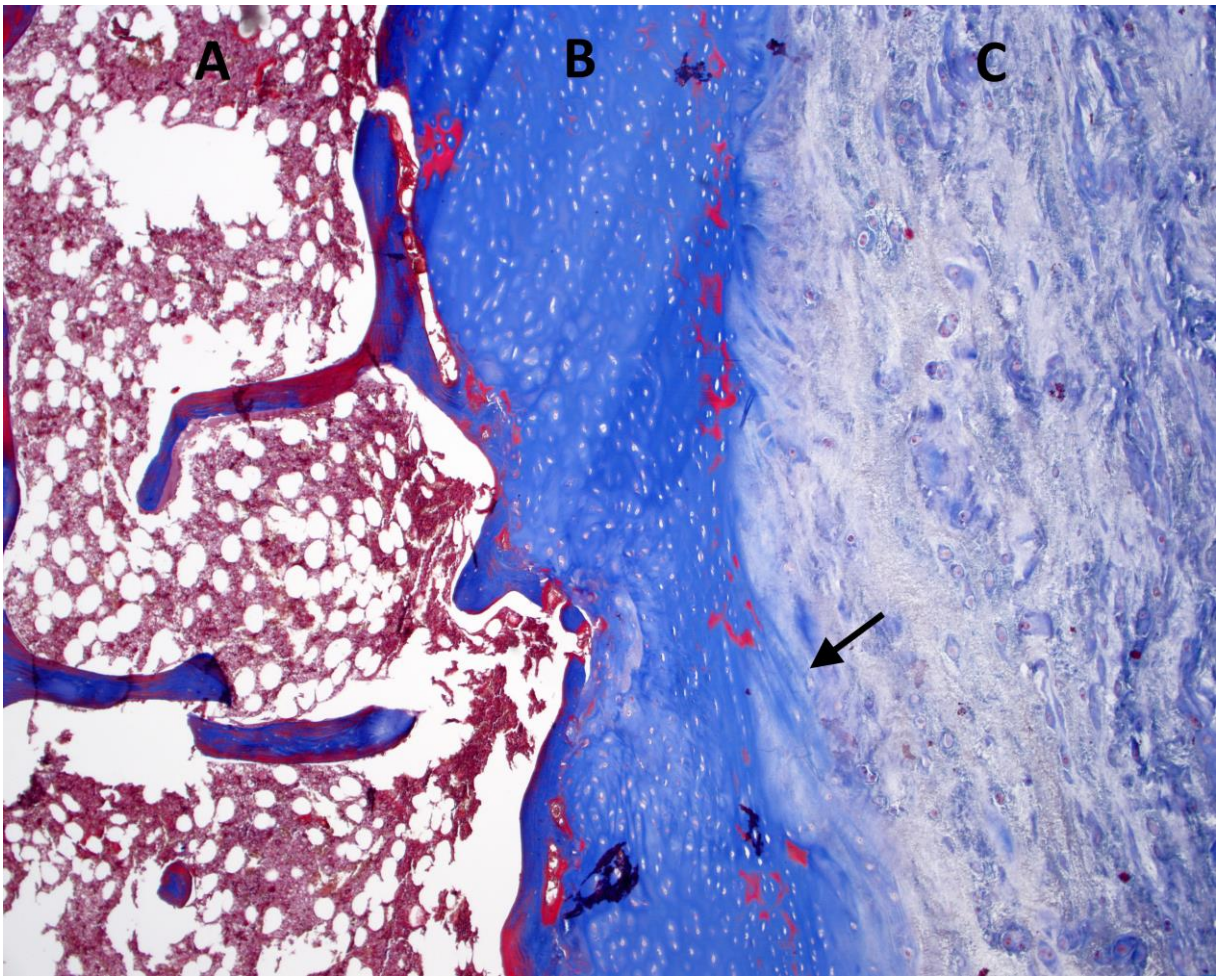

The arrow points to endplate fibers continuing into the intervertebral disc. Red color in the region of the endplate represents calcifications. Masson-Goldner trichrome staining, magnification 200x.

Figure 4. Changes in intervertebral disc and endplate structure due to endplate calcification, fall in nutrient transport and resulting degeneration.

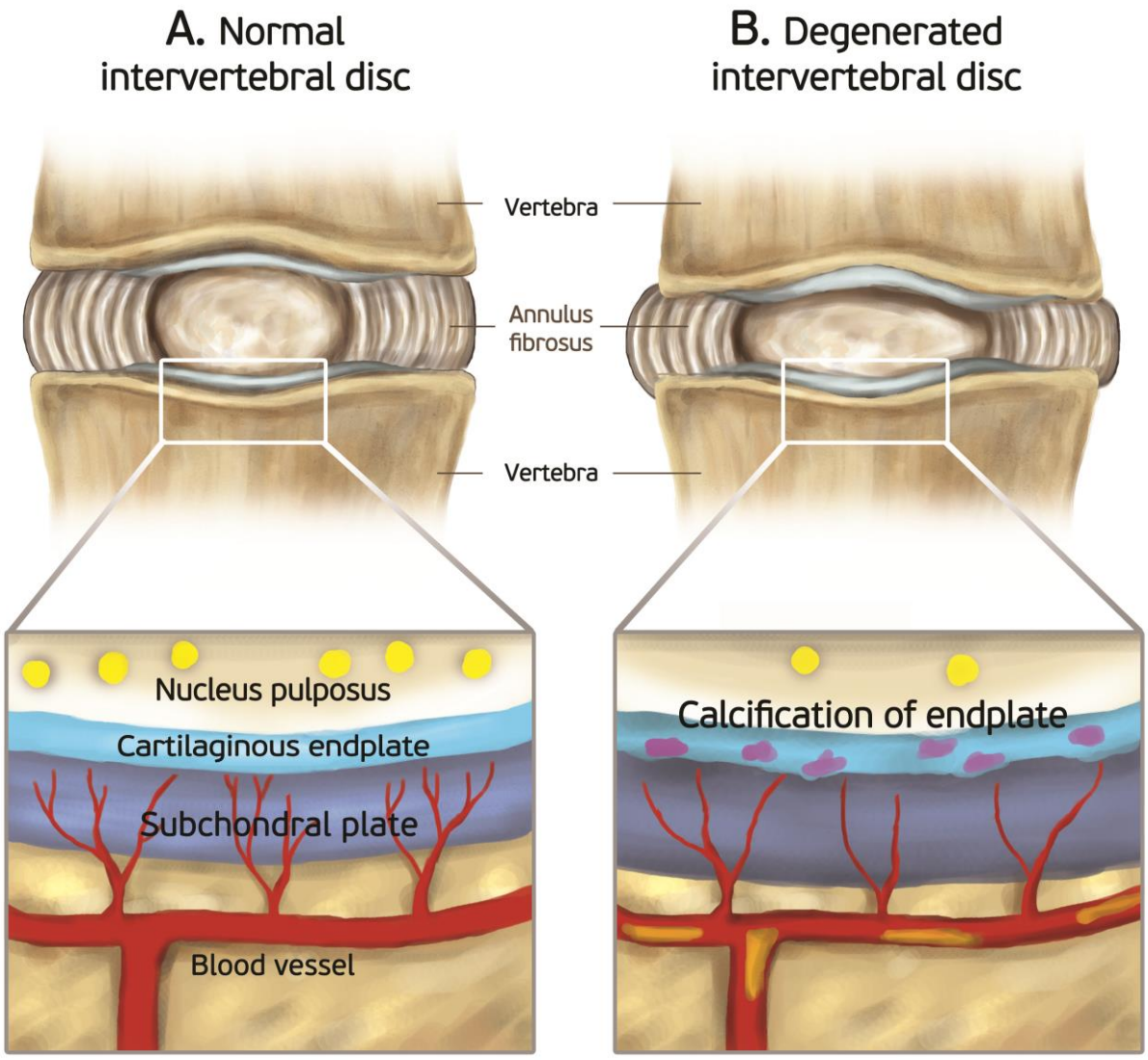

(A) Normal intervertebral disc – note the high number of patent blood vessels penetrating the endplate but not entering into the disc, and the high number of nucleus pulposus cells.

(B) Degenerated intervertebral disc – note the presence of calcifications in the blood vessels, a fall in their number, as well as calcification of the endplate, and a fall in the number of nucleus pulposus cells.

Figure 5. Physiological routes of nutrient supply to the intervertebral disc.

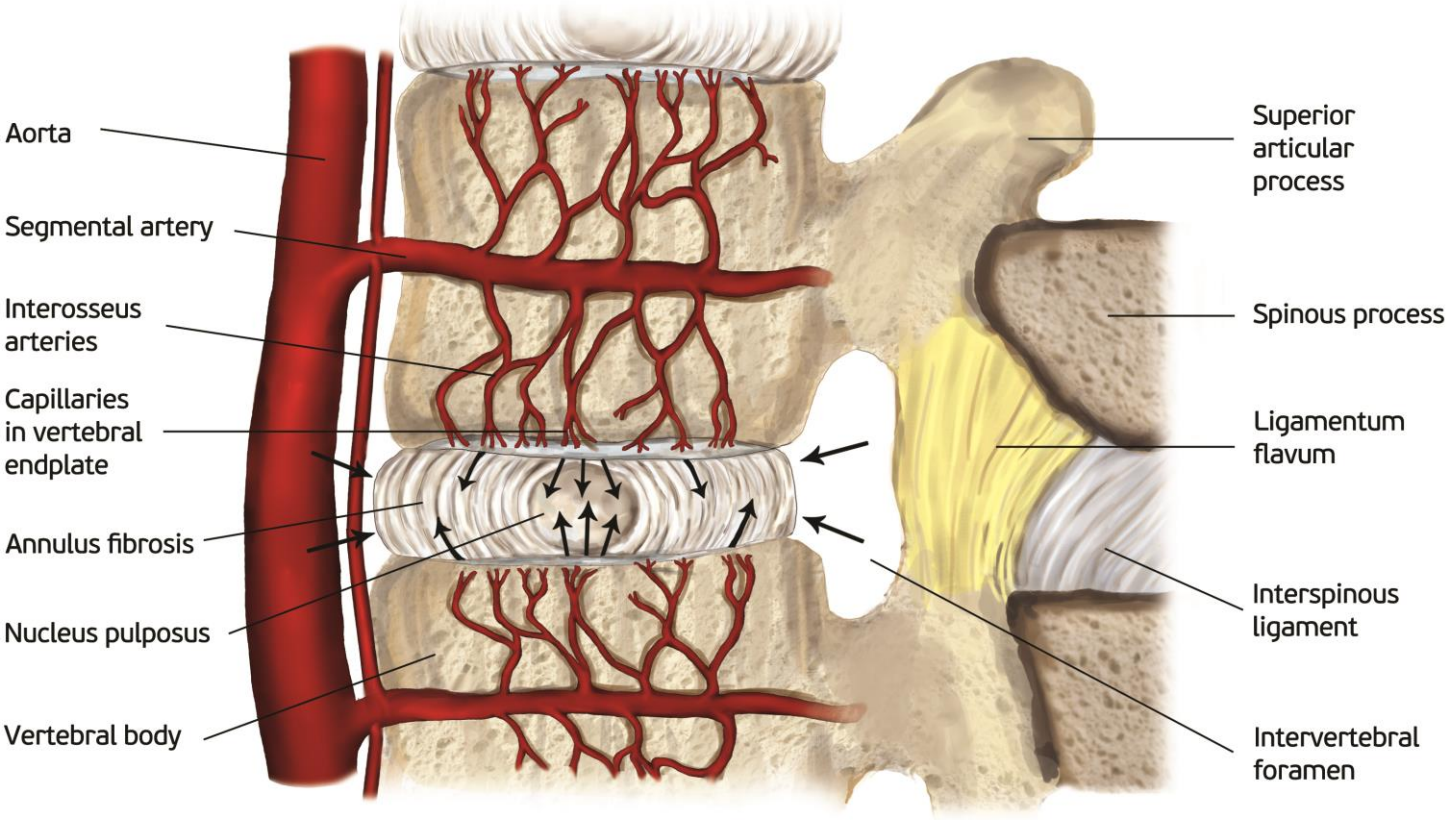

The arrows point to the routes via which nutrients are delivered to the intervertebral disc – via the endplates as well as through the outer annulus fibrosus (in both cases nutrients are delivered through diffusion).

Figure 6. Schematic representation of the innervation of the intervertebral disc.

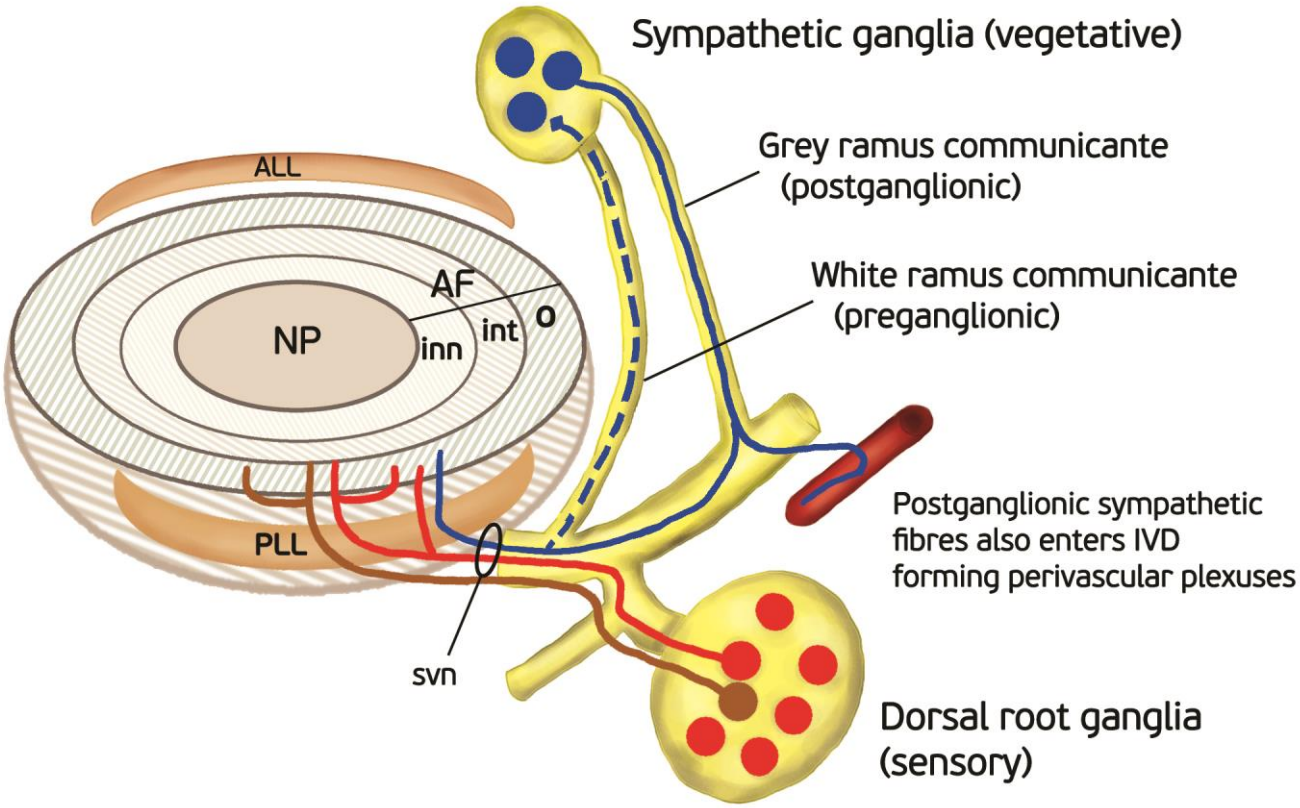

Nociceptive sensory fibers originating in the dorsal root ganglia (red) and postganglionic sensory nerve fibers (blue) enter the outer part of the annulus fibrosus. Nerves in the intervertebral disc arise from the sinuvertebral nerve, from spinal nerves or from grey rami communicantes. In addition, mechanical nerve fibers originate in the dorsal root ganglia and coming from the anterior and posterior longitudinal ligament innervate the external layers of the annulus fibrosus of the intervertebral disc.

All – anterior longitudinal ligament; PLL – posterior longitudinal ligament; NP – nucleus pulposus; AF – annulus fibrosus; inn – inner; int – intermediate; o – outer; svn – sinuvertebral nerve; IVD – intervertebral disc.

Figure adapted from García-Cosamalón et al. [29].

Figure 7. Schematic representation of the innervation of normal (A) and degenerated (B) intervertebral discs, as well as the origin of sensory nerve fibers that innervate them.

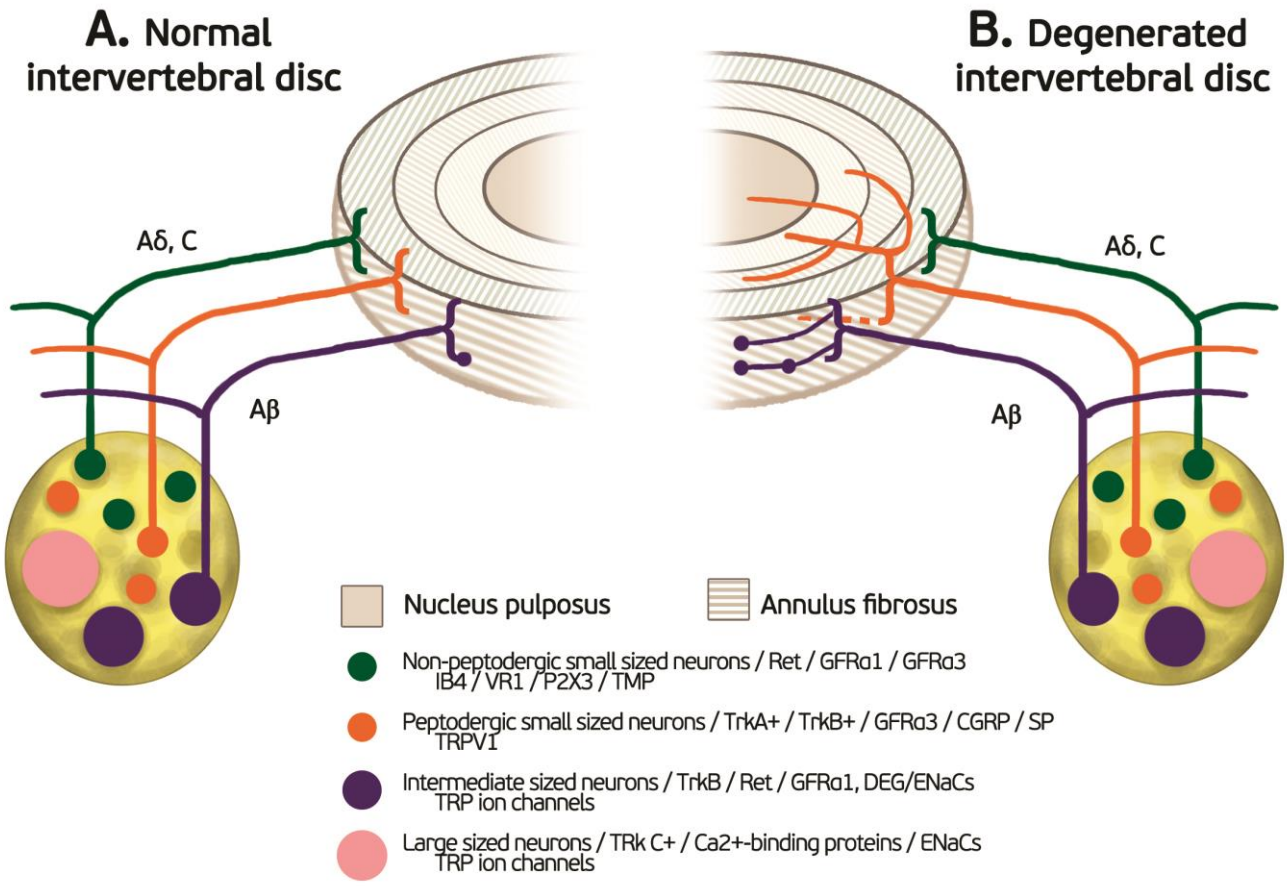

In the normal intervertebral disc, innervation is restricted to the outer layers of the annulus fibrosus and consists of small nerve fibers (orange and green) and some large fibers forming mechanoreceptors (purple).

In the degenerated intervertebral disc, nerve fibers are higher in number and they enter the inner layers of the annulus fibrosus and even the nucleus pulposus. Furthermore, in these conditions, the density of mechanoreceptors in the superficial layers of intervertebral disc are increased.

Dorsal root ganglia contain different types of sensory neurons that project to the intervertebral disx and to the dorsal horn of the spinal cord. Thin myelinated Ad fibers and unmyelinated C fibers arise from small neurons (orange and green), which, in the spinal cord, synapse in

lamina I and II and mediate nociception. The myelinated Ab fibers (purple) arise from intermediate neurons. At the periphery they form slowly and rapidly adapting low-threshold mechanoreceptors, and synapse in lamina III and IV in the dorsal horn of the spinal cord. They mediate sensations of touch, pressure and vibration. Most of the sensory nerve fibers innervating the intervertebral disc are Ad or C fibers. They originate from small peptidergic neurons expressing TrkA ⁄ TrkB (the receptor for nerve growth factor/brain-derived neurotrophic factor; orange) or non-peptidergic neurons expressing the common signaling receptor for glial cell-derived neurotrophic factor family of neurotrophic factors (Ret) (orange). Neurons in dorsal root ganglia can be differentiated based on their pattern of expression of receptors for neurotrophic factors, pattern of expression of different ion channels primarily of the degenerin ⁄ epithelial sodium channels (DEG ⁄ ENaCs) (ENaCa, b and c; acid-sensing ion channel (ASIC)1, ASIC2 and ASIC3) and transient receptor potential (TRP) (TRPA1, TRPC1, TRPC6 and TRPV1-4) families, and peptide content.

CGRP - calcitonin gene-related peptide; GFRa1 and GFRa3 - glial cell-line-derived neurotrophic receptor subtypes a1 and a3; P2X3 - ATP-gated ion channel subtype P2X3; SP - substance P; TMP - thiamine monophosphatase; VR1 - vanilloid receptor subtype 1.

Figure adapted from García-Cosamalón et al. [29].

Figure 8. Intervertebral disc "compression-coping" mechanisms.

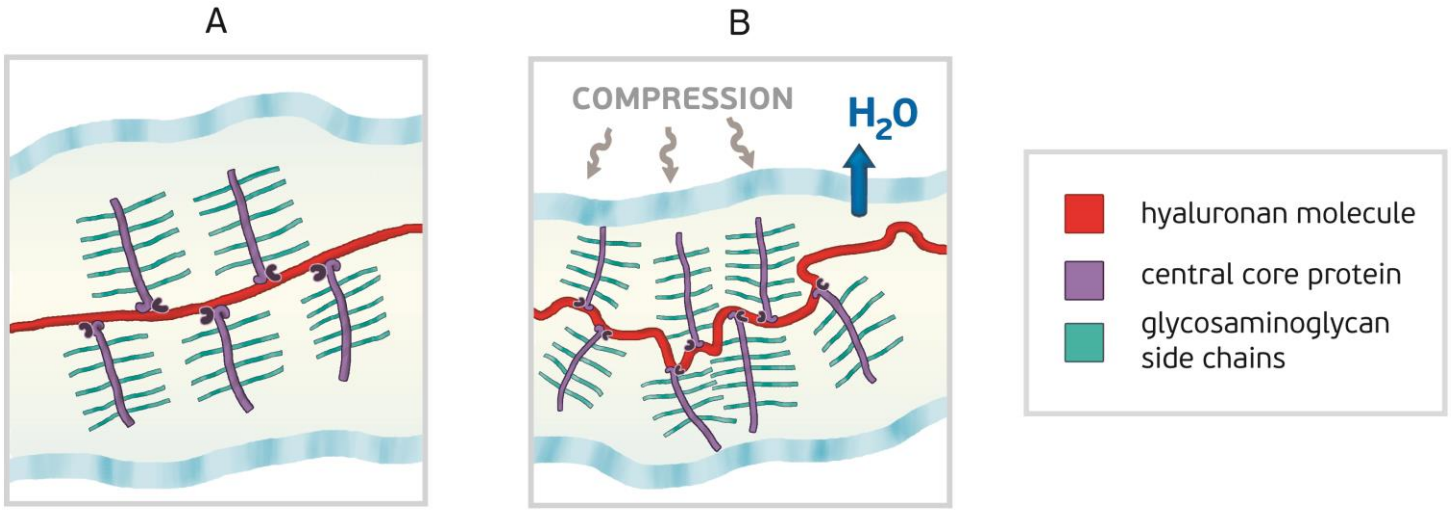

The nucleus pulposus is depicted as containing proteoglycan aggregates entrapped in a collagen fiber network. Proteoglycan aggregates are depicted as a central hyaluronan molecule (red) substituted with aggrecan molecules possessing a central core protein (purple) and sulfated glycosaminoglycan side chains (light green).

(A) State of equilibrium – nucleus pulposus is rich in water due to the high anionic glycosaminoglycan content. This is balanced by tensile forces in the collagen network.

(B) Compressive forces transmitted through the spine to the intervertebral disc lead to part of the water being forced out of the intervertebral disc. This increases aggrecan concentration and subsequently intervertebral disc swelling potential, thus resisting further compression.

On removal of the compressive load, disc height is restored as water is drawn back into the tissue to restore the original equilibrium conditions. Any parameter that decreases proteoglycan concentration or weakens the collagen network will be detrimental to disc function.

5. Artykuł numer 2

Tomaszewski KA, Walocha JA, Mizia E, Gładysz T, Głowacki R, Tomaszewska R. Age- and degeneration-related variations in cell density and glycosaminoglycan content in the human cervical intervertebral disc and its endplates. Polish Journal of Pathology 2014

Table of Contents

Age- and degeneration-related variations in cell density and glycosaminoglycan content in the human cervical intervertebral disc and its endplates

Krzysztof A. Tomaszewski[1], Jerzy A. Walocha[1], Ewa Mizia[1], Tomasz Gładysz[1,2], Roman Głowacki[3], Romana Tomaszewska[4]

[1]Department of Anatomy, Jagiellonian University Medical College, Krakow, Poland

[2]Department of Oral Surgery, Institute of Dentistry, Jagiellonian University Medical College, Krakow, Poland

[3]Department of Otorhinolaryngology, Ludwik Rydygier Specialistic Hospital, Krakow, Poland

[4]Department of Pathology, Jagiellonian University Medical College, Krakow, Poland

Running title: IVD cellularity and GAG content variations

Corresponding author

Krzysztof A. Tomaszewski

Department of Anatomy, Jagiellonian University Medical College

12 Kopernika street, 31-034 Krakow, Poland

Tel./fax. +48-12-422-95-11

e-mail: krtomaszewski@gmail.com

Abstract

The first aim of this study was to quantify cell density in cervical intervertebral discs (IVDs) and endplates of varying age and degeneration grade. The second aim was to analyze glycosaminoglycan (GAG) content in cervical IVDs and their endplates.

Sixty cervical IVDs were excised from 30 human cadavers, not later than 24 hours post-mortem. Each sample underwent sectioning. Half of each sample underwent GAG content analysis using the dimethylmethylene blue binding assay. The other half underwent histological processing, histological degeneration grading, and cell density assessment using the Abercrombie method.

The nucleus pulposus (NP) (4218±417 cells/mm^3) had significantly higher cell density than the anterior annulus fibrosus (AF) (3283±438 cells/mm^3; $p<0.0001$), and similar cell density (4464±551 cells/mm^3; $p=0.36$) to the posterior AF. Cell density was similar throughout the different regions of the endplate. The NP (619±178 μg/mg dry weight) had a significantly higher GAG content than both the anterior (428±199 μg/mg dry weight; $p<0.0001$), and posterior AF (524±218 μg/mg dry weight; $p<0.0001$).

Concluding, this study introduces detailed 3D maps of cervical IVD and endplate cell density and GAG content. Furthermore, it shows that cervical IVDs and their endplates only slightly differ, in terms of cell density and GAG content, from lumbar IVDs.

Keywords: cell density; degeneration; endplate; glycosaminoglycans; intervertebral disc.

Introduction

The intervertebral discs (IVD) are cylindrical in shape, fibrocartilaginous structures responsible for articulation between vertebral bodies. They allow for flexion, extension, and rotation of the otherwise rigid anterior portion of the vertebral column [1]. Macroscopically the IVD can be divided into an outer annulus fibrosus (AF) which surrounds a centrally located nucleus pulposus (NP). This "two-compartment" structure allows the IVD to successfully function as a loadbearing unit [2]. The IVD is bordered, from the cranial and caudal sides by the endplates, which possess an osseous as well as a hyaline cartilage component [3]. One of their main roles is to prevent the highly hydrated NP from bulging into the adjacent vertebrae.

With ageing the IVD undergoes changes, both in terms of its extracellular matrix composition, as well as cell density and character [4, 5]. Since early childhood, the blood supply to the IVD and the endplates decreases [6], together with cell density [7], leading to an increased incidence of structural defects. Since IVD cells are responsible for matrix formation and maintenance, their proper quantity, quality, and distribution in the regional compartments of the IVD may be crucial in preventing degeneration. However, changes in cell density with ageing thus far have only been shown in lumbar IVDs [7, 8]. Recent years have brought about new treatment modalities for disc degenerative disease (DDD) – these include autologous or allogeneic cell transplantation [7, 9, 10], mesenchymal stem cell transfer [11], and genetically modified cell transformation. However, for these treatments to be effective one would have to know the cell density baseline values which can be expected when treating individuals of certain age and level of IVD degeneration. The current literature lacks information on cell density age- and degeneration-related changes in human cervical IVDs and endplates. As a result the number of cells implanted into IVDs, in various animal experiments, varies

significantly [9-11]. This points out the need to establish cell density values in regard to patient age and IVD degeneration. Such knowledge would allow future cell-based therapies to deliver adequate numbers of cells with each treatment.

The correct spatial distribution of proteoglycans (with glycosaminoglycan chains – GAG) in the IVD is crucial for the discs' physiological swelling behaviors, streaming potential, and compressive properties [12]. During IVD degeneration, proteolytic fragmentation of large and small proteoglycans may induce or inhibit essential inflammatory response pathways altering the ability of the extracellular matrix to maintain its structural integrity [13, 14]. Loss of proteoglycans in the NP is a clear sign of early IVD degeneration [15]. Thus far several studies have investigated the distribution of sulfated GAGs in lumbar IVDs, both in the sagittal [16], as well as coronal and axial [17] directions. However no such study has been performed in cervical IVDs. As IVD degeneration is driven partially by aging [14], it is not easy to separate changes that are a consequence of aging itself from those that develop because of tissue degeneration and the accompanying repair process. Additional research is needed to determine how age and degeneration influence IVD and endplate extracellular matrix composition.

The first aim of this study was to quantify cell density in cervical IVDs and endplates of varying age and degeneration grade to produce cell density maps, which would provide a knowledge base for future cell based therapies for cervical DDD. As IVD cells are directly responsible for proteoglycan production, the second aim of the study was to analyze GAG content in cervical IVDs and their endplates. This part of the study aimed at providing additional insight into IVD and endplate physiology and pathology, and was meant to supply data for future computer modelling of IVD behavior.

Materials and Methods

Material acquisition

Sixty cervical IVDs were excised from 30 human cadavers (at the Department of Forensic Medicine, Jagiellonian University Medical College), using the anterior approach, not later than 24 hours post-mortem [18]. The material was excised in one block comprising vertebral bodies, IVDs, endplates and blood vessels supplying these structure, wrapped in saline soaked gauze, vacuum-sealed to prevent dehydration, and kept at 4° Celsius for transport, and until further processing. Excision started at the level of the lower half of the C4 vertebra and ended at the level of the upper half of the C6 [Figure 1].

The study inclusion criterion was the ability to excise a section of the anterior spinal column (from the lower half of the C4 vertebra to the upper half of the C6), with the anterior and posterior longitudinal ligaments and blood vessels supplying the vertebrae. Study exclusion criteria were: (1) injury to the cervical spine, preventing from excising the required section; (2) previous cervical spine surgery; (3) receiving chemotherapy in the last 12 months; (4) previous radiation therapy to the perispinal region; (5) long-standing paralysis (6 or more months); (6) ankylosing spondylitis.

Material processing

On the same day each sample was unpacked from the vacuum-sealed container. Intervertebral discs were isolated by removing extraneous soft tissue and adjacent vertebrae using a scalpel/microscalpel under an operating microscope (OPMI Pico, Zeiss). Special attention was paid not to remove the cartilaginous endplates (both cranial and caudal), and leave them intact with the IVDs. To assure this a thin layer of subchondral bone was left attached to the IVD.

Each IVD was then dissected, using a custom made 3 mm x 3 mm die-cutter, in order to obtain an array of square samples spanning the sagittal direction from anterior to posterior (4-7 sections, depending on IVD size) and also spanning the coronal direction from left lateral to central to right lateral locations (5-8 sections) [17]. Additionally, IVD sections from 5 different regions (anterior, posterior, lateral, and nucleus pulposus) were further divided – first into 2 sections (sagittal plane). Then, one of the two sections was further divided into 5 sections to evaluate the distribution of GAG content in the axial direction. Material acquisition and processing are depicted in Figure 1.

Macroscopic degeneration grading and tissue processing

During die-cutting, each IVD was sectioned at the midsagittal plane, which allowed for macroscopic IVD degeneration scoring according to Thompson's 5-grade classification [19]. Grade 1 corresponds to a healthy IVD while Grade 5 represents the most severely degenerated IVD. Each specimen was assessed by two of the authors, and the grade was averaged. Next, the samples chosen for further histological analysis [Figure 1] were placed in a 10% solution of formaldehyde (pH 7.4) for a minimum of 14 days for fixing. The samples chosen for GAG content analysis were immediately processed (see below).

Macroscopic degeneration grading and histological processing

Microscopic IVD and endplate (both cranial and caudal) degeneration was assessed using the histologic degeneration score (HDS) [6]. In brief, HDS semiquantitatively scores cellular organization (cell proliferation), cleft/tear formations, granular changes, and mucoid degeneration in anterior/posterior annulus fibrosus (AF) and nucleus pulposus (NP) regions. It produces a summary score separately for the AF/NP (0-22), and the endplate (0-18).

The NP/AF scores were grouped as follows [7]: group I: 0-2; group II: 3-7; group III: 8-12; group IV: 13-17; group V: 18-22 (tissue defects, scar). The EP scores were grouped as follows: group I: 0-2; group II: 3-5; group III: 6-9; group IV: 10-12; group V: 13-18 (tissue defects, scar, ossification). Group V did not encompass normal disc tissue and thus was not included in the calculation of cell density.

Tissue samples were acquired from the midsagittal and midcoronal planes of each of the IVD regions [Figure 1]. Fixed samples were decalcified, dehydrated, embedded in paraffin, sectioned midsagittaly at 4 μm, and stained with haematoxylin and eosin (H&E), Masson-Goldner trichrome and alcian blue-PAS (Department of Pathology, Jagiellonian University Medical College). Each sample was assessed and scored, using light microscopy (Nikon Eclipse 80i), by two observers, and the final score per sample was averaged [20].

Additional horizontal sections, of each sample, were prepared in the same manner with H&E staining to determine the calculated cell density using the Abercrombie method [7, 21]. Each sample was photographed and analyzed using Java ImageJ (developed by Wayne Rasband) [22].

The degree of endplate calcification was analyzed as the percentage of calcified tissue (red on Masson-Goldner trichrom staining) to the non-calcified part. The fact of endplate calcification was verified on corresponding H&E stained samples. The percentage of calcification was averaged for all examined endplate regions.

Cell density analysis and cell nucleus correction factor

A morphometric analysis was performed to determine the cell number per analyzed region [Figure 1] of IVD and EP, using sagittal slices. All measurements were performed using a light microscope (Nikon Eclipse 80i) with an ocular grid (10x10 fields). The number of cell nuclei were counted from the superior to the inferior part of the section (magnification 400x)

[7]. Twenty consecutive grids in the anterior-posterior dimension and a variable number of grids (depending on the thickness of the sample) in the superior-inferior direction were analyzed. Different cell types were distinguished based on their morphology.

As the nuclei of IVD cells are usually larger than 5 μm, they may appear in more than 1 section, which results in an overestimation of the total cell number. Abercrombie [21] developed a correction factor to determining cell density (T) including the number of nuclei (N) per area (N/mm2), the section thickness (S), and the diameter of the cell nucleus (D). Based on this method we included a correction factor of 240 to obtain the cell number per mm^3. The number of cell nuclei was counted using ImageJ software.

Measuring GAG content

After dissection [Figure 1] each sample was placed in pre-weighed vials, weighed, and lyophilized to obtain dry weights using a balance with ± 0.01 mg resolution (DV215CD, Ohaus).

Dry tissue was solubilized using proteinase K (0.5 mg/mL, Sigma Aldrich) and assayed for GAG content using the dimethylmethylene blue (DMMB) dye binding assay as previously described for disc tissue [15]. The GAG content was calculated based on a standard curve using an aqueous solution of chondroitin sulfate sodium salt from shark cartilage (chondroitin 6-sulfate, Sigma Aldrich, cat. no. C4384). All GAG content measurements were performed in duplicate, and expressed as μg/mg of dry tissue.

Statistical analysis

Statistical analysis was conducted using Statistica 10.0 (Statsoft). Elements of descriptive statistics were used (mean, standard deviation percentage distribution). Differences between groups were tested with the paired Student's t test. To assess the correlation between scores,

Pearson's correlation was used. Inter-rater reliability of the histologic assessment of cell density and the HDS was assessed using intraclass correlation coefficient (ICC). Statistical significance was set at $p<0.05$.

Ethics

The research protocol was approved by the Jagiellonian University Medical College Ethics Committee (registry number KBET/319/B/2012). The study has been performed in accordance with the ethical standards laid down in the 1964 Declaration of Helsinki and its later amendments. The specimen excision method was chosen so as not to destabilize the cadaver's spinal column.

Results

The study group comprised 30 female and 30 male IVDs. The mean age±SD of the specimens was 51.4±19.5. The basic characteristics of the study group are presented in Table 1.

Interobserver reliability

The interclass correlation coefficient for the assessment of cell density from two randomly selected midsagittal sections per Thompson degeneration grade with a total of 100 ROIs displayed a very high reliability coefficient alpha of 0.92.

Cell density in the intervertebral disc

Cell density per chosen IVD region in relation to the HDS grade is displayed in Table 2. The average cell number differed significantly between the anterior (3283±438 cells/mm^3) and posterior (4464±551 cells/mm^3) AF ($p<0.0001$). The NP (4218±417 cells/mm^3) had significantly higher cell density than the anterior AF ($p<0.0001$), and similar cell density

(p=0.36) to the posterior AF. Comparison by side of AF, showed no difference (p=0.51) between the left (4875±378 cells/mm^3) and right (4735±385 cells/mm^3) sides in terms of cell density.

The HDS negatively correlated with cell density in all of the IVD regions (r=-0.31-(-0.55); p<0.003). This correlation was strongest for the NP.

Age significantly negatively correlated with cell density only in the anterior AF (r=-0.28; p=0.009), and the NP (r=-0.37; p<0.0001). Maps of average IVD cell density for typical 20-30, 40-50, 60-70, and 80-90 year olds are shown in Figure 2A.

There were no statistical differences between sexes in terms of IVD cell density with the exception of the NP (males 3162±886 cells/mm^3 vs. females 5069±5269 cells/mm^3; p<0.001).

Cell density in the endplate

Differences in cell density between the cranial and caudal endplates were not statistically significant (p>0.05), thus the results were presented as an average value of cranial and caudal endplate cellularity.

Cell density per chosen endplate region in relation to the HDS grade is displayed in Table 3. When comparing the average cell number between the endplate region underlying the anterior (18624±1774 cells/mm^3) and posterior (18829±1569 cells/mm^3) AF no significant difference was noted (p=0.89). The endplate region underlying the NP (19744±1698 cells/mm^3) had similar cell density when compared to the anterior (p=0.39), and posterior (p=0.40) AF regions. Comparison by side of endplate region underlying the AF, showed no difference (p=0.93) between the left (18463±1543 cells/mm^3) and right (18540±1622 cells/mm^3) sides in terms of cell density.

The HDS significantly negatively correlated with cell density in all of the endplate regions (r=-0.72-(-0.77); p<0.0001). This correlation was strongest for the region underlying the posterior AF.

Age significantly negatively correlated with cell density in all of the endplate regions (r=-0.44-(-0.53); p<0.0001), and was strongest for the region underlying the anterior AF (r=-0.53; p<0.0001). Maps of average endplate cell density for typical 20-30, 40-50, 60-70, and 80-90 year olds are shown in Figure 2B.

Endplate calcification strongly negatively correlated with cell density in the endplate (r=-0.51-(-0.56); p<0.0001).

There were no statistical differences between sexes in terms of endplate cell density for all analyzed regions (p>0.05).

Glycosaminoglycan content in the intervertebral disc

Glycosaminoglycan content per chosen IVD region in relation to the HDS grade is displayed in Table 4. When comparing the average GAG content between the anterior (428±199 μg/mg dry weight) and posterior (524±218 μg/mg dry weight) AF a significant difference was noted (p<0.001). The NP (619±178 μg/mg dry weight) had a significantly higher GAG content than both the anterior (p<0.0001), and posterior AF (p<0.0001). Comparison by side of AF, showed no difference (p=0.63) between the left (479±201 μg/mg dry weight) and right (470±192 μg/mg dry weight) sides in terms of GAG content.

The HDS negatively correlated with GAG content in all of the IVD regions (r=-0.47-(-0.71); p<0.0001). This correlation was strongest for the NP.

Age significantly negatively correlated with GAG content in all of the IVD regions (r=-0.60-(-0.90); p<0.0001), and was strongest for the region of the NP. Maps of average IVD GAG content for typical 20-30, 40-50, 60-70, and 80-90 year olds are shown in Figure 3A.

There were no statistical differences between sexes in terms of GAG content in any of the IVD regions ($p>0.05$).

Glycosaminoglycan content in the endplate

Differences in GAG content between the cranial and caudal endplates were not statistically significant ($p>0.05$), thus the results were presented as an average value of cranial and caudal endplate GAG content.

Glycosaminoglycan content per chosen endplate region in relation to the HDS grade is displayed in Table 5. When comparing the average GAG content between the endplate region underlying the anterior (169±52 μg/mg dry weight) and posterior (192±57 μg/mg dry weight) AF a significant difference was noted ($p<0.0001$). The endplate region underlying the NP (209±58 μg/mg dry weight) had significantly higher GAG content than the anterior ($p<0.0001$), and posterior ($p<0.0001$) AF regions. Comparison by side of endplate region underlying the AF, showed no difference ($p=0.84$) between the left (199±56 cells/mm^3) and right (200±57 μg/mg dry weight) sides in terms of GAG content.

The HDS significantly negatively correlated with GAG content in all of the endplate regions ($r=-0.57$-(-0.64); $p<0.0001$),. The correlation was strongest for the region underlying the NP.

Age significantly negatively correlated with GAG content in all of the endplate regions ($r=-0.82$-(-0.88); $p<0.0001$), and was strongest for the regions underlying the left and right AF. Maps of average endplate GAG content for typical 20-30, 40-50, 60-70, and 80-90 year olds are shown in Figure 3B.

Endplate calcification strongly negatively correlated with cell density of the endplate ($r=-0.58$-(-0.68); $p<0.0001$).

There were no statistical differences between sexes in terms of endplate GAG content for all analyzed regions ($p>0.05$).

Figure 4 shows IVD GAG content variation in the axial direction in regards to HDS grade.

Cell density and glycosaminoglycan content correlations in the intervertebral disc and the endplates

Weak correlations existed between IVD cell density, and cell density in corresponding EP regions ($r=0.25$-0.33; $p<0.01$). This was not true only for the NP ($p>0.05$).

Cell density in the IVD weakly correlated with IVD GAG content ($r=0.30$-0.37; $p>0.03$) only in the NP regions. In the endplate no correlations were found between cell density and GAG content in the region underlying the NP. However moderate correlations between GAG content and cell density were found in endplate regions underlying the right and left sides of the inner AF ($r=0.39=0.48$; $p<0.01$), and in the regions underlying the anterior ($r=0.37$; $p<0.02$), and posterior outer AF ($r=0.39$; $p<0.01$).

Discussion

This study aimed at establishing cell density values as well as providing data on GAG content across different regions of the cervical IVD and its endplates. Recent years have seen a multitude of studies focusing on the analysis of changes in the extracellular matrix of the IVD during ageing [4-6, 12-17]. However, despite tremendous research efforts, we still lack knowledge regarding cell density and GAG content throughout the IVD. To the authors best knowledge this is the first study to analyze cell density and GAG content in cervical IVDs and their endplates.

For our study we decided to use the well validated Abercrombie method [21] of cell counting. Basing on the previous experience of Liebscher et al. [7] with using the Abercrombie method, we determined the “true” cell density in a three-dimensional space using 2-dimensional

histological sections. As IVD cells have nuclei larger than 4 μm (section thickness), the employed method prevented us from missing any nuclei during counting.

Cell density in the IVD and the endplates

Overall, taking into account the IVD, cell density was highest in the NP and gradually decreased outwards, with the anterior AF having significantly lower cell density than the posterior AF. The differences in the anterior-posterior cell density might originate from the fact that nutrient supply to the posterior part of the IVD is generally thought to be better [23]. Nerlich et al. [24] have also found that posterior vessels can be located deeper in the posterior AF in juvenile discs. In consequence, there is a small chance that some of these vessels persist, at least for a certain period of time, into adulthood. Though generally studies consider this unlikely [24]. There is still no agreement as to whether cell density decreases outwards from the NP [8] or remains constant throughout the IVD [7], as different studies present conflicting results. As this is the first study to analyze cervical IVDs, we support the theory that cell density is not homogeneous throughout the whole IVD. No significant side-related variations in cell density were noted, however this might be explained by the fact, that the IVD receives nutrients not only through the endplate but also from segmental artery branches that run along the vertebral bodies, and allow nutrients to diffuse to the IVD from its sides [25].

With progressing degeneration cell density in the IVD decreased. Age did not have a strong effect on cell density, which remained more or less constant with progressing age of the patients, with the exception of the NP and the anterior AF were cell density decreased with ageing. This finding is in line with previous studies [7] which found that the most significant decrease of IVD cell density takes place between the 3rd and 16th year of life. This period is a witness to dramatic changes occurring in the IVD, with the volume of the IVD increasing

with a simultaneous decrease in blood supply (due to vascular regression) [24]. This results in reduced diffusion rate [26] and therefore lower oxygen and glucose concentrations in the NP region, leading to a harsher cell environment [27]. This "vicious cycle" is further potentiated by endplate calcification, which impedes nutrient diffusion even more [20]. The above mentioned facts, together with age which seemingly does not correlate with a decrease in cell density, might lead us to conclude that degenerative changes cause impairment of cell function rather than their death. This finding is in line with previously reported results [7, 15, 28]. It further elucidates the fact that even though in HDS grade IV IVDs a rise in cell density can be seen, these new cells remain "inactive" and do not produce extracellular matrix elements. Thus cannot contribute to IVD regeneration. Though the overall cell density does not significantly decrease with age, Figure 2 shows that with age the spatial distribution of cells changes. Progressive loss of cells in the anterior and middle part (and not in the outer parts) of the IVD can be seen, further supporting the theory that nutrition is the key factor in preventing age- and degeneration-related IVD changes (as with endplate calcification the outer regions of the IVD tend to receive more nutrients).

Cranial and caudal endplates exhibited similar cell density and GAG content, as was also found by Rodriguez et al. [29]. The endplate presented similar cell density throughout all of its structure, in some cases "matching" IVD regions of low cell density with endplate areas of high cell density [eg. Figure 2 - A1 and B1]. As could be expected, increasing endplate calcification leads to a decrease in the number of cells. However, contrary to what we found in the IVD, in the endplate age significantly negatively correlated with endplate cell density. This finding might either stem from simple endplate calcification (which markedly progressed with age) and physical destruction of cells or suggest that IVD cells are more resistant in nature, due to the "harsher" environment [27] that is present in the IVD when compared with the endplate.

Glycosaminoglycans in the IVD and the endplates

Proteoglycan molecules within the endplate matrix are necessary for the control of solute transport and maintenance of water content throughout the IVD. Depletion of proteoglycans from the endplate cartilage is associated with loss of proteoglycans from the NP [30]. This translates further that proteoglycan loss would ultimately lead to degeneration of the IVD [31].

Similar to other studies [17] we found that the highest concentration of GAGs can be found in the region of the NP. Overall GAG content, both in the IVD and the endplates, followed cell density values. GAG production is considered a measure of IVD/endplate cell activity [29]. Interestingly sagittal and coronal variations in IVD GAG content were rather high when compared to previous studies [17]. However, this was only true for the IVD, while the endplate, regardless of donor age or IVD/endplate degeneration, had similar GAG content throughout all of its regions [Figure 3B1-4]. Axial variations in IVD GAG content were small, and resembled those from lumbar IVDs [17].

Age and HDS score significantly negatively correlated with GAG content both in the IVD and the endplate. It is well recognized that GAG content decreases with degeneration [32]. Additionally, Rodriguez et al. [29] have found that endplate porosity increases with age, while GAG content, as in our study, decreases. Collectively, the presented findings support the theory that endplate porosity increases with age, and that this may be an adaptive response to a reduction of nuclear swelling pressure. It is worth to additionally underline the fact that GAG content decreases with ageing, as this decrease might be suggestive of an age-related generalized decrease in cellular biochemical activity [14]. While it is hard to generalize the significance of this decrease, it is suggestive of a decreasing cellular response and extra-

cellular matrix production that may have a significant role in how tissue injury is managed as a consequence of ageing.

Gender did not have an influence either on cell density or GAG content in both the IVD and the endplates. This finding is in line with previous studies [7, 29].

The strong sides of this study include a large study group (one of the largest to date), a detailed histological analysis combined with a significant number of examined IVD and endplate regions in axial, coronal, and sagittal directions. To the authors best knowledge this is the first study to assess cell density and GAG content in cervical IVDs and their endplates. However, this study has also one drawback. The youngest specimen in our study came from a 19-year-old person. This precluded us from analyzing how cell density and GAG content changes during years (3-16) when the IVD and the endplates undergo the highest degree of changes.

Conclusions

Concluding, this study introduces several detailed 3D maps of cervical IVD and cervical endplate cell density and GAG content. The most important prerequisite for successful IVD cell injection in cell-based tissue engineering approaches is a clear understanding of the actual cell numbers in normal and degenerated IVDs. Knowledge from this study may partially bridge the gap on IVD cell numbers in normal and degenerated discs.

Furthermore, the results from this study show that cervical IVDs and their endplates only slightly differ, in terms of cell density and GAG content, from their lumbar counterparts.

Additionally this study provides new information characterizing GAG content distributions in the three primary directions in the IVD. This information may be helpful for future computer modelling of human IVD tissue. The data presented also points out an overall age-related trend towards decreased IVD cellular metabolic activity as manifested by decreasing concentrations of GAGs.

Conflict of Interest Statement

All authors declare that they have no conflict of interest or financial relationship to disclose.

Acknowledgements

This study was funded by the National Science Center – Poland under grant number DEC-2012/07/N/NZ5/00078, and by Jagiellonian University statutory funds for young scientists number K/DSC/002093. Krzysztof A. Tomaszewski received a scholarship to prepare his PhD thesis from the National Science Center – Poland under award number DEC-2013/08/T/NZ5/00020.

Author contribution

Design and planning of the study – KAT, JAW, RT. Sample collection – KAT, EM, TG, RG. Sample preparation – KAT, RG, RT. Histological analysis – KAT, RT. Biochemical analysis – KAT. Data interpretation – KAT, JAW, EM, RT (sample measurement and result verification), KAT (statistical analysis). Bibliographic search – KAT, TG. Drafting and revising the manuscript – KAT. Obtaining funding – KAT. Critical revision of the manuscript – JAW, RT. All authors have read and approved the final version of the manuscript.

All co-authors confirm the above-mentioned contributions and consent to the fact that this study is a part of Krzysztof A. Tomaszewski's PhD thesis. The co-authors confirm that Krzysztof A. Tomaszewski has contributed significantly (80% in total) to every part of this study, as stated above.

References

1. Roberts S, Evans H, Trivedi J, et al. Histology and pathology of the human intervertebral disc, J Bone Joint Surg Am 2006; 88: 10-14.
2. Niosi CA, Oxland TR. Degenerative mechanics of the lumbar spine. Spine J 2004; 4: 202S-208S.
3. Taylor JR, Twomey LT. Growth of human intervertebral discs and vertebral bodies. J Anat 1988; 120: 49-68.
4. Gruber HE, Hanley EN Jr. Ultrastructure of the human intervertebral disc during aging and degeneration: comparison of surgical and control specimens. Spine 2002; 27: 798-805.
5. Nerlich AG, Schleicher ED, Boos N. 1997 Volvo award winner in basic science studies. Immunohistologic markers for age-related changes of human lumbar intervertebral discs. Spine 1997; 22: 2781-2795.
6. Boos N, Weissbach S, Rohrbach H, et al. Classification of age-related changes in lumbar intervertebral discs: 2002 Volvo Award in basic science. Spine 2002; 27: 2631-2644.
7. Liebscher T, Haefeli M, Wuertz K, et al. Age-related variation in cell density of human lumbar intervertebral disc. Spine (Phila Pa 1976) 2011; 36: 153-159.
8. Hastreiter D, Ozuna RM, Spector M. Regional variations in certain cellular characteristics in human lumbar intervertebral discs, including the presence of alpha-smooth muscle actin. J Orthop Res 2001; 19: 597-604.
9. Meisel HJ, Siodla V, Ganey T, et al. Clinical experience in cell based therapeutics: disc chondrocyte transplantation a treatment for degenerated or damaged intervertebral disc. Biomol Eng 2007; 24: 5-21.

10. Gruber HE, Johnson TL, Leslie K, et al. Autologous intervertebral disc cell implantation: a model using Psammomys obesus, the sand rat. Spine 2002; 27: 1626-1633.
11. Revell PA, Damien E, Di Silvio L, et al. Tissue engineered intervertebral disc repair in the pig using injectable polymers. J Mater Sci Mater Med 2007; 18: 303-308.
12. Perie DS, Maclean JJ, Owen JP, et al. Correlating material properties with tissue composition in enzymatically digested bovine annulus fibrosus and nucleus pulposus tissue. Ann Biomed Eng 2006; 34: 769-777.
13. Cs-Szabo G, Ragasa-Sanjuan D, Turumella V. Changes in mRNA and protein levels of proteoglycans of the anulus fibrosus and nucleus pulposus during intervertebral disc degeneration. Spine 2002; 27: 2212-2219.
14. Singh K, Masuda K, Thonar EJ, et al. Age-related changes in the extracellular matrix of nucleus pulposus and anulus fibrosus of human intervertebral disc. Spine (Phila Pa 1976) 2009; 34: 10-16.
15. Antoniou J, Steffen T, Nelson F, et al. The human lumbar intervertebral disc: evidence for changes in the biosynthesis and denaturation of the extracellular matrix with growth, maturation, ageing, and degeneration. J Clin Invest 1996; 98: 996-1003.
16. Urban JPG, Maroudas A. The measurement of fixed charge density in the intervertebral disc. Biochim Biophys Acta 1979; 586: 166-178.
17. Iatridis JC, MacLean JJ, O'Brien M, et al. Measurements of proteoglycan and water content distribution in human lumbar intervertebral discs. Spine (Phila Pa 1976) 2007; 32: 1493-1497.
18. Le Maitre CL, Freemont AJ, Hoyland JA. The role of interleukin-1 in the pathogenesis of human intervertebral disc degeneration. Arthritis Res Ther 2005; 7: R732-745.

19. Thompson JP, Pearce RH, Schechter MT, et al. Preliminary evaluation of a scheme for grading the gross morphology of the human intervertebral disc. Spine 1990; 15: 411-415.
20. Tomaszewski KA, Adamek D, Pasternak A, et al. Degeneration and calcification of the cervical endplate is connected with a decreased expression of ANK, ENPP-1, OPN and TGF-β1 in the intervertebral disc. Pol J Pathol 2014; 65: 204-211.
21. Abercrombie M. Estimation of nuclear population from microtome sections. Anat Rec 1946; 94: 239-247.
22. Mizia E, Tomaszewski KA, Lis GJ, et al. The use of computer-assisted image analysis in measuring the histological structure of the human median nerve. Folia Morphol (Warsz) 2012; 71: 82-85.
23. Crock HV, Yoshizawa H. The blood supply of the lumbar vertebral column. Clin Orthop Relat Res 1976; 115: 6-21.
24. Nerlich AG, Schaaf R, Walchli B, et al. Temporospatial distribution of blood vessels in human lumbar intervertebral discs. Eur Spine J 2007; 16: 547-555.
25. Raj PP. Intervertebral disc: anatomy-physiology-pathophysiology-treatment. Pain Pract 2008; 8: 18-44.
26. Rajasekaran S, Babu JN, Arun R, et al. ISSLS prize winner: a study of diffusion in human lumbar discs: a serial magnetic resonance imaging study documenting the influence of the endplate on diffusion in normal and degenerate discs. Spine 2004; 29: 2654-2667.
27. Bibby SR, Urban JP. Effect of nutrient deprivation on the viability of intervertebral disc cells. Eur Spine J 2004; 13: 695-701.

28. Antoniou J, Goudsouzian NM, Heathfi eld TF, et al. The human lumbar endplate. Evidence of changes in biosynthesis and denaturation of the extracellular matrix with growth, maturation, aging, and degeneration. Spine 1996; 21: 1153-1161.
29. Rodriguez AG, Slichter CK, Acosta FL, et al. Human disc nucleus properties and vertebral endplate permeability. Spine (Phila Pa 1976) 2011; 36: 512-520.
30. Roberts S, Urban JP, Evans H, et al. Transport properties of the human cartilage endplate in relation to its composition and calcification. Spine 1996; 21: 415-420.
31. Pearce RH, Grimmer BJ, Adams ME. Degeneration and the chemical composition of the human intervertebral disc. J Orthop Res 1987; 5: 198-205.
32. Urban JP, McMullin JF. Swelling pressure of the lumbar intervertebral discs: influence of age, spinal level, composition, and degeneration. Spine 1988; 13: 179-187.

Tables

Table 1. Basic characteristics of the study group.

	Female (n=30)	**Male (n=30)**	**Total (n=60)**	**p-value[1]**
Age (SD)	52.8 (19.8)	50.0 (19.4)	51.4 (19.5)	0.57
IVD degeneration Thompson classification (SD)	2.6 (1.3)	3.2 (1.3)	2.9 (1.3)	0.08
IVD degeneration HDS score (0-22) (SD)	12.0 (6.1)	14.3 (5.3)	13.1 (5.8)	0.13
Endplate degeneration HDS score (0-18) (SD)	8.9 (5.3)	11.5 (4.8)	10.2 (5.2)	0.06
Endplate calcification [%] (SD)	28.4 (25.1)	44.1 (26.0)	36.2 (26.5)	0.02
IVD degeneration Thompson classification vs. degree of endplate calcification [%] (SD)				
Grade I	6.2 (2.6)	6.7 (0.6)	6.3 (2.1)	0.31
Grade II	13.2 (2.8)	17.7 (1.9)	14.8 (3.3)	<0.0001
Grade III	29.6 (8.7)	37.1 (7.3)	34.4 (8.4)	0.0006
Grade IV	53.3 (6.9)	61.6 (4.8)	57.9 (7.0)	<0.0001
Grade V	77.3 (8.5)	79.1 (2.8)	78.5 (5.2)	0.28

[1] – for differences between females and males

SD – standard deviation; IVD – intervertebral disc; HDS – histologic degeneration score.

Table 2. Cell density per intervertebral disc region in relation to the histologic grade of disc degeneration.

IVD region [cell/mm^3]	HDS I	HDS II	HDS III	HDS IV
AOA	22124 (2333)	2412 (192)	1864 (211)	2586 (179)
AIA	22549 (2058)	2484 (188)	2225 (201)	2715 (124)
AONP	22182 (2035)	3790 (727)	4007 (914)	2624 (273)
NP	21462 (3577)	3521 (715)	4481 (564)	2599 (378)
PONP	24523 (962)	3850 (824)	3654 (1141)	2805 (326)
PIA	28662 (1061)	2891 (931)	2190 (338)	5139 (798)
POA	26623 (779)	2391 (595)	1908 (359)	4454 (669)
LLOA	19184 (906)	2821 (463)	2255 (303)	5273 (1063)
LLIA	20759 (401)	4914 (674)	4106 (473)	4930 (1576)
LONP	21124 (1894)	4364 (752)	3638 (827)	2761 (247)
RONP	21199 (2741)	3718 (887)	3667 (1160)	2598 (261)
RLIA	20663 (411)	4798 (647)	3744 (522)	4699 (1571)
RLOA	19868 (840)	3001 (668)	2163 (294)	5105 (1007)
Anterior AF (averaged)	22337 (1813)	2448 (188)	2045 (273)	2651 (165)
NP (averaged)	22098 (2238)	3849 (799)	3889 (978)	2677 (307)
Posterior AF (averaged)	27642 (1401)	2641 (801)	2049 (371)	4797 (805)

Values in brackets represent standard deviations. HDS – histologic degeneration score; IVD – intervertebral disc; AOA – anterior outer annulus; AIA – anterior inner annulus; PIA – posterior inner annulus; POA – posterior outer annulus; LLOA – left lateral outer annulus; LLIA – left lateral inner annulus; RLIA – right lateral inner annulus; RLOA – right lateral outer annulus; NP – nucleus pulposus; AONP – anterior outer nucleus pulposus; PONP – posterior outer nucleus pulposus; LONP – left outer nucleus pulposus; RONP – right outer nucleus pulposus; AF – annulus fibrosus.

Table 3. Cell density per endplate region in relation to the histologic grade of endplate degeneration.

EP region [cell/mm^3]	HDS I	HDS II	HDS III	HDS IV
AOA	37252 (3408)	45174 (17896)	8925 (1438)	9538 (884)
AIA	35855 (4445)	40046 (9071)	8579 (1763)	9458 (1070)
AONP	36033 (3946)	50041 (13619)	8870 (1317)	13207 (2372)
NP	46639 (12563)	20779 (5995)	12135 (3084)	12703 (1839)
PONP	45596 (3108)	39961 (13779)	11821 (2003)	12551 (1712)
PIA	40745 (12186)	44512 (11810)	10842 (2365)	9541 (1035)
POA	35523 (12122)	27132 (5237)	12899 (2472)	9953 (959)
LLOA	35828 (8999)	40827 (11537)	10198 (2552)	9637 (1104)
LLIA	34843 (6904)	35117 (12003)	11681 (2235)	9506 (665)
LONP	47531 (6811)	45340 (11793)	12189 (3216)	13569 (2206)
RONP	46565 (7560)	41029 (8911)	12803 (3228)	12987 (2144)
RLIA	34805 (7937)	39635 (9556)	9928 (3145)	9992 (971)
RLOA	34617 (9562)	41427 (12338)	9474 (2657)	10009 (1096)
Anterior AF (averaged)	36554 (3806)	42610 (13888)	8752 (1589)	9498 (962)
NP (averaged)	44473 (8168)	39430 (14619)	11564 (2955)	13003 (2036)
Posterior AF (averaged)	38134 (11785)	35822 (12584)	11870 (2596)	9747 (1000)

Values in brackets represent standard deviations. HDS – histologic degeneration score; EP – endplate; AOA – anterior outer annulus; AIA – anterior inner annulus; PIA – posterior inner annulus; POA – posterior outer annulus; LLOA – left lateral outer annulus; LLIA – left lateral inner annulus; RLIA – right lateral inner annulus; RLOA – right lateral outer annulus; NP – nucleus pulposus; AONP – anterior outer nucleus pulposus; PONP – posterior outer nucleus pulposus; LONP – left outer nucleus pulposus; RONP – right outer nucleus pulposus; AF – annulus fibrosus.

Table 4. Glycosaminoglycan content per intervertebral disc region in relation to the histologic grade of disc degeneration.

IVD region [GAG µg/mg dry weight]	HDS I	HDS II	HDS III	HDS IV	HDS V
AOA	471 (5.0)	385 (92)	393 (88)	268 (94)	181 (48)
AIA	805 (48)	690 (149)	662 (108)	526 (172)	364 (70)
AONP	864 (20)	802 (96)	744 (135)	598 (165)	467 (90)
NP	851 (28)	754 (129)	697 (122)	550 (141)	424 (84)
PONP	908 (12)	781 (88)	745 (121)	602 (158)	485 (90)
PIA	866 (5.0)	794 (79)	774 (98)	665 (147)	529 (95)
POA	609 (13)	481 (122)	447 (107)	316 (89)	236 (92)
LLOA	543 (98)	529 (78)	480 (113)	350 (104)	225 (97)
LLIA	898 (5.0)	730 (122)	716 (121)	517 (169)	368 (95)
LONP	879 (81)	767 (163)	742 (132)	548 (142)	435 (96)
RONP	882 (45)	776 (112)	726 (157)	555 (159)	418 (89)
RLIA	841 (35)	748 (114)	679 (123)	502 (152)	362 (90)
RLOA	587 (1.4)	477 (71)	484 (102)	359 (102)	219 (99)
Anterior AF (averaged)	638 (195)	537 (198)	528 (168)	397 (190)	273 (110)
NP (averaged)	877 (39)	776 (116)	731 (132)	570 (152)	446 (91)
Posterior AF (averaged)	737 (148)	637 (189)	611 (195)	491 (214)	383 (175)

Values in brackets represent standard deviations. HDS – histologic degeneration score; IVD – intervertebral disc; GAG - glycosaminoglycans; AOA – anterior outer annulus; AIA – anterior inner annulus; PIA – posterior inner annulus; POA – posterior outer annulus; LLOA – left lateral outer annulus; LLIA – left lateral inner annulus; RLIA – right lateral inner annulus; RLOA – right lateral outer annulus; NP – nucleus pulposus; AONP – anterior outer nucleus pulposus; PONP – posterior outer nucleus pulposus; LONP – left outer nucleus pulposus; RONP – right outer nucleus pulposus; AF – annulus fibrosus.

Table 5. Glycosaminoglycan content per endplate region in relation to histologic grade of disc degeneration.

EP region [GAG µg/mg dry weight]	HDS I	HDS II	HDS III	HDS IV	HDS V
AOA	178 (37)	182 (16)	168 (31)	153 (25)	123 (25)
AIA	225 (50)	247 (31)	213 (54)	192 (52)	139 (41)
AONP	242 (31)	260 (29)	241 (46)	222 (43)	151 (44)
NP	252 (36)	254 (23)	240 (50)	224 (36)	158 (47)
PONP	245 (23)	258 (29)	236 (45)	223 (39)	157 (50)
PIA	220 (62)	244 (36)	221 (44)	191 (45)	137 (38)
POA	252 (42)	251 (37)	210 (56)	204 (46)	156 (38)
LLOA	238 (39)	251 (34)	214 (46)	195 (46)	148 (35)
LLIA	246 (51)	266 (28)	227 (50)	206 (52)	162 (43)
LONP	231 (53)	261 (31)	231 (57)	198 (55)	155 (42)
RONP	237 (52)	263 (33)	224 (53)	201 (51)	153 (37)
RLIA	250 (42)	271 (26)	227 (49)	210 (49)	155 (40)
RLOA	232 (48)	242 (27)	218 (55)	195 (49)	153 (39)
Anterior AF (averaged)	202 (48)	215 (41)	190 (49)	172 (44)	131 (35)
NP (averaged)	242 (38)	259 (27)	234 (49)	214 (46)	155 (44)
Posterior AF (averaged)	236 (53)	247 (36)	215 (50)	198 (45)	147 (39)

Values in brackets represent standard deviations. HDS – histologic degeneration score; EP – endplate; GAG - glycosaminoglycans; AOA – anterior outer annulus; AIA – anterior inner annulus; PIA – posterior inner annulus; POA – posterior outer annulus; LLOA – left lateral outer annulus; LLIA – left lateral inner annulus; RLIA – right lateral inner annulus; RLOA – right lateral outer annulus; NP – nucleus pulposus; AONP – anterior outer nucleus pulposus; PONP – posterior outer nucleus pulposus; LONP – left outer nucleus pulposus; RONP – right outer nucleus pulposus; AF – annulus fibrosus.

Figures

Figure 1. Study material acquisition and processing.

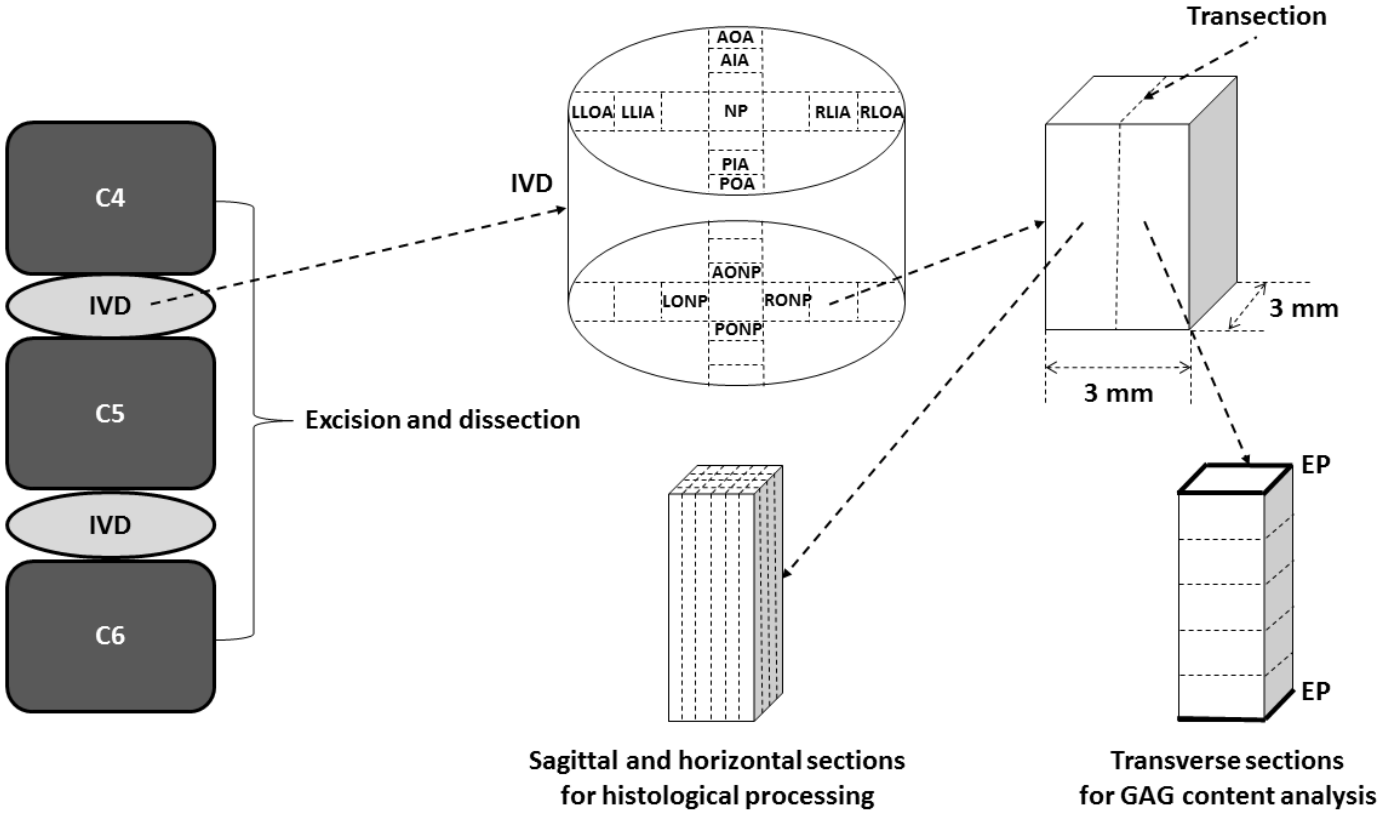

C4-C6 – fourth to sixth cervical vertebrae; IVD – intervertebral disc; AOA – anterior outer annulus; AIA – anterior inner annulus; PIA – posterior inner annulus; POA – posterior outer annulus; LLOA – left lateral outer annulus; LLIA – left lateral inner annulus; RLIA – right lateral inner annulus; RLOA – right lateral outer annulus; NP – nucleus pulposus; AONP – anterior outer nucleus pulposus; PONP – posterior outer nucleus pulposus; LONP – left outer nucleus pulposus; RONP – right outer nucleus pulposus; EP – endplate; GAG – glycosaminoglycan.

Figure 2. Three-dimensional maps of average intervertebral disc (A) and endplate (B) cell density shown for different age groups.

Please note the change in scale between different maps. Values are expressed as number of cells per mm^3.

A1 – intervertebral disc (20-30 years old); B1 – endplate (20-30 years old); A2 – intervertebral disc (40-50 years old); B2 – endplate (40-50 years old); A3 – intervertebral disc (60-70 years old); B3 – endplate (60-70 years old); A4 – intervertebral disc (80-90 years old); B5 – endplate (80-90 years old).

C - center; LI - left inner; LO - left outer; RI - right inner; RO - right outer; AO - anterior outer; AI - anterior inner; PI - posterior inner; PO - posterior outer.

Please see next page for Figure 2.

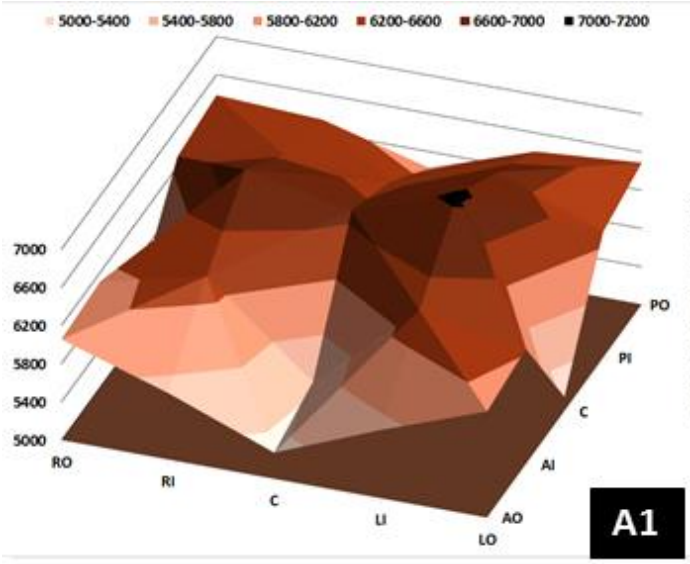
5000-5400
5400-5800
5800-6200
6200-6600
6600-7000
7000-7200
7000
6600
6200
5800
5400
5000
RO
RI
C
LI
AO
LO
AI
C
PI
PO
A1

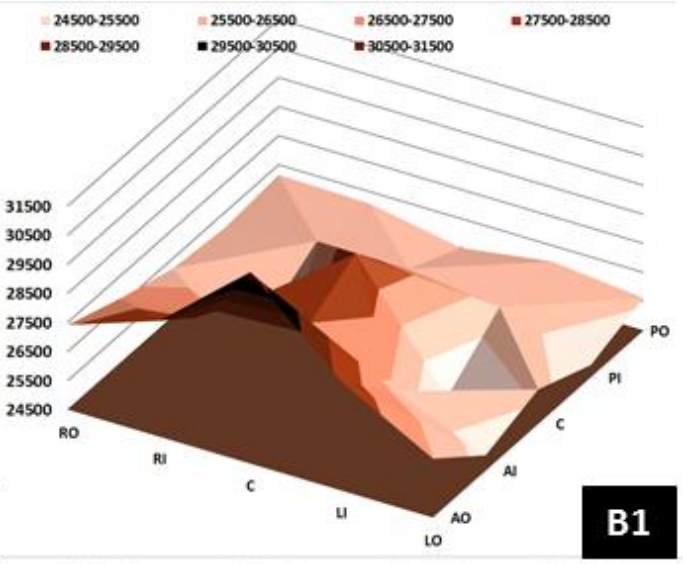
24500-25500
25500-26500
26500-27500
27500-28500
28500-29500
29500-30500
30500-31500
31500
30500
29500
28500
27500
26500
25500
24500
RO
RI
C
LI
AO
LO
AI
C
PI
PO
B1

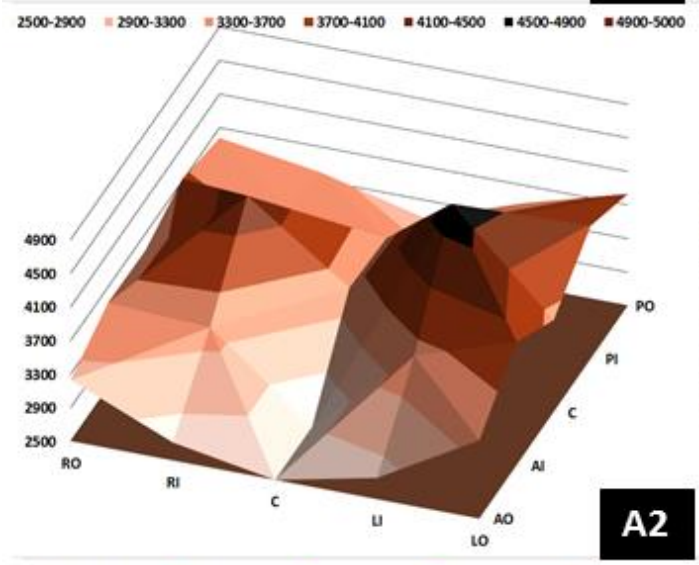
2500-2900
2900-3300
3300-3700
3700-4100
4100-4500
4500-4900
4900-5000
4900
4500
4100
3700
3300
2900
2500
RO
RI
C
LI
AO
LO
AI
C
PI
PO
A2

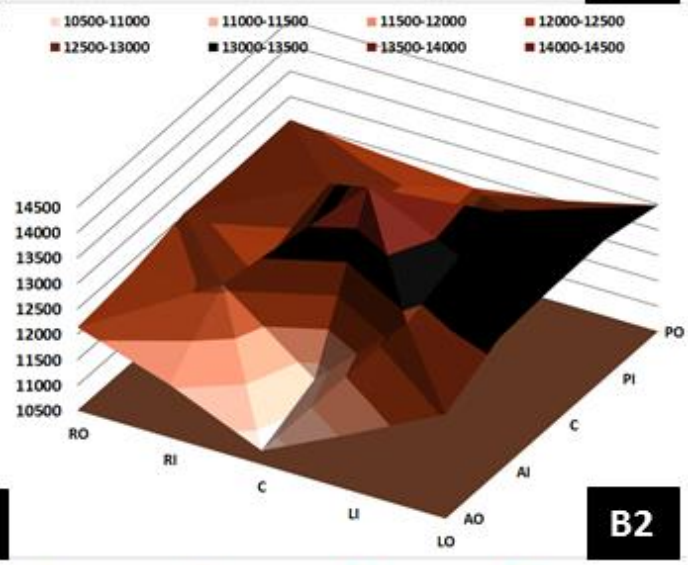
10500-11000
11000-11500
11500-12000
12000-12500
12500-13000
13000-13500
13500-14000
14000-14500
14500
14000
13500
13000
12500
12000
11500
11000
10500
RO
RI
C
LI
AO
LO
AI
C
PI
PO
B2

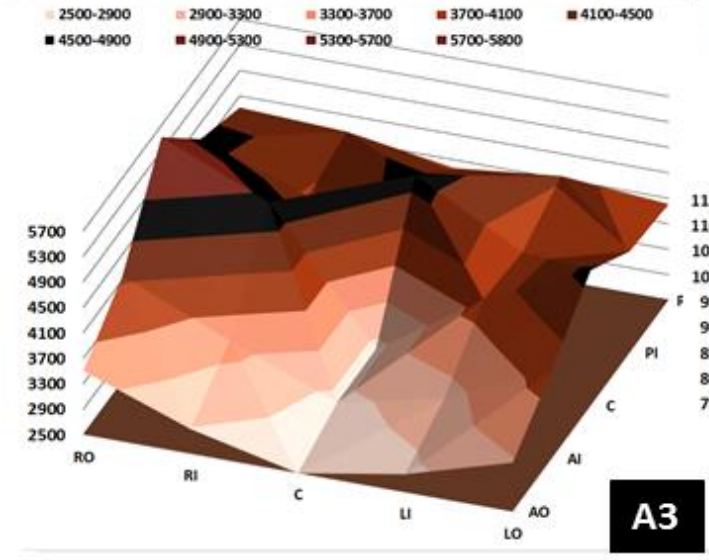
2500-2900
2900-3300
3300-3700
3700-4100
4100-4500
4500-4900
4900-5300
5300-5700
5700-5800
5700
5300
4900
4500
4100
3700
3300
2900
2500
RO
RI
C
LI
AO
LO
AI
C
PI
PO
A3

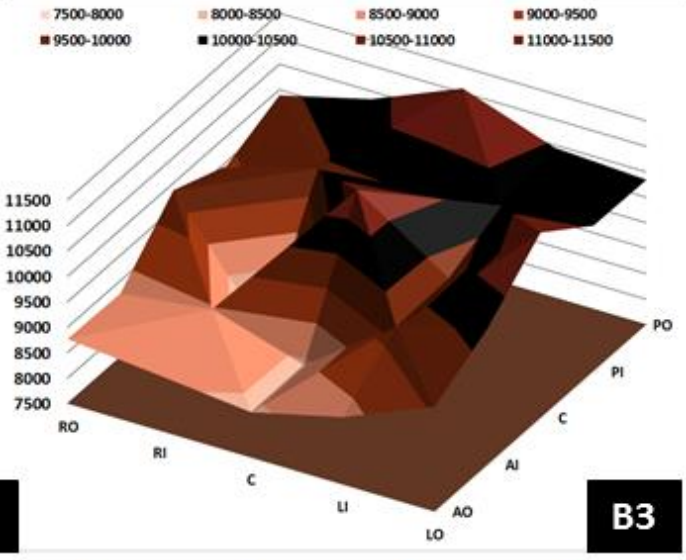
7500-8000
8000-8500
8500-9000
9000-9500
9500-10000
10000-10500
10500-11000
11000-11500
11500
11000
10500
10000
9500
9000
8500
8000
7500
RO
RI
C
LI
AO
LO
AI
C
PI
PO
B3

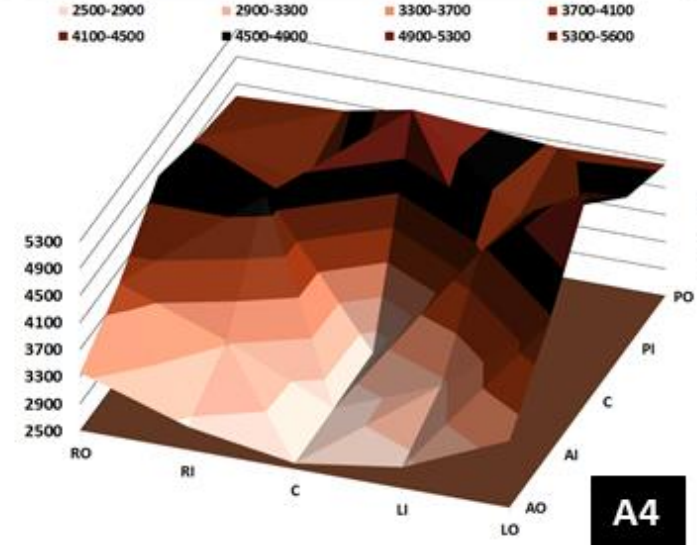
2500-2900
2900-3300
3300-3700
3700-4100
4100-4500
4500-4900
4900-5300
5300-5600
5300
4900
4500
4100
3700
3300
2900
2500
RO
RI
C
LI
AO
LO
AI
C
PI
PO
A4

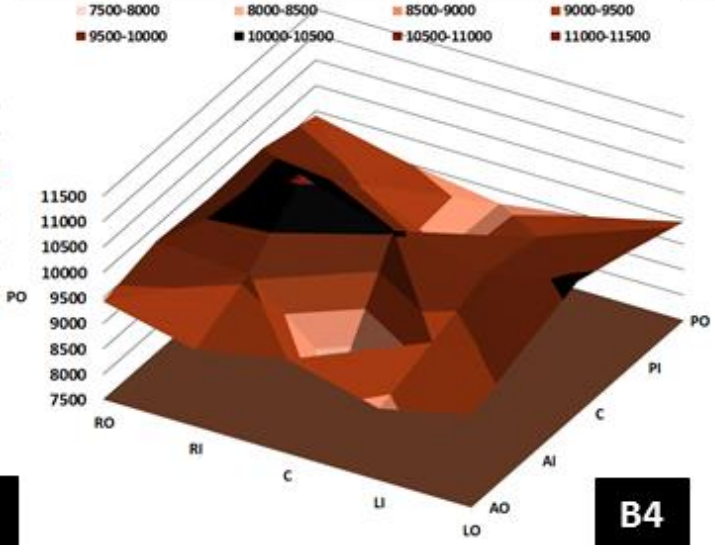
7500-8000
8000-8500
8500-9000
9000-9500
9500-10000
10000-10500
10500-11000
11000-11500
11500
11000
10500
10000
9500
9000
8500
8000
7500
RO
RI
C
LI
AO
LO
AI
C
PI
PO
B4

Figure 3. Three-dimensional maps of average glycosaminoglycan content in the intervertebral disc (A) and endplate (B) shown for different age groups.

Please note the change in scale between different maps. Values are expressed as μg of GAG per mg of dry tissue weight.

A1 – intervertebral disc (20-30 years old); B1 – endplate (20-30 years old); A2 – intervertebral disc (40-50 years old); B2 – endplate (40-50 years old); A3 – intervertebral disc (60-70 years old); B3 – endplate (60-70 years old); A4 – intervertebral disc (80-90 years old); B5 – endplate (80-90 years old).

C - center; LI - left inner; LO - left outer; RI - right inner; RO - right outer; AO - anterior outer; AI - anterior inner; PI - posterior inner; PO - posterior outer.

Please see next page for Figure 3.

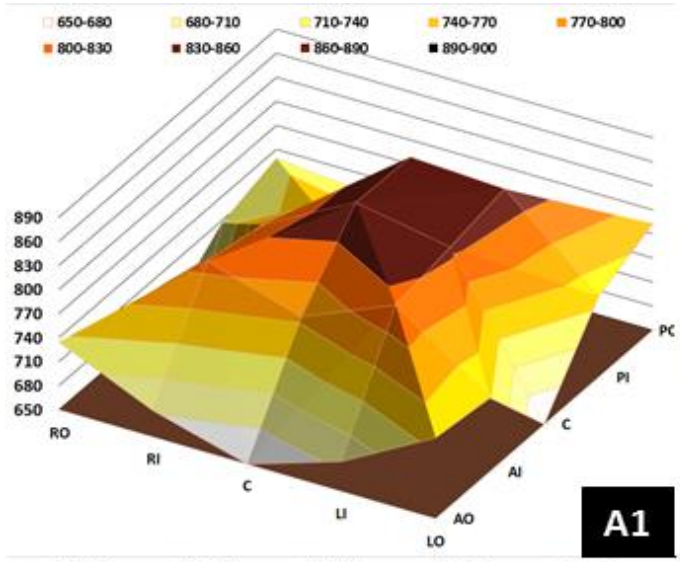

A1

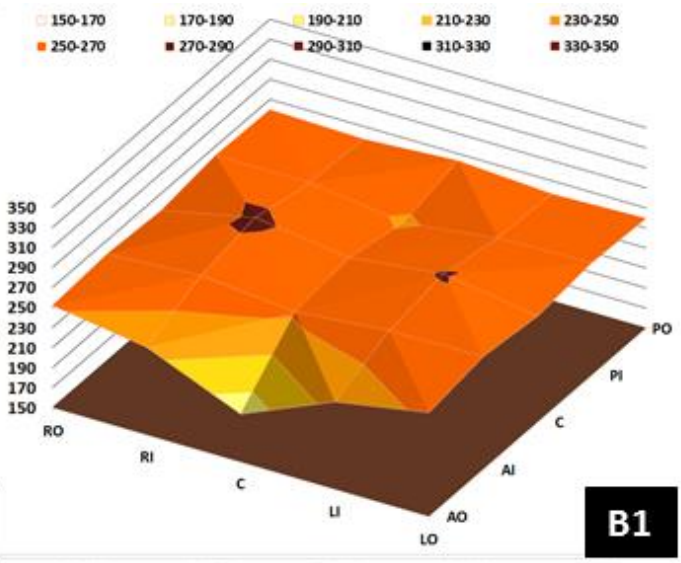

B1

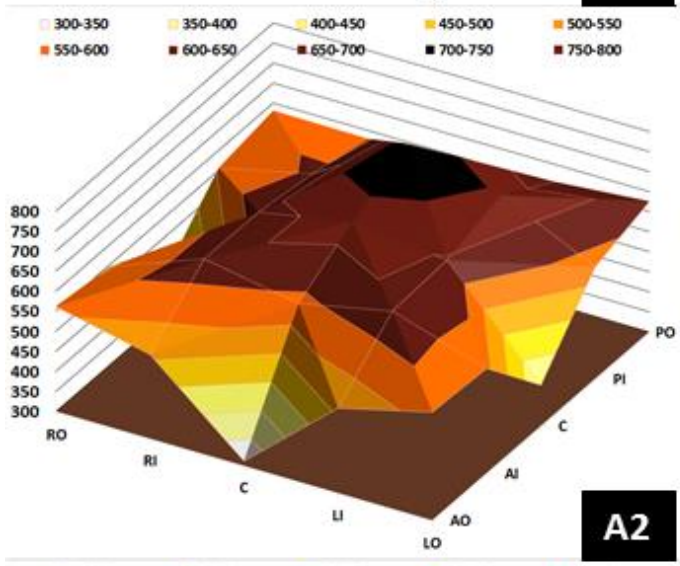

A2

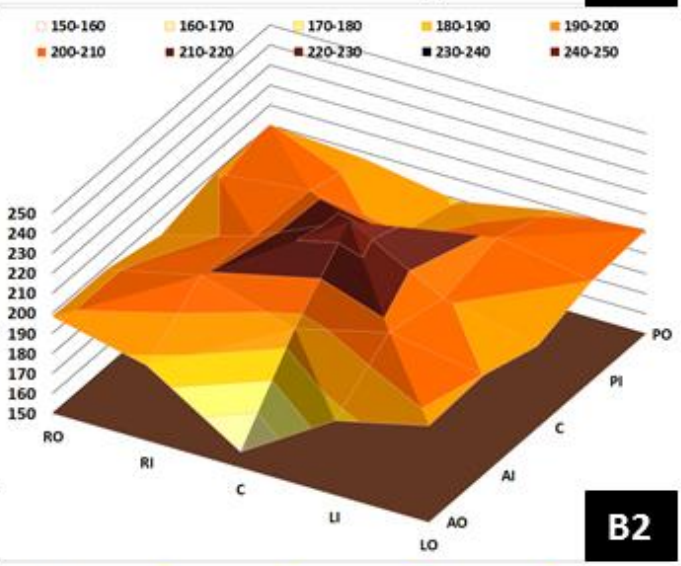

B2

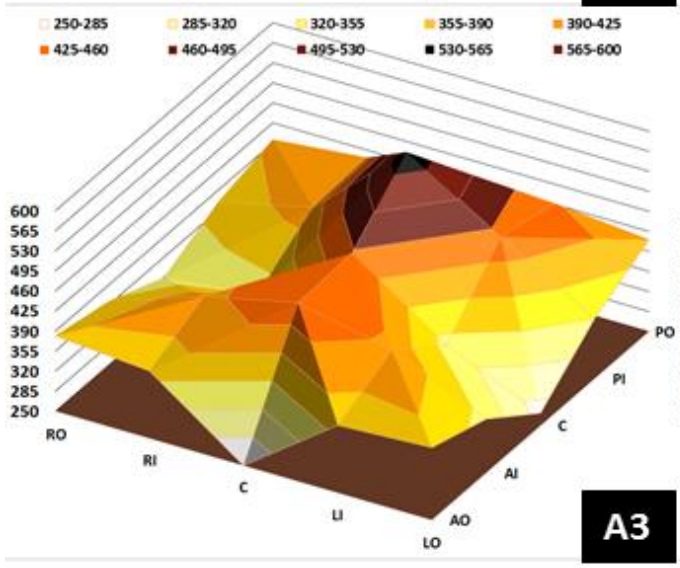

A3

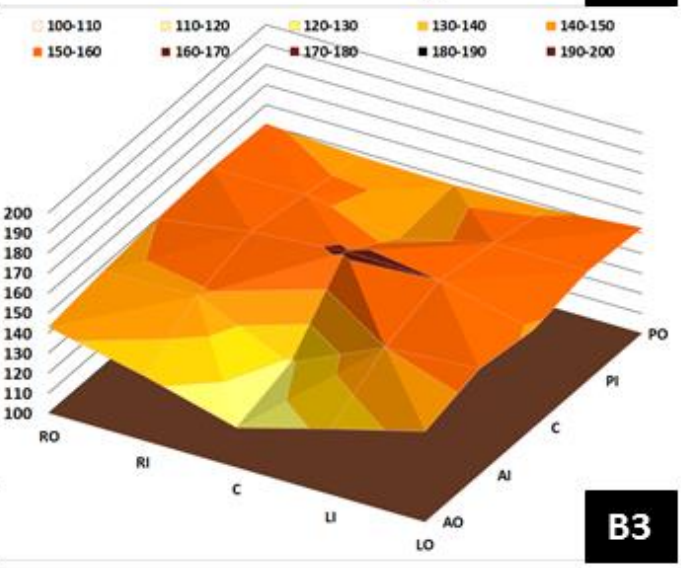

B3

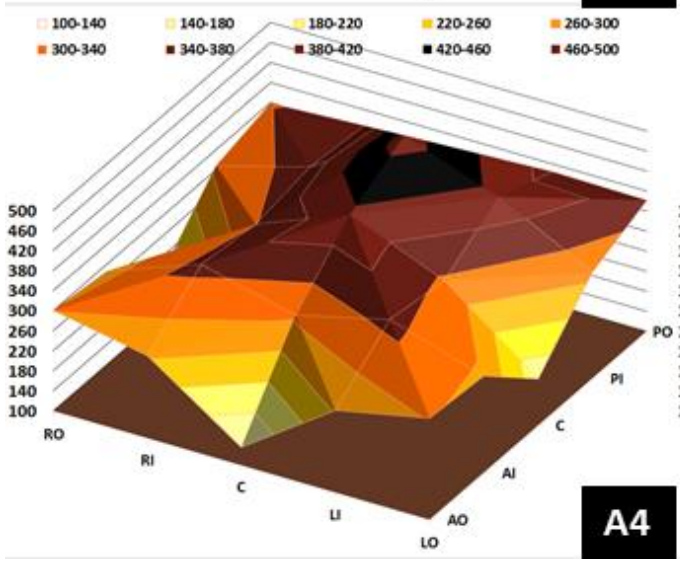

A4

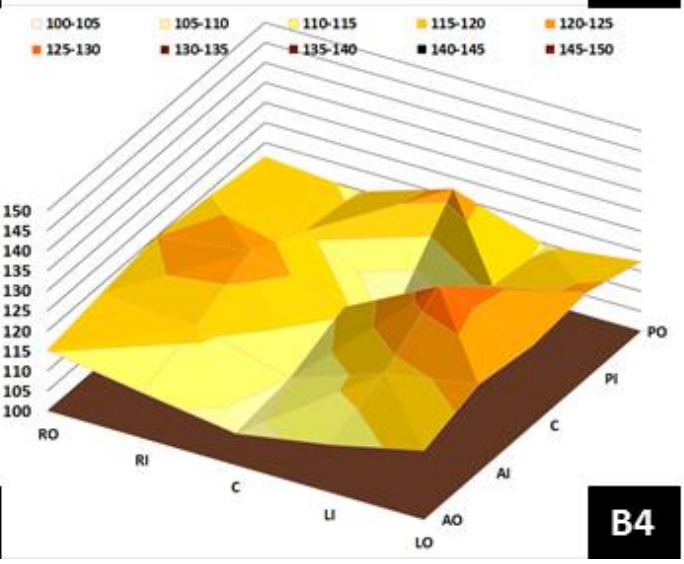

B4

Figure 4. Intervertebral disc glycosaminoglycan content variation in the axial direction in regards to histological degeneration score grade.

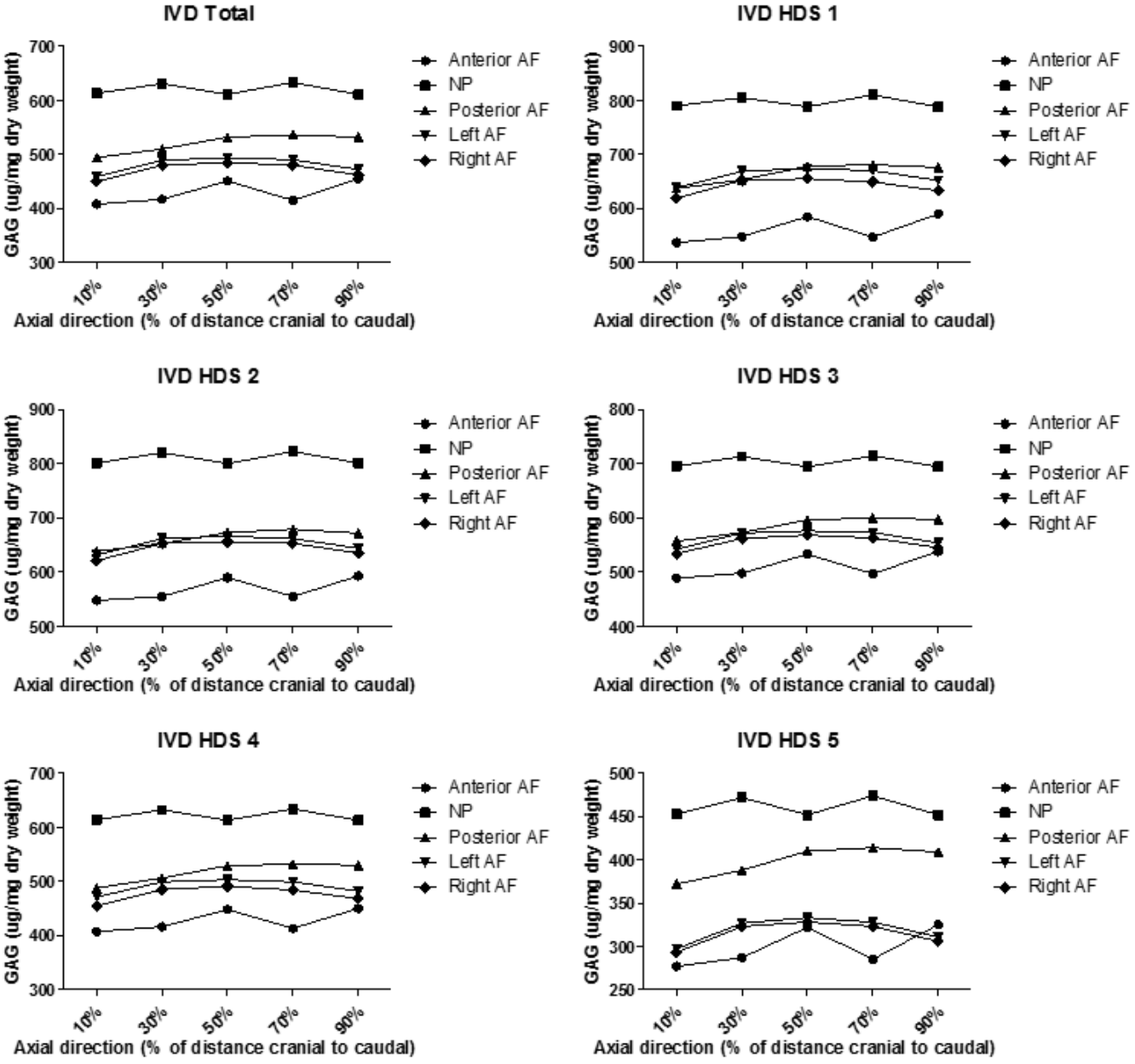

Please note the change in scale between different graphs.

IVD – intervertebral disc; GAG – glycosaminoglycan; HDS – histological degeneration score; AF – annulus fibrosus; NP – nucleus pulposus.

6. Artykuł numer 3

Tomaszewski KA, Adamek D, Pasternak A, Głowacki R, Tomaszewska R, Walocha JA. Degeneration and calcification of the cervical endplate is connected with a decreased expression of ANK, ENPP-1, OPN and TGF-β1 in the intervertebral disc. Polish Journal of Pathology 2014;65(3):204-211

Table of Contents

Degeneration and calcification of the cervical endplate is connected with a decreased expression of ANK, ENPP-1, OPN and TGF-β1 in the intervertebral disc

Krzysztof A. Tomaszewski[1], Dariusz Adamek[2], Artur Pasternak[1], Roman Głowacki[3], Romana Tomaszewska[2], Jerzy A. Walocha[1]

[1] – Department of Anatomy, Jagiellonian University Medical College, Krakow, Poland

[2] – Department of Pathology, Jagiellonian University Medical College, Krakow, Poland

[3] – Department of Otorhinolaryngology, Rydygier Specialistic Hospital, Krakow, Poland

Running title: Decreased PPi related proteins in cervical IVDs

Corresponding author

Krzysztof A. Tomaszewski

Department of Anatomy, Jagiellonian University Medical College

12 Kopernika street, 31-034 Krakow, Poland

Tel./fax. +48-12-422-95-11

e-mail: krtomaszewski@gmail.com

Abstract

The aim of this study was to clarify the relationship between the expression of ALP, ANK, ENPP-1, OPN and TGF-β1 in the intervertebral disc (IVD), and cervical vertebral endplate calcification and degeneration. Sixty cervical IVDs were excised from 30 human cadavers. Each specimen was assessed macroscopically for degeneration (Thompson's classification), and then underwent histological processing, regular staining (haematoxylin and eosin, Masson-Goldner trichrome and alcian blue-PAS), immunohistochemistry (ALP, ANK, ENPP-1, OPN and TGF-β1), microscopic degeneration grading (Boos classification), and assessment of endplate calcification. The mean age±SD of the specimens was 51.4±19.5. The percentage of endplate calcification significantly correlated with the degree of endplate and IVD degeneration graded using Boos'es score (both $r=0.91$; $p<0.0001$). The intensity and number of stained cells per FOV markedly decreased, for ANK, ENPP-1, and TGF-β1, with the grade of IVD degeneration, regardless of the analyzed IVD region. This was not true only for ALP which demonstrated an increasing trend corresponding to the degree of IVD degeneration. The expression of OPN was low throughout all analyzed regions, regardless of the degree of degeneration. Modulating the expression of the abovementioned proteins, especially ANK and TGF-β1, may be a new way to prevent the degeneration and calcification of the IVD.

Keywords: ANK; calcification; cervical intervertebral disc; degeneration; endplate.

Introduction

In the most recent Global Burden of Disease Study [1] low back pain (LBP) was found to be the biggest contributor to Years Lived with Disability (YLDs). LBP is the most common form of chronic pain, costing the UK's economy over 6.6 billion pounds in 1998 [2]. The prevalence rates range from 12% to 35% with around 10% of patients becoming chronically disabled [3].

Back pain has a strong association with intervertebral disc (IVD) degeneration [4]. Discs degenerate far earlier than other musculoskeletal tissues, and the first findings of degeneration in the lumbar discs are seen between 11-16 years of age [5]. The process of degeneration increases steeply with age, especially in males – around 10% of 50-year-olds and 60% of 70-year-olds have severely degenerate IVDs [4, 5].

Although the complex and dynamic relationships between disc degeneration and sclerosis of the vertebral endplate are well recognized, they are poorly understood. IVD degenerative disease is known to be caused by a series of factors including ageing, biochemical changes (loss of proteoglycan, collagen fibers and increased enzymatic activity), genetics, mechanical loading and injury, as well as impaired disc nutrition [4]. The IVD is the largest avascular structure in the human body [6], and the main way for it to receive nutrients is through diffusion from the capillary buds penetrating the vertebral endplate [7]. Endplate calcification, through a decrease in its permeability, may lead to a fall in nutrient delivery to the cells of the IVD [7], and through that to its degeneration and mechanical failure [8].

The ANKH gene is the human homologue of the gene responsible for progressive ankylosis in a naturally occurring mutant mouse [9]. It produces a multiple-pass transmembrane protein (ANK) which regulates intracellular inorganic pyrophosphate (PPi) transportation from the cytoplasm to the extracellular space, thereby maintaining the PPi steady-state concentration, and thus possibly preventing increased calcification of the tissue [10]. Findings from previous

studies show that mRNA and protein products of ANKH decrease with endplate degeneration [11].

Transforming growth factor-beta-1 (TGF-β1) plays a significant role in regulating crystal deposition in endplate cartilage, and is able to induce PPi elaboration via TGF-β1-induced ANKH gene expression, thus being an important factor in the regulation of the calcification process [12].

Calcification involves the deposition of calcium phosphates, with alkaline phosphatase (ALP) playing an active role in initiating this process [13]. It hydrolyzes organic phosphates and PPi [14], yielding monophosphate ions (Pi), which, in the presence of calcium ions, form hydroxyapatite crystals [15]. This process is however far more complicated with ANKH (conjointly with ectoenzyme PC-1 – ENPP1) deficiencies causing a possible decrease in PPi and osteopontin (OPN) levels [16].

However, most of the above mentioned studies were performed on animal models or on a small number of human lumbar IVDs. None of them ventured to analyze the correlation between different PPi associated proteins. Thus, the aim of this study was to clarify the relationship between the expression of ALP, ANK, ENPP-1, OPN and TGF-β1 in the IVD, and cervical vertebral endplate calcification and degeneration.

Materials and Methods

Material acquisition

Sixty cervical IVDs were excised from 30 human cadavers (at the Department of Forensic Medicine, Jagiellonian University Medical College), using the anterior approach, not later than 24 hours post-mortem [17]. The material was excised in one block comprising vertebral bodies, IVDs, endplates and blood vessels supplying these structure, and wrapped in saline soaked gauze, vacuum-sealed to prevent dehydration, and kept at 4° Celsius until further

processing. Excision started at the level of the lower half of the C4 vertebra and ended at the level of the upper half of the C6.

The study inclusion criterion was the ability to excise a section of the anterior spinal column (from the lower half of the C4 vertebra to the upper half of the C6), with the anterior and posterior longitudinal ligaments and blood vessels supplying the vertebrae. Study exclusion criteria were: (1) injury to the cervical spine, preventing from excising the required section; (2) previous cervical spine surgery; (3) receiving chemotherapy in the last 12 months; (4) previous radiation therapy to the perispinal region; (5) long-standing paralysis (6 or more months); (6) ankylosing spondylitis.

Macroscopic and microscopic degeneration grading

On the same day each sample was unpacked from the vacuum-sealed container, and sectioned transversally at the middle of the C5 vertebral body. This produced two samples from each cadaver encompassing the IVD with its both endplates, surrounded from both ends by part of the vertebral bodies. Next each sample was sectioned along the midsagittal plane for macroscopic IVD degeneration scoring according to Thompson's classification [18]. Each specimen was assessed by two of the authors, and the grade was averaged. Next, the samples were placed in a 10% solution of formaldehyde (pH 7.4) for a minimum of 14 days for fixing.

Microscopic IVD and endplate degeneration was assessed using Boos classification [19]. Each endplate and IVD was divided into 5 regions - anterior outer annulus (AO), anterior inner annulus (AI), nucleus pulposus (NP), posterior inner annulus (PI), and posterior outer annulus (PO). Tissue samples acquired from the midsagittal plane (of each of the 5 IVD regions) were decalcified, dehydrated, embedded in paraffin, sectioned at 4 μm, and stained with haematoxylin and eosin, Masson-Goldner trichrome and alcian blue-PAS (Department of Pathology, Jagiellonian University Medical College). Each sample was assessed and scored,

using light microscopy (Nikon Eclipse 80i), by two observers, and the final score per sample was averaged.

The degree of endplate calcification was analyzed as the percentage of calcified tissue (red on Masson-Goldner trichrom staining) to the non-calcified part. The fact of endplate calcification was verified on corresponding H&E stained samples. The percentage of calcification was averaged for all examined endplate regions.

Immunohistochemistry

For immunohistochemical localization, formalin-fixed tissue sections were treated for 10 min with 3% H_2O_2. Heat induced epitope retrieval was performed in EDTA (pH 8.0)/citrate (pH 6.0) at 98° for 30 or 60 min depending on the antibody (as per the producer's recommendations). Sections were than incubated at room temperature with the following antibodies – ANK1 (1:50 concentration, Santa Cruz Biotechnology), SPP1 (1:50 concentration, Lab Vision), alkaline phosphatase (1:50 concentration, Lab Vision), ENPP1 (1:100 concentration, Santa Cruz Biotechnology), TGF- β1 (1:50 concentration, Abcam). After incubation the samples were washed in TBS (DAKO corp.). For antigen-antibody visualization the Ultra Vision LP Values Detection System (Lab Vision) together with DAB (3,30-diaminobenzidine) (DAKO) were used according to the manufacturer's recommendations. Finally, sections were washed and then counterstained with Mayer's hematoxylin.

For each antibody and for each sample a negative control was processed. Negative controls were carried out by incubation in the absence of the primary antibody and always yielded negative results [20].

The intensity of the immunohistochemical reaction was measured using the following semi-quantitative grading scheme: (-) no stained cells; (+) 1-4 positive cells; (++) 5-9 positive cells;

(+++) ≥10 positive cells. Each sample was photographed and analyzed using Java ImageJ [21], by assessing 3 consecutive fields of view (FOV) (magnification x200) and calculating the average number of stained cells for each sample. Then the results from all the samples were averaged to obtain the final number of cells per FOV.

Ethics

The research protocol was approved by the Jagiellonian University Medical College Ethics Committee (registry number KBET/319/B/2012). The study has been performed in accordance with the ethical standards laid down in the 1964 Declaration of Helsinki and its later amendments. The specimen excision method was chosen so as not to destabilize the cadaver's spinal column.

Statistical analysis

Statistical analysis was conducted using Statistica 10.0 PL (Statsoft). Elements of descriptive statistics were used (mean, standard deviation percentage distribution). Differences between groups were tested with the unpaired Student's t test or Mann–Whitney U test as appropriate. To assess the correlation between scores, Pearson's correlation was used. Statistical significance was set at $p<0.05$.

Results

The study group comprised 30 female and 30 male IVDs. The mean age±SD of the specimens was 51.4±19.5. The basic characteristics of the study group are presented in Table I.

IVD degeneration, graded using Thompson's classification, significantly correlated with Boos'es IVD degeneration score ($r=0.77$; $p<0.0001$). IVD and endplate degeneration, graded using Boos'es score also strongly correlated with each other ($r=0.96$; $p<0.0001$). The

percentage of endplate calcification significantly correlated with both the degree of endplate and IVD degeneration graded using Boos'es score (both $r=0.91$; $p<0.0001$).

Specimen's age strongly correlated with both IVD degeneration (Thompson's and Boos'es scores) and endplate degeneration (Boos score), as well as the averaged percentage of endplate calcification ($r=0.76$; $r=0.77$; $r=0.73$; $r=0.75$ respectively; $p<0.0001$).

Staining intensity of selected proteins per Thompson's degeneration grade for different IVD regions is presented in Tables II-VI. The intensity and number of stained cells per FOV markedly decreased, for the majority of analyzed proteins (ANK, ENPP-1, and TGF-β1), with the grade of IVD degeneration, regardless of the analyzed region. This was not true only for ALP which demonstrated an increasing trend corresponding to the degree of IVD degeneration. The expression of OPN was low throughout all analyzed regions, regardless of the degree of IVD degeneration.

Figure 1 presents selected intervertebral disc regions (all from the annulus fibrosus) stained (immunohistochemistry) for ankyrin, and their corresponding endplate zones stained with Masson's trichrome. A distinct negative correlation can be seen between the expression of ankyrin in the IVD and the degree of calcification of the vertebral endplate.

Discussion

The aim of this study was to clarify the relationship between the expression of ALP, ANK, ENPP-1, OPN and TGF-β1 in the IVD, and cervical vertebral endplate calcification and degeneration. The most significant finding of this study is the fact that, for the first time in a large group of cervical IVDs, it was possible to confirm that there exists a strong relationship between a decreased expression of ANK, ENPP-1, and TGF-β1 in the IVD and an increase in IVD degeneration and endplate degeneration and calcification. This finding was probably most evident for ANK and TGF-β1 as both proteins are strongly intertwined with each other

in the process of calcification [12]. ALP, as expected, was expressed more intensively in IVDs with a higher degree of calcification, as ALP is a marker of ongoing mineral deposition [14].

It is still not clear whether calcification is the cause or the effect of IVD and/or endplate degeneration. Some authors safely reply that both processes exist simultaneously and are strongly associated with each other [22]. However, the results of our previous study (results not yet published) have signaled that endplate calcification is rather the cause, than the effect of a fall in nutrient transport, as it starts in the well-vascularized center of the endplate, and not in the outer regions where the number of endplate openings (marrow contact channels) is lower. Unfortunately, definitive sentences have to be withheld until "cause and effect" studies provide further data.

This study has demonstrated that there exists a strong correlation between the degree of endplate and IVD degeneration and the intensity of endplate calcification, as well as the age of the specimen. The latter has already been shown in previous studies [23, 24], showing at the same time that currently it is impossible to differentiate between changes related purely to ageing, from those occurring due to pathological degeneration. This has also been shown to be true for the cervical spine, where in a longitudinal study no other factor except for age was related to the progression of degeneration [25]. The correlation between IVD calcification and degeneration has also been shown before [26], however never so clearly for the relationship between endplate calcification and IVD degeneration. Our study also confirms that the first calcifications in the endplate can be seen as early as in the third decade of life [26]. However in this young age-group the occurrence of calcifications is rather rare, with the majority being found in the cervical or thoracic spine – sites not so prone to degeneration as the lumbosacral region [26, 27]. A study by Rutges et al. [26] has shown that part of the calcifications found in the IVD are located around viable cells, suggesting the origin of calcium salt production,

which may result from end stage hypertrophic differentiation. However, Rutges et al. [26] found that in the nucleus pulposus of young patients, calcifications were always associated with notochordal cells, indicating a different mechanism underlying calcification – probably associated with the activity of Runx2, ALP and osteoprotegerin.

The differences in the staining intensity found between IVD region (nucleus pulposus vs. different regions of the annulus fibsosus) may possibly originate from the fact that endplate cartilage and annulus fibrosus cells are derived from mesenchymal cells, while cells of the nucleus pulpous are derived from notochordal cells [28].

The expression of ANK, ENPP-1, and TGF-β1 markedly decreased with the grade of IVD degeneration. ANK is a transmembrane protein responsible for regulating the intra- and extracellular transport of PPi [9], and is considered a significant "anti-calcification" protein [11]. It has been mentioned [9] that when the ANK channel protein fails in its function, than calcium pyrophosphate dehydrate deposits in the cartilage. The current study confirms earlier findings from animal models that ANK protein expression decreases with degeneration [10], suggesting its significant role in the mechanism of pathological calcification. It has been reported that TGF-β1 plays an important part in regulating the expression of ANK in chondrocytes, through Ras/Raf-1/ERK and Ca^{2+}-dependent PKC signal-regulated kinase pathways [12]. Also cyclic mechanical tension applied to cultured endplate chondrocytes increased both the expression of ANK and TGF-β1 [8]. What is more, ANK protein expression increases in a dose-dependent manner when treated with TGF-β1 [8]. All of the above facts would explain the strong association between ANK and TGF-β1 expression found in our study. The somewhat weaker, but still significant, association found in this study between ANK, ENPP1, and TGF-β1 expression further proves that ANK is more sensitive to TGF-β1 than ENPP1 [12].

The reason for poor expression of OPN, both in the vertebral endplate and the IVD, is not clear. We expected to see an increasing expression of OPN correlating with the degree of degeneration and endplate calcification, as OPN plays and important role is mineralization [29]. The obtained results stand in opposition to the calcification mechanisms discovered in tendons and blood vessels where hydroxyapatite deposition is strongly related to osteopontin, type X collagen, and osteonectin [30, 31]. It is probable that the fact of the IVD being an avascular structure plays an important role in modulating the process of calcification [29].

ALP expression was found to increase with the progression of endplate and IVD degeneration and calcification, with the exception of Thompson grade V IVDs. This finding suggests that ALP is involved in extracellular mineralization. More likely so as the localization of ALP activity coincided with the location where many of the calcifications were found. ALP is one of the most important proteins in the process of calcification, and its increase in more calcified IVDs was expected. However, it is not only ALP that could be responsible for increased IVD calcification. Primary annulus fibrosus cells are also likely responsible for this process in the IVD [32]. The significant decrease of ALP expression in the most degenerated IVDs is most probably caused by the large degree of cell death found in Thompson grade V specimens.

Concluding, this study has pointed out the important and intertwined role of ANK, TGF-β1, ENPP1, and OPN in the process of IVD and endplate degeneration and calcification. Modulating the expression of the abovementioned proteins, especially ANK and TGF-β1, may be a new way to prevent the degeneration and calcification of the IVD. Further studies are still needed to elucidate the cause and effect relationship between endplate calcification and IVD degeneration.

Conflict of Interest Statement

All authors declare that they have no conflict of interest.

Acknowledgements

The authors want to thank Mr Krzysztof Skomski for his excellent microphotographs. This study was funded by the National Science Center – Poland under grant number DEC-2012/07/N/NZ5/00078. Krzysztof A. Tomaszewski received a scholarship to prepare his PhD thesis from the National Science Center – Poland under award number DEC-2013/08/T/NZ5/00020.

Author contribution

Design and planning of the study – KAT, DA, RT, JAW. Sample collection – KAT, AP. Sample preparation – KAT, RG, RT. Histological analysis – KAT, DA, RT. Data interpretation – KAT, RT, DA, JAW (sample measurement and result verification), KAT (statistical analysis). Bibliographic search – KAT, AP. Drafting and revising the manuscript – KAT. Obtaining funding – KAT. Critical revision of the manuscript – DA, RT, JAW. All authors have read and approved the final version of the manuscript.

All co-authors confirm the above-mentioned contributions and consent to the fact that this study is a part of Krzysztof A. Tomaszewski's PhD thesis. The co-authors confirm that Krzysztof A. Tomaszewski has contributed significantly (80% in total) to every part of this study, as stated above.

References

1. Vos T, Flaxman AD, Naghavi M, et al. Years lived with disability (YLDs) for 1160 sequelae of 289 diseases and injuries 1990-2010: a systematic analysis for the Global Burden of Disease Study 2010. Lancet 2012;3 80: 2163-2196.

2. Froud R, Patterson S, Eldridge S, et al. A systematic review and meta-synthesis of the impact of low back pain on people's lives. BMC Musculoskelet Disord 2014; 15: 50.

3. Maniadakis N, Gray A. The economic burden of back pain in the UK. Pain 2000; 84: 95-103.

4. Raj PP. Intervertebral disc: anatomy-physiology-pathophysiology-treatment. Pain Pract 2008; 8: 18-44.

5. Boos N, Weissbach S, Rohrbach H, et al. Classification of age-related changes in lumbar intervertebral discs. Volvo Award in basic science. Spine 2002; 27: 2631-2644.

6. Moore RJ. The vertebral endplate: disc degeneration, disc regeneration. Eur Spine J 2006; 15: S333-337.

7. van der Werf M, Lezuo P, Maissen O, et al. Inhibition of vertebral endplate perfusion results in decreased intervertebral disc intranuclear diffusive transport. J Anat 2007; 211: 769-774.

8. Xu H, Zhang X, Wang H, et al. Continuous cyclic mechanical tension increases ank expression in endplate chondrocytes through the TGF-β1 and p38 pathway. Eur J Histochem 2013; 57: e28.

9. Zaka R, Williams CJ. Role of the progressive ankylosis gene in cartilage mineralization. Curr Opin Rheumatol. 2006; 18: 181-186.

10. Xu HG, Hu CJ, Wang H, et al. Effects of mechanical strain on ANK, ENPP1 and TGF-β1 expression in rat endplate chondrocytes in vitro. Mol Med Report 2011; 4: 831-835.

11. Xu HG, Song JX, Cheng JF, et al. JNK phosphorylation promotes degeneration of cervical endplate chondrocytes through down-regulation of the expression of ANK in humans. Chin Med J (Engl). 2013; 126: 2067-2073.

12. Cailotto F, Bianchi A, Sebillaud S, et al. Inorganic pyrophosphate generation by transforming growth factor-beta-1 is mainly dependent on ANK induction by Ras/Raf-1/extracellular signal-regulated kinase pathways in chondrocytes. Arthritis Res Ther 2007; 9: R122.

13. Miller GJ, DeMarzo AM. Ultrastructural localization of matrix vesicles and alkaline phosphatase in the Swarm rat chondrosarcoma: their role in cartilage calcification. Bone. 1988; 9: 235-241.

14. Hristova GI, Jarzem P, Ouellet JA, et al. Calcification in human intervertebral disc degeneration and scoliosis. J Orthop Res. 2011; 29: 1888-1895.

15. Anderson HC, Sipe JB, Hessle L, et al. Impaired calcification around matrix vesicles of growth plate and bone in alkaline phosphatase-deficient mice. Am J Pathol 2004; 164: 841-847.

16. Harmey D, Hessle L, Narisawa S, et al. Concerted regulation of inorganic pyrophosphate and osteopontin by akp2, enpp1, and ank: an integrated model of the pathogenesis of mineralization disorders. Am J Pathol 2004; 164: 1199-1209.

17. Le Maitre CL, Freemont AJ, Hoyland JA. The role of interleukin-1 in the pathogenesis of human intervertebral disc degeneration. Arthritis Res Ther 2005; 7: R732-745.

18. Thompson JP, Pearce RH, Schechter MT, et al. Preliminary evaluation of a scheme for grading the gross morphology of the human intervertebral disc. Spine 1990; 15: 411-415.

19. Boos N, Weissbach S, Rohrbach H, et al. Classification of age-related changes in lumbar intervertebral discs. Volvo Award in basic science. Spine 2002; 27: 2631-2644.

20. Pyziak L, Stasikowska-Kanicka O, Danilewicz M, et al. Immunohistochemical analysis of mast cell infiltrates and microvessel density in oral squamous cell carcinoma. Pol J Pathol 2013; 64: 276-280.

21. Mizia E, Tomaszewski KA, Lis GJ, et al. The use of computer-assisted image analysis in measuring the histological structure of the human median nerve. Folia Morphol (Warsz) 2012; 71: 82-85.

22. Gruber HE, Ashraf N, Kilburn J, et al. Vertebral endplate architecture and vascularization: application of microcomputerized tomography, a vascular tracer, and immunocytochemistry in analyses of disc degeneration in the aging sand rat. Spine 2005; 30: 2593-2600.

23. Sowa G, Vadala G, Studer R, et al. Characterization of intervertebral disc aging: longitudinal analysis of a rabbit model by magnetic resonance imaging, histology, and gene expression. Spine 2008; 33: 1821-1828.

24. Miller JA, Schmatz C, Schultz AB. Lumbar disc degeneration: correlation with age, sex, and spine level in 600 autopsy specimens. Spine 1988; 13: 173-178.

25. Okada E, Matsumoto M, Ichihara D, et al. Aging of the cervical spine in healthy volunteers: a 10-year longitudinal magnetic resonance imaging study. Spine 2009; 34: 706-712.

26. Rutges JPHJ, Duit RA, Kummer JA, et al. Hypertrophic differentiation and calcification during intervertebral disc degeneration. Osteoarthritis and Cartilage 2010; 18: 1487-1495.

27. Dai LY, Ye H, Qian QR. The natural history of cervical disc calcification in children. J Bone Joint Surg Am 2004; 86: 1467-1472.

28. Sive JI, Baird P, Jeziorsk M, et al. Expression of chondrocyte markers by cells of normal and degenerate intervertebral discs. Mol Pathol 2002; 55: 91-97.

29. Melrose J, Burkhardt D, Taylor TK, et al. Calcification in the ovine intervertebral disc: a model of hydroxyapatite deposition disease. Eur Spine J 2009; 18: 479-489.

30. Takeuchi E, Sugamoto K, Nakase T, et al. Localization and expression of osteopontin in the rotator cuff tendons in patients with calcifying tendinitis. Virchows Arch 2001; 438: 612-617.

31. Moe SM, Chen NX. Pathophysiology of vascular calcification in chronic kidney disease. Circ Res 2004; 95: 560-567.

32. Nosikova Y, Santerre JP, Grynpas MD, et al. Annulus fibrosus cells can induce mineralization: an in vitro study. Spine J 2013; 13: 443-453.

Tables

Table I. Basic characteristics of the study group.

	Female (n=30)	**Male (n=30)**	**Total (n=60)**	**p-value[1]**
Age (SD)	52.8 (19.8)	50.0 (19.4)	51.4 (19.5)	0.57
IVD degeneration - Thompson classification (SD)	2.6 (1.3)	3.2 (1.3)	2.9 (1.3)	0.08
IVD degeneration - Boos classification (SD)	12.0 (6.1)	14.3 (5.3)	13.1 (5.8)	0.13
Endplate degeneration - Boos classification (SD)	8.9 (5.3)	11.5 (4.8)	10.2 (5.2)	0.06
Endplate calcification [%] (SD)	28.4 (25.1)	44.1 (26.0)	36.2 (26.5)	0.02
IVD degeneration - Thompson classification vs. degree of endplate calcification [%] (SD)				
Grade I	6.2 (2.6)	6.7 (0.6)	6.3 (2.1)	0.31
Grade II	13.2 (2.8)	17.7 (1.9)	14.8 (3.3)	<0.0001
Grade III	29.6 (8.7)	37.1 (7.3)	34.4 (8.4)	0.0006
Grade IV	53.3 (6.9)	61.6 (4.8)	57.9 (7.0)	<0.0001
Grade V	77.3 (8.5)	79.1 (2.8)	78.5 (5.2)	0.28

[1] – for differences between females and males

SD – standard deviation; IVD – intervertebral disc.

Table II. Staining intensity of selected proteins per Thompson's degeneration grade for the anterior outer annulus of the intervertebral disc.

Anterior Outer Annulus (AO)	**Thompson grade I (n=9)**	**Thompson grade II (n=17)**	**Thompson grade III (n=14)**	**Thompson grade IV (n=9)**	**Thompson grade V (n=11)**
ALP	+	++	++	+++	+
ANK	++	++	+	+	+
ENPP-1	+++	+++	++	+	+
OPN	-	+	+	++	+
TGF-β1	+++	++	+	+	-

Grading scheme: (-) no stained cells; (+) 1-4 positive cells; (++) 5-9 positive cells; (+++) ≥10 positive cells.

ALP – alkaline phosphatase; ANK – ankyrin; ENPP-1 – ectoenzyme PC-1; OPN – osteopntin; TGF-β1 – transforming growth factor β1.

Each sample was analyzed by assessing 3 consecutive fields of view (FOV) (magnification x200) and calculating the average number of stained cells for each sample. Then the results from all the samples were averaged to obtain the final number of cells per FOV.

Table III. Staining intensity of selected proteins per Thompson's degeneration grade for the anterior inner annulus of the intervertebral disc.

Anterior Inner Annulus (AI)	**Thompson grade I (n=9)**	**Thompson grade II (n=17)**	**Thompson grade III (n=14)**	**Thompson grade IV (n=9)**	**Thompson grade V (n=11)**
ALP	+	++	+++	+++	+
ANK	+++	+++	++	+	+
ENPP-1	++	+++	++	-	-
OPN	-	+	++	+	+
TGF-β1	+++	+++	++	+	+

Grading scheme: (-) no stained cells; (+) 1-4 positive cells; (++) 5-9 positive cells; (+++) ≥10 positive cells.

ALP – alkaline phosphatase; ANK – ankyrin; ENPP-1 – ectoenzyme PC-1; OPN – osteopntin; TGF-β1 – transforming growth factor β1.

Each sample was analyzed by assessing 3 consecutive fields of view (FOV) (magnification x200) and calculating the average number of stained cells for each sample. Then the results from all the samples were averaged to obtain the final number of cells per FOV.

Table IV. Staining intensity of selected proteins per Thompson's degeneration grade for the nucleus pulposus region of the intervertebral disc.

Nucleus Pulposus (NP)	**Thompson grade I (n=9)**	**Thompson grade II (n=17)**	**Thompson grade III (n=14)**	**Thompson grade IV (n=9)**	**Thompson grade V (n=11)**
ALP	-	+	++	++	+
ANK	+++	++	+	+	-
ENPP-1	+++	+++	++	+	-
OPN	+	+	+	+	+
TGF-β1	++	++	+	+	+

Grading scheme: (-) no stained cells; (+) 1-4 positive cells; (++) 5-9 positive cells; (+++) ≥10 positive cells.

ALP – alkaline phosphatase; ANK – ankyrin; ENPP-1 – ectoenzyme PC-1; OPN – osteopntin; TGF-β1 – transforming growth factor β1.

Each sample was analyzed by assessing 3 consecutive fields of view (FOV) (magnification x200) and calculating the average number of stained cells for each sample. Then the results from all the samples were averaged to obtain the final number of cells per FOV.

Table V. Staining intensity of selected proteins per Thompson's degeneration grade for the posterior inner annulus of the intervertebral disc.

Posterior Inner Annulus (PI)	**Thompson grade I (n=9)**	**Thompson grade II (n=17)**	**Thompson grade III (n=14)**	**Thompson grade IV (n=9)**	**Thompson grade V (n=11)**
ALP	+	+	+++	++	+
ANK	++	++	+	-	-
ENPP-1	+++	+++	++	+	-
OPN	+	-	++	+	-
TGF-β1	+++	++	+	+	+

Grading scheme: (-) no stained cells; (+) 1-4 positive cells; (++) 5-9 positive cells; (+++) ≥10 positive cells.

ALP – alkaline phosphatase; ANK – ankyrin; ENPP-1 – ectoenzyme PC-1; OPN – osteopntin; TGF-β1 – transforming growth factor β1.

Each sample was analyzed by assessing 3 consecutive fields of view (FOV) (magnification x200) and calculating the average number of stained cells for each sample. Then the results from all the samples were averaged to obtain the final number of cells per FOV.

Table VI. Staining intensity of selected proteins per Thompson's degeneration grade for the posterior outer annulus of the intervertebral disc.

Posterior Outer Annulus (PO)	**Thompson grade I (n=9)**	**Thompson grade II (n=17)**	**Thompson grade III (n=14)**	**Thompson grade IV (n=9)**	**Thompson grade V (n=11)**
ALP	+	++	+++	++	++
ANK	++	++	+	+	+
ENPP-1	++	++	+	+	-
OPN	-	+	+	-	+
TGF-β1	++	++	+	+	-

Grading scheme: (-) no stained cells; (+) 1-4 positive cells; (++) 5-9 positive cells; (+++) ≥10 positive cells.

ALP – alkaline phosphatase; ANK – ankyrin; ENPP-1 – ectoenzyme PC-1; OPN – osteopntin; TGF-β1 – transforming growth factor β1.

Each sample was analyzed by assessing 3 consecutive fields of view (FOV) (magnification x200) and calculating the average number of stained cells for each sample. Then the results from all the samples were averaged to obtain the final number of cells per FOV.

Figures

Figure 1. Selected intervertebral disc regions (annulus fibrosus) stained (immunohistochemistry) for ankyrin, and their corresponding endplate zones stained with Masson's trichrome.

A, C, E, G – immunohistochemistry staining for ankyrin

B, D, F, H – Masson's trichrome staining (red marks calcification)

Figure lettering	Patient's age	Thompson's IVD degeneration grade	Boos IVD degeneration grade	Boos endplate degeneration grade
A & B	22	I	2	2
C & D	37	II	7	5
E & F	54	III	13	10
G & H	82	V	19	17

Please see next page for Figure 3.

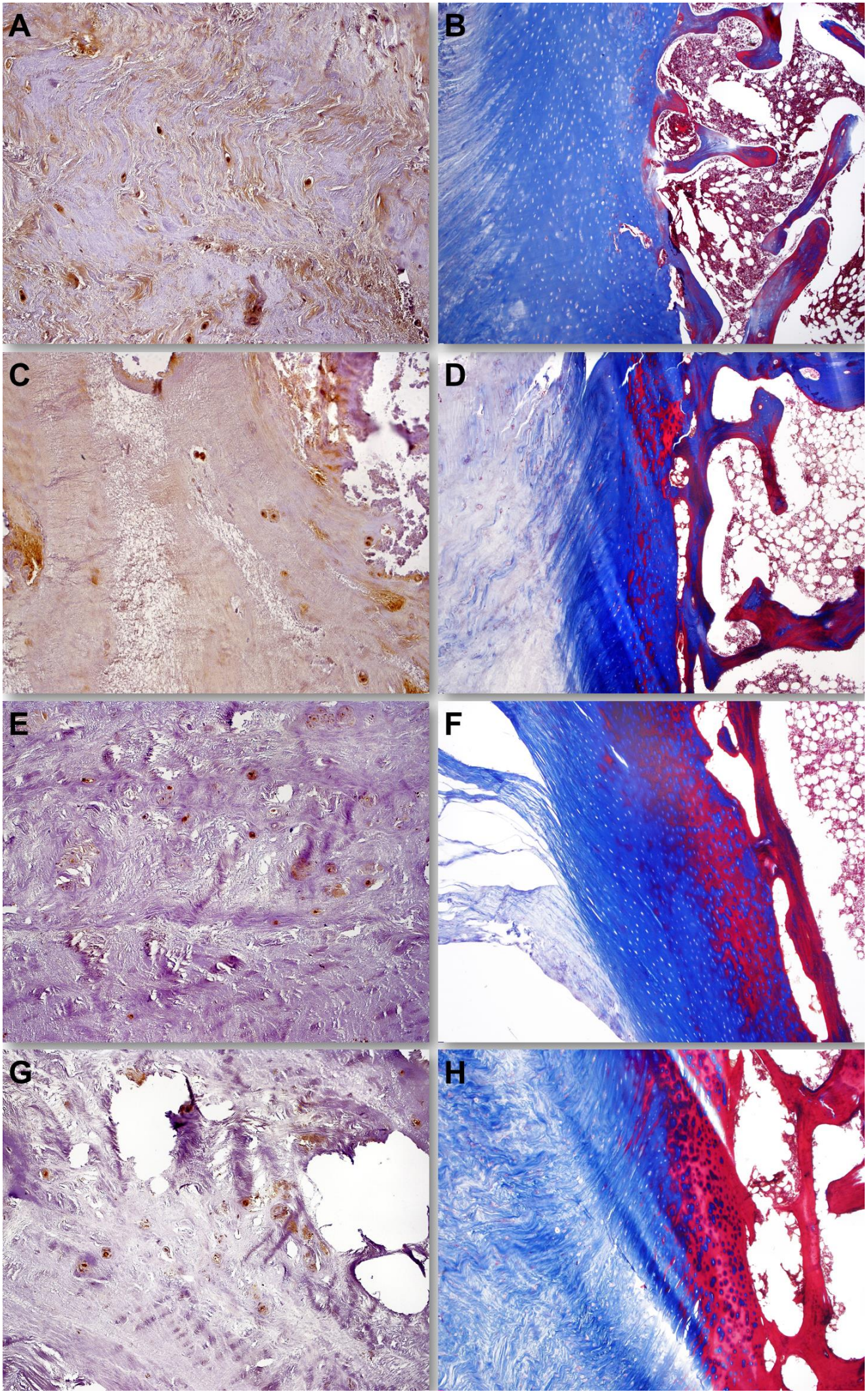
A
B
C
D
E
F
G
H

7. Artykuł numer 4

Tomaszewski KA, Adamek D, Konopka T, Tomaszewska R, Walocha JA. Endplate calcification and cervical intervertebral disc degeneration – the role of endplate marrow contact channel occlusion. Folia Morphologica 2014

Table of Contents

Endplate calcification and cervical intervertebral disc degeneration – the role of endplate marrow contact channel occlusion

Krzysztof A. Tomaszewski[1], Dariusz Adamek[2], Tomasz Konopka[3], Romana Tomaszewska[2], Jerzy A. Walocha[1]

[1] – Department of Anatomy, Jagiellonian University Medical College, Krakow, Poland

[2] – Department of Pathology, Jagiellonian University Medical College, Krakow, Poland

[3] – Department of Forensic Medicine, Jagiellonian University Medical College, Krakow, Poland

Running title: Endplate calcification and MCC occlusion

Corresponding author

Krzysztof A. Tomaszewski

Department of Anatomy, Jagiellonian University Medical College

12 Kopernika street, 31-034 Krakow, Poland

Tel./fax. +48-12-422-95-11

e-mail: krtomaszewski@gmail.com

Abstract

Background. The aim of this study was to determine the fundamental relationships between cervical intervertebral disc (IVD) degeneration, endplate calcification, and the patency of endplate marrow contact channels (MCC).

Materials and Methods. Sixty cervical IVDs were excised from 30 human cadavers. After sectioning the specimens underwent micro computed tomography (microCT) – from all images the number, caliber, diameter and distribution of endplate openings were measured using ImageJ. Next, the specimens were scored for macroscopic degeneration (Thompson's classification), and subsequently underwent histological analysis for both IVD and endplate degeneration (Boos classification) and calcification.

Results. The study group comprised 30 female and 30 male IVDs (mean age±SD 51.4±19.5). Specimen's age, macroscopic and microscopic degeneration correlated negatively with the number of MCCs ($r=-0.33$-(-0.95); $p<0.0001$), apart from the MCCs >300 μm in diameter ($r=0.66$-0.79; $p<0.0001$). The negative relationship was strongest for the MCCs 10-50 μm in diameter.

Conclusions. There is a strong negative correlation between the number of endplate MCCs, and both macroscopic and microscopic cervical IVD and endplate degeneration. This could further support the thesis that endplate calcification, through the occlusion of MCCs, leads to a fall in nutrient transport to the IVD, and subsequently causes its degeneration.

Keywords: calcification; cervical intervertebral disc; degeneration; endplate; marrow contact channel occlusion.

Introduction

The intervertebral disc (IVD) is the largest avascular structure in the human body [19] – in the lumbar spine some IVD cells can be up to 8 mm from the nearest direct blood supply [1, 19].

The IVD can be separated macroscopically into three different components. A centrally located gelatinous mass (the nucleus pulposus) is enclosed in concentrically organized layers of collagen fibers (the inner and outer annulus fibrosus), which are framed, at the cranial and caudal ends of each disc, by hyaline-like cartilaginous end-plates forming a transition zone to the adjacent vertebral bodies [21]. The endplates are typically less than 1 mm thick, and while this varies considerably across the width of any single disc, they tend to be thinnest in the central region adjacent to the nucleus [6]. The endplates are identifiable from an early embryological stage and have an osseous, as well as a hyaline cartilage component [19, 29]. A network of microscopic blood vessels penetrates the endplates during development of the growing spine, principally to provide nutrition for the disc, before disappearing around the time of skeletal maturity [19]. After this point in development the mineralized portion of the endplate is penetrated only by marrow contact channels (MCC), through which capillary buds emerge. These capillary buds connect the trabecular spaces to the cartilaginous endplate, but do not penetrate into it [20]. Apart from a sparse vascular supply in the outer lamellae of the annulus, mature discs are almost totally dependent on diffusion of essential solutes across the endplates for nutrition and metabolic exchange [33]. In addition, several studies have shown that it is the central portion of the endplate that is responsible for the diffusion of the majority of nutritional substances [22, 24].

One of the primary causes of disc degeneration is thought to be failure of nutrient supply to the disc cells [31]. In vitro, the activity of disc cells is very sensitive to changes in extracellular oxygen and pH levels [10-12]. Disc cells do not survive prolonged exposure to low pH or glucose concentrations [9, 10]. A fall in nutrient supply that leads to a lowering of

oxygen tension or of pH (a result of raised lactic acid concentrations) could thus affect the ability of disc cells to synthesize and maintain the disc's extracellular matrix and could ultimately lead to disc degeneration [24, 31]. The pathway from the blood supply to the nucleus cells is hazardous because these cells are supplied almost entirely by capillaries that originate in the vertebral bodies, penetrate the subchondral plate and terminate just above the cartilaginous endplate [31]. Nutrients must then diffuse from the capillaries through the cartilaginous endplate and the dense extracellular matrix of the nucleus pulposus to the cells [1, 19]. Nutrient supply to nucleus cells can be disturbed at several points. Factors that affect the blood supply to the vertebral body such as atherosclerosis [8], sickle cell anemia, caisson disease, and Gaucher's disease [24] all appear to lead to a significant increase in disc degeneration. Finally, even if the blood supply remains undisturbed, nutrients may not reach the disc cells if the cartilaginous endplate calcifies [1, 13, 25, 33]. Intense calcification of the endplate is seen in scoliotic discs [32].

The above relationship has been proven for lumbar IVDs [1], however it was not directly related to the degeneration of their endplates. When compared with lumbar disc degenerative disease, little is known about the degeneration of cervical IVDs and their endplates. Thus, the aim of this study was to determine the fundamental relationships between cervical IVD degeneration, endplate calcification, and the patency of endplate marrow contact channels (MCC).

Materials and Methods

Material acquisition

Sixty cervical IVDs were excised from 30 human cadavers (at the Department of Forensic Medicine, Jagiellonian University Medical College), using the anterior approach, not later than 24 hours post-mortem [17]. The material was excised in one block comprising vertebral

bodies, IVDs, endplates and blood vessels supplying these structure, and wrapped in saline soaked gauze, vacuum-sealed to prevent dehydration, and kept at 4° Celsius until micro computed tomography (microCT) scanning (on the same day). Excision started at the level of the lower half of the C4 vertebra and ended at the level of the upper half of the C6.

The study inclusion criterion was the ability to excise a section of the anterior spinal column (from the lower half of the C4 vertebra to the upper half of the C6), with the anterior and posterior longitudinal ligaments and blood vessels supplying the vertebrae. Study exclusion criteria were: (1) injury to the cervical spine, preventing from excising the required section; (2) previous cervical spine surgery; (3) receiving chemotherapy in the last 12 months; (4) previous radiation therapy to the perispinal region; (5) long-standing paralysis (6 or more months); (6) ankylosing spondylitis.

MicroCT scanning

Before scanning each sample was unpacked from the vacuum-sealed container, and sectioned transversally at the middle of the C5 vertebral body. This produced two samples from each cadaver encompassing the IVD with its both endplates, surrounded from both ends by part of the vertebral bodies.

The samples were scanned using a microCT scanner (SkyScan 1172 N.V., Aartselaar, Belgium) (Department of Medical Physics, Institute of Physics, Jagiellonian University). The spatial resolution was set to 13.68μm per pixel. The shadow images were obtained using an X-ray source energy of 80keV using the 0.5mm Al filter. The angular step between image acquisitions was 0.4º and each image was averaged from 5 frames. Scanning was performed perpendicular to the cranial-caudal axis of the sample, which was mounted on a custom plasticine attachment (this allowed for precise repositioning of the specimen along the z-axis with minimal rotational error) [27, 28].

3D sample reconstruction

Virtual reconstructions were prepared using NRecon software (SkyScan). Each reconstructed cross-section had a resolution of 2000x2000 pixels. CTVox was used for primary volume rendering of every sample. The transfer function was appropriately set to visualize canals (empty spaces) inside the sample.

The 3D analysis was performed using CTVox, CTAnalyser and CTVol (SkyScan) applications. Before analysis, all cross-sections were binarised using CTAnalyser software to reconstruct virtual solid 3D models of the sample. These models were visualized in CTVol software (Figure 1a and 1b).

Image analysis

From all images the number, caliber, diameter and distribution of endplate openings were measured using ImageJ [18]. Following the recommendations of Benneker et al. [1] we decided to neglect all holes smaller than 10 μm in diameter, as these were found to be mostly artifacts. Images from both the cranial and caudal endplates were acquired and analyzed. Each endplate was divided into 5 regions - anterior outer annulus (AO), anterior inner annulus (AI), nucleus pulposus (NP), posterior inner annulus (PI), and posterior outer annulus (PO). The number of MCCs was counted per $10mm^2$.

IVD and endplate degeneration assessment

Directly after microCT scanning, each sample was sectioned along the midsagittal plane for macroscopic IVD degeneration scoring according to Thompson's classification [30]. Each specimen was assessed by two of the authors, and the grade was averaged. Next, the samples were placed in a 10% solution of formaldehyde (pH 7.4) for a minimum of 14 days.

Microscopic IVD and endplate degeneration was assessed using Boos classification [4]. Tissue samples acquired from the midsagittal plane (of each of the 5 IVD regions) were dehydrated, embedded in paraffin, sectioned at 4 μm, and stained with haematoxylin and eosin, Masson-Goldner trichrome and alcian blue-PAS (Department of Pathology, Jagiellonian University Medical College). Each sample was assessed and scored, using light microscopy, by two observers, and the final score per sample was averaged.

The degree of endplate calcification was analyzed as the percentage of calcified tissue (red on Masson-Goldner trichrom staining) (Figure 2a) to the non-calcified part (Figure 2b). The fact of endplate calcification was verified on corresponding H&E stained samples. The percentage of calcification was averaged for all examined endplate regions.

Ethics

The research protocol was approved by the Jagiellonian University Medical College Ethics Committee (registry number KBET/319/B/2012). The study has been performed in accordance with the ethical standards laid down in the 1964 Declaration of Helsinki and its later amendments. The specimen excision method was chosen so as not to destabilize the cadaver's spinal column.

Statistical analysis

Statistical analysis was conducted using Statistica 10.0 PL (Statsoft). Elements of descriptive statistics were used (mean, standard deviation percentage distribution). Differences between groups were tested with t test, Mann–Whitney U test or analysis of variance (ANOVA) as appropriate. To assess the correlation between scores, Pearson's correlation was used. Backward elimination was applied ($p>0.1$) to identify the MCC size ranges that correlated

best with endplate degeneration scored using Boos classification [2]. Statistical significance was set at $p<0.05$.

Results

The study group comprised 30 female and 30 male IVDs. The mean age±SD of the specimens was 51.4±19.5. The basic characteristics of the study group are shown in Table 1.

IVD degeneration, graded using Thompson's classification, significantly correlated with Boos'es IVD degeneration score ($r=0.77$; $p<0.0001$). IVD and endplate degeneration, graded using Boos'es score also strongly correlated with each other ($r=0.96$; $p<0.0001$).

Specimen's age strongly correlated with both IVD degeneration (Thompson's and Boos'es) and endplate degeneration (Boos score), as well as the averaged percentage of endplate calcification ($r=0.76$; $r=0.77$; $r=0.73$; $r=0.75$ respectively; $p<0.0001$). Age also showed a strong negative correlation with the total number of endplate openings ($r=-0.68$; $p<0.0001$), as well as the number of openings (averaged from all endplate regions) of varying diameters ($r=-0.33$-(-0.76); $p<0.0001$), with the exception of openings over 300 μm in diameter ($r=0.66$; $p<0.0001$) (Figure 3). The number of the 300 μm endplate openings negatively correlated with the number of all other openings ($r=-0.62$-(-0.82); $p<0.0001$). This correlation was strongest for openings 10 – 50 μm in diameter ($r=-0.82$; $p<0.0001$). Figure 3 shows the age-distribution of endplate openings of different sizes among both sexes.

A similar relationship between the number of endplate openings and IVD and endplate degeneration/calcification was seen (Table 2). Figure 4 shows the number of endplate openings grouped according to Thompson's grade of degeneration.

By backward elimination we have determined that openings between 10 – 50 μm ($r=-0.91$; $p<0.0001$) in diameter accounted for 85% of the variability in the "total number of endplate openings – degree of endplate degeneration" ($r=-0.85$; $p<0.0001$) correlation.

Discussion

This study aimed at revealing the relationships between cervical IVD degeneration, endplate calcification, and the patency of endplate MCCs. The major finding presented in this manuscript is the fact that there is a strong negative correlation between the number of endplate MCCs, and both macroscopic and microscopic cervical IVD and endplate degeneration. Similar to lumbar IVDs [1], this study has also shown that the relationship between MCC closure and IVD degeneration was the strongest for the region corresponding to the nucleus pulposus. This corresponds well with what was written earlier, that the central portion of the endplate is responsible for the diffusion of the majority of nutritional substances [22, 24].

This study is the first to use microCT together with histological analysis to allow for the localization, quantification, and characterization of MCCs in the cervical endplate. Up-to-date only one similar study [1] explored such a relationship in lumbar IVDs, using scanning electron microscopy (SEM). Other studies assessing this relationship based solely on histological analysis [7], which allows only to visualize a certain portion of the endplate, and not its entire structure. The method used in the current study is easily reproducible – both through the use of microCT, and also due to the fact that both Thompson's and Boos'es grading systems were tested for interobserver reliability, practicability, and validity [14]. All the above mentioned allow to perform accurate measurements of endplate MCCs. This study has also brought to light the fact that, if used properly, Thompson's grade of IVD degeneration closely correlates with Boos'es score of microscopic IVD and endplate degeneration. This gives clinicians performing cervical spine surgeries a useful tool to support their post-operative discussion with their patients, when the results of pathological analysis are not yet known.

In opposition to the study by Benneker et al. [1] our findings showed a strong correlation between age and the decreasing number of MCCs (Figure 3), with the exclusion of openings larger than 300 μm. The strong correlation between IVD degeneration and the decreasing number of endplate openings has been noted before [1, 20] but only for lumbar IVD's. Figure 3 also points to an important fact, that the age at which the number of MCCs decreases can vary considerably between individuals. This has been reported before for lumbar IVDs [1, 4].

The lack of correlation between the total area of all endplate openings, both averaged and divided by region, and endplate or IVD degeneration grade can be partially explained by the fact that with increasing endplate degeneration there was a significant increase in the number of endplate openings larger than 300 μm (largest noted were ~600 μm in diameter). Basing on our results and the SEM findings of Benneker et al. [1] we concur that the increased size of the openings was caused by endplate cracking during degeneration. These openings do not contain capillary buds [5], and are the offspring of age-associated endplate thinning, clefts and fissures [4].

Similarly to previous studies on lumbar IVD samples [1, 23] we have observed that the correlation between endplate degeneration and the number of endplate openings is the strongest for those MCCs that hold capillary buds [3]. However, in contrast to other studies, we have chosen to investigate openings 10-50 μm in diameter, as animal studies report that capillary buds, within the endplate's cartilage can be between 5-50 μm in size [15]. However, as mentioned earlier, we did not include into our analysis openings smaller than 10 μm, as they have been found to be mostly artifacts [1]. The vascular buds are capillary structures, morphologically similar among humans, monkeys, and rabbits [35]. Capillaries can be classified into 3 types – discontinuous, fenestrated, and continuous. Capillary permeability increases in this order, and the morphological features of the endothelium indicate organ specificity [2]. The vascular buds were found to be fenestrated capillaries, which are usually

observed in metabolically very active tissues such as endocrine glands, kidneys, intestinal mucosa and dorsal root ganglion [15, 16]. This would mean that there is enhanced permeability and metabolism in both the cartilaginous endplate and the IVD.

This study points out important correlations between endplate calcification, MCC occlusion and IVD degeneration. However, the exact mechanisms by which the endplate calcifies are yet to be discovered. Several factors are thought to play a role in the pathogenesis of endplate calcification e.g. calcium-binding collagen type X [3], ankyrin [36], ENPP1 and TGF-β1 [34]. We cannot state for certain, as this study does not answer cause and effect questions, but one could presume that endplate calcification is rather the cause, than the effect of a fall in nutrient transport, as it begins in the well-vascularized center of the endplate, and not in the outer regions where the number of endplate openings is lower.

In our study we have not decided to go beyond microCT and histological analysis, even though some studies [1, 20, 26] reached out for biochemical parameters to supplement their search for the cause of endplate-IVD degeneration. This is something worth exploring in future studies, as different studies [1, 20, 26] produce conflicting results – especially when it comes to the role of glycosaminoglycans in the interplay between age, endplate bone porosity and IVD degeneration. Rodriguez et al. [26] observed that endplate porosity increased with age while GAG content decreased. This conflicts with the study by Nachemson et al. [20] which showed a decrease in endplate porosity with age and degeneration. The findings of Nachemson et al. are also supported by the result obtained by Benneker et al. [1] as well as the present study.

Concluding, this is the first study to perform such an investigation on human cervical spine samples. It has brought to light that, similarly to lumbar IVDs, there is a strong negative correlation between the number of endplate MCCs, and both macroscopic and microscopic cervical IVD and endplate degeneration. This could further support the idea that endplate

calcification, through the occlusion of MCCs, leads to a fall in nutrient transport to the IVD, and subsequently causes its degeneration. Additionally, the method demonstrated in this study allows to perform accurate and easily reproducible measurements of the number, size and shape of endplate MCCs. What is more, we have shown that Thompson's classification corresponds well to Boos'es histological classification of endplate and IVD degeneration, allowing to use Thompson's classification as a surrogate of microscopic degeneration, until the results of pathological analysis are known.

Conflict of Interest Statement

All authors declare that they have no conflict of interest.

Acknowledgements

This study was funded by the National Science Center – Poland under grant number DEC-2012/07/N/NZ5/00078. Krzysztof A. Tomaszewski received a scholarship to prepare his PhD thesis from the National Science Center – Poland under award number DEC-2013/08/T/NZ5/00020.

Author contribution

Design and planning of the study – KAT, DA, RT, JAW. Sample collection – KAT, TK. Sample preparation – KAT, RT. Histological analysis – KAT, DA, RT. Data interpretation – KAT, RT, DA, JAW (sample measurement and result verification), KAT (statistical analysis). Bibliographic search – KAT. Drafting and revising the manuscript – KAT. Obtaining funding – KAT. Critical revision of the manuscript – DA, TK, RT, JAW. All authors have read and approved the final version of the manuscript.

All co-authors confirm the above-mentioned contributions and consent to the fact that this study is a part of Krzysztof A. Tomaszewski's PhD thesis. The co-authors confirm that Krzysztof A. Tomaszewski has contributed significantly (80% in total) to every part of this study, as stated above.

References

1. Benneker LM, Heini PF, Alini M, Anderson SE, Ito K (2005) 2004 Young Investigator Award Winner: vertebral endplate marrow contact channel occlusions and intervertebral disc degeneration. Spine (Phila Pa 1976), 30: 167-173.

2. Bennett HS, Luft JH, Hampton JC (1959) Morphological classification of vertebrate blood capillaries. Am J Physiol, 196: 381-390.

3. Boos N, Nerlich AG, Wiest I, von der Mark K, Aebi M (1997) Immunolocalization of type X collagen in human lumbar intervertebral discs during ageing and degeneration. Histochem Cell Biol 108: 471-480.

4. Boos N, Weissbach S, Rohrbach H, Weiler C, Spratt KF, Nerlich AG (2002) Classification of age-related changes in lumbar intervertebral discs. Volvo Award in basic science. Spine, 272631-2644.

5. Coventry MB, Ghormley RK, Kernohan JW (1945) The intervertebral disc: its microscopic anatomy and pathology: Part II. Changes in the intervertebral disc concomitant with age. J Bone Joint Surg Am, 27: 233-247.

6. Edwards WT, Zheng Y, Ferrara LA, Yuan HA (2001) Structural features and thickness of the vertebral cortex in the thoracolumbar spine. Spine (Phila Pa 1976), 26: 218-225.

7. Grignon B, Grignon Y, Mainard D, Braun M, Netter P, Roland J (2000) The structure of the cartilaginous end-plates in elder people. Surg Radiol Anat, 22: 13-19.

8. Hangai M, Kaneoka K, Kuno S, Hinotsu S, Sakane M, Mamizuka N, Sakai S, Ochiai N (2008) Factors associated with lumbar intervertebral disc degeneration in the elderly. Spine J, 8: 732-740.

9. Horner HA, Urban JP (2001) 2001 Volvo Award Winner in Basic Science Studies: Effect of nutrient supply on the viability of cells from the nucleus pulposus of the intervertebral disc. Spine (Phila Pa 1976), 26: 2543-2549.

10. Huang CY, Gu WY (2008) Effects of mechanical compression on metabolism and distribution of oxygen and lactate in intervertebral disc. J Biomech, 41: 1184-1196.

11. Ishihara H, Urban JP (1999) Effects of low oxygen concentrations and metabolic inhibitors on proteoglycan and protein synthesis rates in the intervertebral disc. J Orthop Res, 17: 829-835.

12. Jackson AR, Huang CY, Brown MD, Gu WY (2011) 3D finite element analysis of nutrient distributions and cell viability in the intervertebral disc: effects of deformation and degeneration. J Biomech Eng, 133: 091006.

13. Jackson AR, Huang CY, Gu WY (2011) Effect of endplate calcification and mechanical deformation on the distribution of glucose in intervertebral disc: a 3D finite element study. Comput Methods Biomech Biomed Engin, 14: 195-204.

14. Kettler A, Wilke HJ (2006) Review of existing grading systems for cervical or lumbar disc and facet joint degeneration. Eur Spine J, 15: 705-718.

15. Kobayashi S, Baba H, Takeno K, Miyazaki T, Uchida K, Kokubo Y, Nomura E, Morita C, Yoshizawa H, Meir A (2008) Fine structure of cartilage canal and vascular buds in the rabbit vertebral endplate. Laboratory investigation. J Neurosurg Spine, 9: 96-103.

16. Kobayashi S, Yoshizawa H (2002) Effect of mechanical compression on the vascular permeability of the dorsal root ganglion. J Orthop Res, 20: 730-739.

17. Le Maitre CL, Freemont AJ, Hoyland JA (2005) The role of interleukin-1 in the pathogenesis of human intervertebral disc degeneration. Arthritis Res Ther, 7: R732-745.

18. Mizia E, Tomaszewski KA, Lis GJ, Goncerz G, Kurzydło W (2012) The use of computer-assisted image analysis in measuring the histological structure of the human median nerve. Folia Morphol (Warsz), 71: 82-85.

19. Moore RJ (2006) The vertebral endplate: disc degeneration, disc regeneration. Eur Spine J, 15: S333-337.

20. Nachemson A, Lewin T, Maroudas A, Freeman MA (1970) In vitro diffusion of dye through the end-plates and the annulus fibrosus of human lumbar inter-vertebral discs. Acta Orthop Scand, 41: 589-607.

21. Nerlich AG, Boos N, Wiest I, Aebi M (1998) Immunolocalization of major interstitial collagen types in human lumbar intervertebral discs of various ages. Virchows Arch, 432: 67-76.

22. Ogata K, Whiteside LA (1981) 1980 Volvo award winner in basic science. Nutritional pathways of the intervertebral disc. An experimental study using hydrogen washout technique. Spine, 6: 211-216.

23. Oki S, Matsuda Y, Itoh T, Shibata T, Okumura H, Desaki J (1994) Scanning electron microscopic observations of the vascular structure of vertebral endplates in rabbits. J Orthop Res, 12: 447-449.

24. Raj PP (2008) Intervertebral disc: anatomy-physiology-pathophysiology-treatment. Pain Pract, 8: 18-44.

25. Roberts S, Urban JPG, Evans H, Eisenstein SM (1996) Transport properties of the human cartilage end-plate in relation to its composition and calcification. Spine, 21: 415-420.

26. Rodriguez AG, Slichter CK, Acosta FL, Rodriguez-Soto AE, Burghardt AJ, Majumdar S, Lotz JC (2011) Human disc nucleus properties and vertebral endplate permeability. Spine (Phila Pa 1976), 36: 512-520.

27. Skrzat J, Kozerska M, Wróbel A (2014) Micro-computed tomography study of the abnormal osseous extensions of sella turcica. Folia Morphol (Warsz), 73: 19-23.

28. Skrzat J, Leszczyński B, Kozerska M, Wróbel A (2013) Topography and morphometry of the subarcuate canal. Folia Morphol (Warsz), 72: 357-361.

29. Taylor JR, Twomey LT (1998) Growth of human intervertebral discs and vertebral bodies. J Anat, 120: 49-68.

30. Thompson JP, Pearce RH, Schechter MT, Adams ME, Tsang IK, Bishop PB (1990) Preliminary evaluation of a scheme for grading the gross morphology of the human intervertebral disc. Spine, 15: 411-415.

31. Urban JP, Smith S, Fairbank JC (2004) Nutrition of the intervertebral disc. Spine (Phila Pa 1976), 29: 2700-2709.

32. Urban MR, Fairbank JC, Etherington PJ, Loh FRCA L, Winlove CP, Urban JP (2001) Electrochemical measurement of transport into scoliotic intervertebral discs in vivo using nitrous oxide as a tracer. Spine (Phila Pa 1976), 26: 984-990.

33. van der Werf M, Lezuo P, Maissen O, van Donkelaar CC, Ito K (2007) Inhibition of vertebral endplate perfusion results in decreased intervertebral disc intranuclear diffusive transport. J Anat, 211: 769-774.

34. Xu HG, Hu CJ, Wang H, Liu P, Yang XM, Zhang Y, Wang LT (2011) Effects of mechanical strain on ANK, ENPP1 and TGF-β1 expression in rat endplate chondrocytes in vitro. Mol Med Rep, 4: 831-835.

35. Yoshizawa H, Ohiwa T, Kubota K (1986) Morphological study on the vertebral route for the nutrition of the intervertebral disc. Neuro-Orthopedics. 1: 17-32.

36. Zaka R, Williams CJ (2006) Role of the progressive ankylosis gene in cartilage mineralization. Curr Opin Rheumatol, 18: 181-186.

Tables

Table 1. Basic characteristics of the study group.

	Female (n=30)	**Male (n=30)**	**Total (n=60)**	**p-value[1]**
Age (SD)	52.8 (19.8)	50.0 (19.4)	51.4 (19.5)	0.57
IVD degeneration - Thompson classification (SD)	2.6 (1.3)	3.2 (1.3)	2.9 (1.3)	0.08
IVD degeneration - Boos classification (SD)	12.0 (6.1)	14.3 (5.3)	13.1 (5.8)	0.13
Endplate degeneration - Boos classification (SD)	8.9 (5.3)	11.5 (4.8)	10.2 (5.2)	0.06
Endplate calcification (%)	28.4 (25.1)	44.1 (26.0)	36.2 (26.5)	0.02
Number of endplate openings (10-50 µm)[2]	40.6 (9.3)	35.7 (11.5)	38.2 (10.6)	0.07
Number of endplate openings (50-100 µm)[2]	16.9 (4.7)	16.5 (5.7)	16.7 (5.2)	0.75
Number of endplate openings (100-300 µm)[2]	12.3 (2.7)	12.9 (4.1)	12.6 (3.4)	0.55
Number of endplate openings (>300 µm)[2]	6.0 (2.7)	6.2 (3.3)	6.1 (3.0)	0.77
Number of endplate openings (total)[2]	75.8 (13.1)	71.3 (17.9)	73.6 (15.7)	0.26
Number of endplate openings under NP (10-50 µm)[3]	61.2 (18.2)	51.6 (18.8)	56.4 (19.0)	0.047

[1] – for differences between females and males; [2] – Opening density per 10 mm^2 of endplate area, averaged from all endplate regions (sizes represent opening diameter); [3] – Opening density per 10 mm^2 of endplate area, number of openings given only for the endplate region underlying the nucleus pulposus (sizes represent opening diameter). SD – standard deviation; IVD – intervertebral disc; NP – nucleus pulposus.

Table 2. Correlations between Thompson and Boos degeneration scores and endplate calcification (%), and the number of endplate openings of varying sizes.

	Thompson IVD degeneration score	Boos IVD degeneration score	Boos endplate degeneration score	Endplate calcification (%)
Number of endplate openings (10-50 µm)[1]	r=-0.94 p<0.0001	r=-0.90 p<0.0001	r=-0.91 p<0.0001	r=-0.93 p<0.0001
Number of endplate openings (50-100 µm)[1]	r=-0.83 p<0.0001	r=-0.77 p<0.0001	r=-0.79 p<0.0001	r=-0.79 p<0.0001
Number of endplate openings (100-300 µm)[1]	r=-0.54 p<0.0001	r=-0.51 p<0.0001	r=-0.51 p<0.0001	r=-0.51 p<0.0001
Number of endplate openings (>300 µm)[1]	r=0.79 p<0.0001	r=0.78 p<0.0001	r=0.72 p<0.0001	r=0.79 p<0.0001
Number of endplate openings (total)[1]	r=-0.88 p<0.0001	r=-0.83 p<0.0001	r=-0.85 p<0.0001	r=-0.85 p<0.0001
Number of endplate openings under NP (10-50 µm)[2]	r=-0.95 p<0.0001	r=-0.92 p<0.0001	r=-0.94 p<0.0001	r=-0.94 p<0.0001

[1] – Opening density per 10 mm^2 of endplate area, averaged from all endplate regions (sizes represent opening diameter); [2] – Opening density per 10 mm^2 of endplate area, number of openings given only for the endplate region underlying the nucleus pulposus (sizes represent opening diameter). IVD – intervertebral disc; NP – nucleus pulposus.

Figures

Figure 1. MicroCT virtual reconstruction of endplate – intervertebral disc junction.

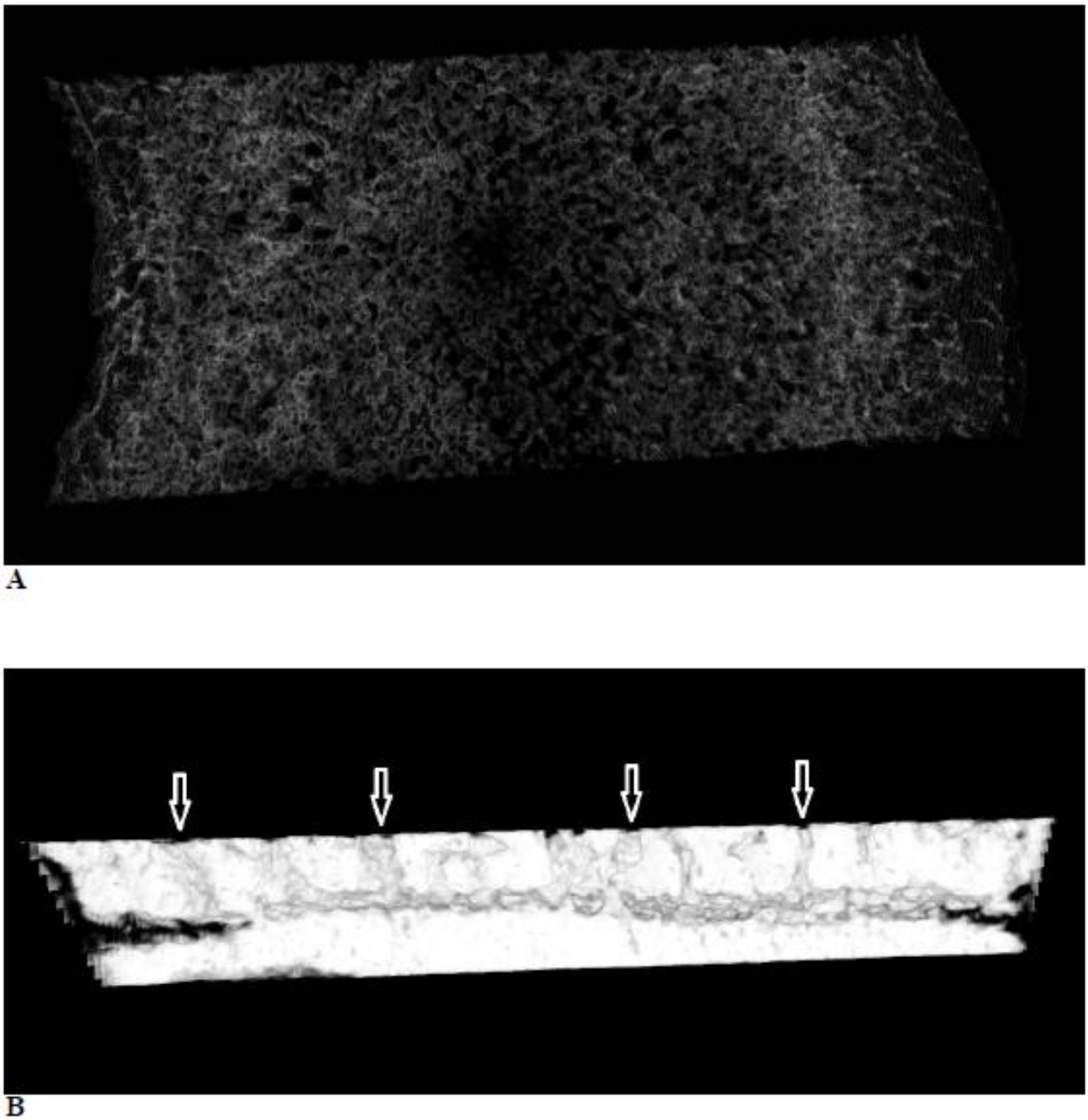

(A) endplate viewed from the side of the disc. Numerous holes of different sizes can be seen. (B) midsagittal section – above – endplate with several marrow contact channels (marked with white arrows); below – intervertebral disc with no marrow contact channels penetrating its core.

Figure 2. Histological slide - Masson-Goldner trichrome staining, magnification x100.

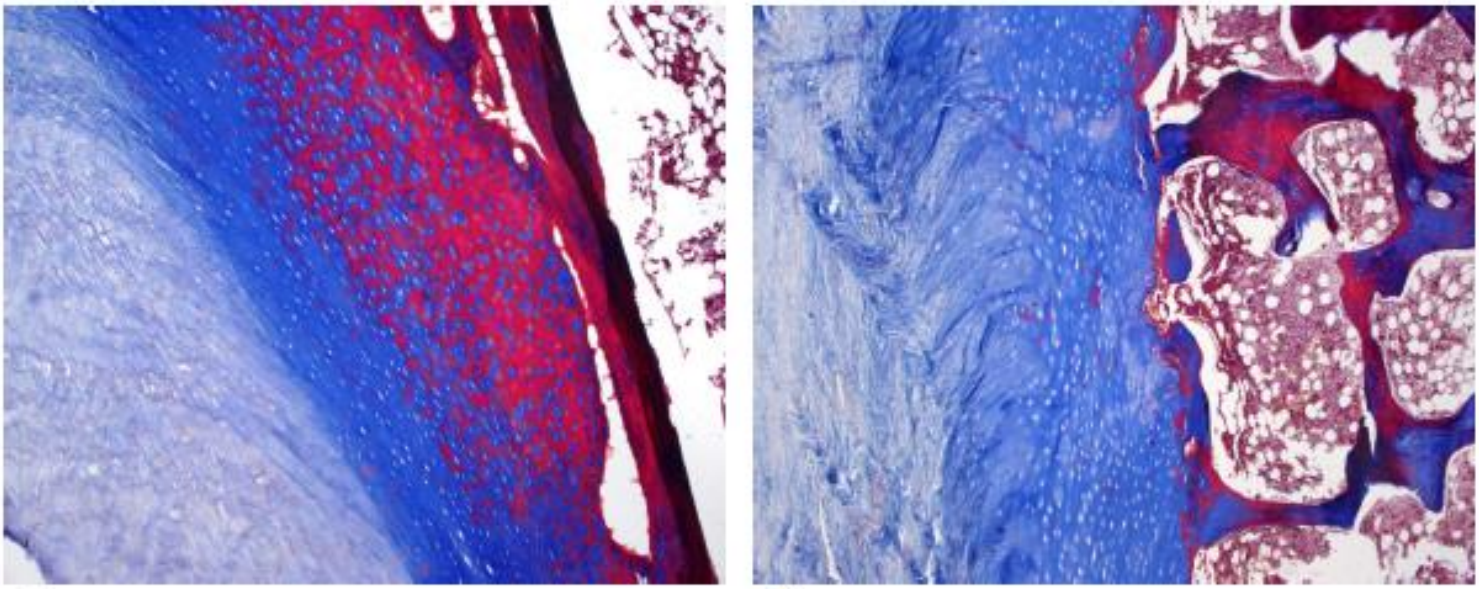

Midsagittal section showing, from the left IVD connective tissue, cartilaginous endplate with chondrocyte holes, and lamellar bone with bone marrow.

(A) 70y.o. male, significant calcification (red) of the endplate. (B) 30y.o. male, only slight endplate calcification can be seen.

Figure 3. Scatter diagram of age vs. number endplate openings of different sizes among both sexes.

The black line represents the regression line. The dash line is the 95%% confidence interval. The white circles represent female specimens and the black triangles represent male specimens.

A – age vs. total number of endplate openings 10-50 μm in diameter averaged from all endplate regions/10mm^2

B – age vs. total number of endplate openings 50-100 μm in diameter averaged from all endplate regions/10mm^2

C – age vs. total number of endplate openings 100-300 μm in diameter averaged from all endplate regions/10mm^2

D – age vs. total number of endplate openings >300 μm in diameter averaged from all endplate regions/10mm^2

E – age vs. total number of endplate openings of all sizes averaged from all endplate regions/10mm^2

F – age vs. total number of endplate openings 10-50 μm in diameter underlying the nucleus pulposus (NP) only/10mm^2

Please see next page for Figure 3.

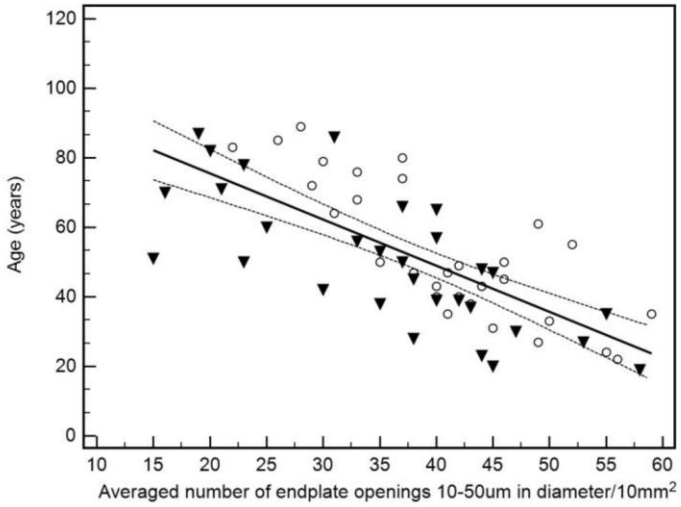
Age (years)
Averaged number of endplate openings 10-50um in diameter/10mm2

A

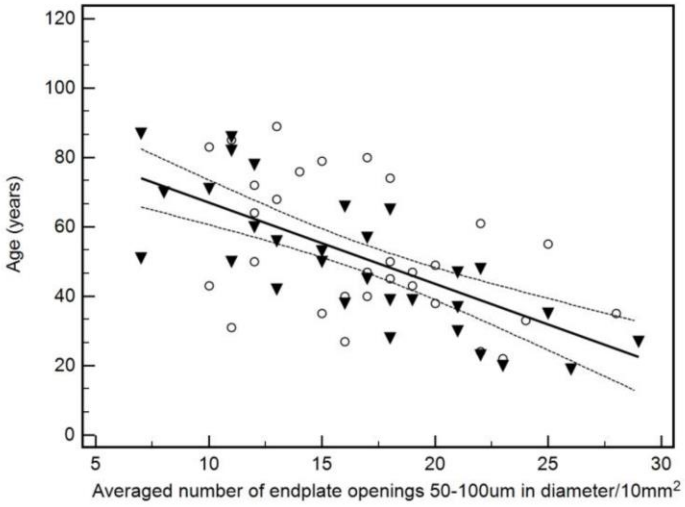
Age (years)
Averaged number of endplate openings 50-100um in diameter/10mm2

B

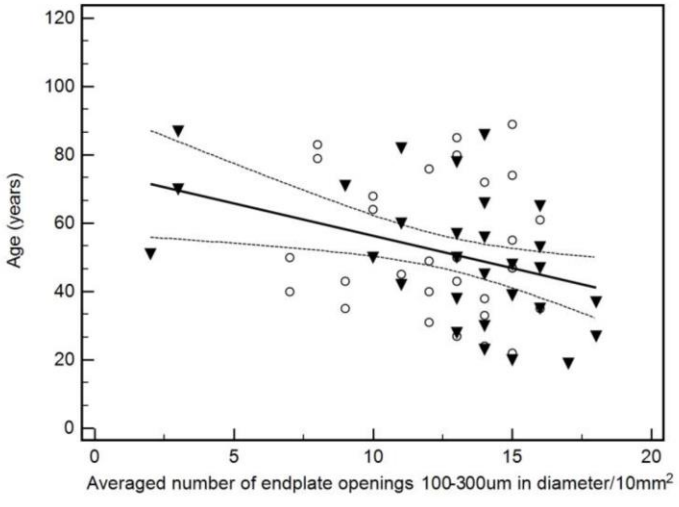
Age (years)
Averaged number of endplate openings 100-300um in diameter/10mm2

C

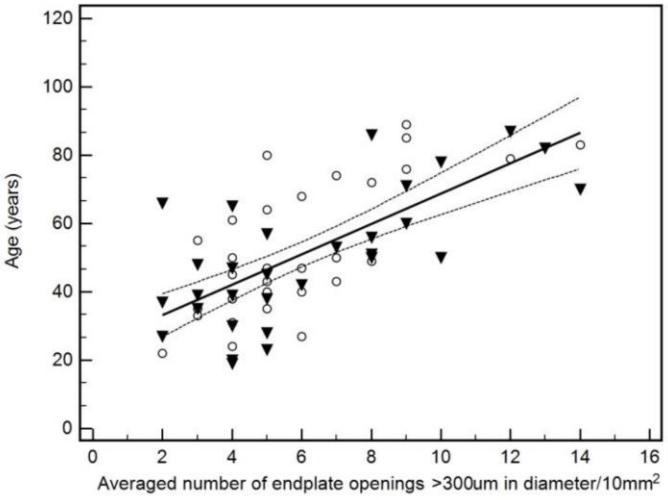
Age (years)
Averaged number of endplate openings >300um in diameter/10mm2

D

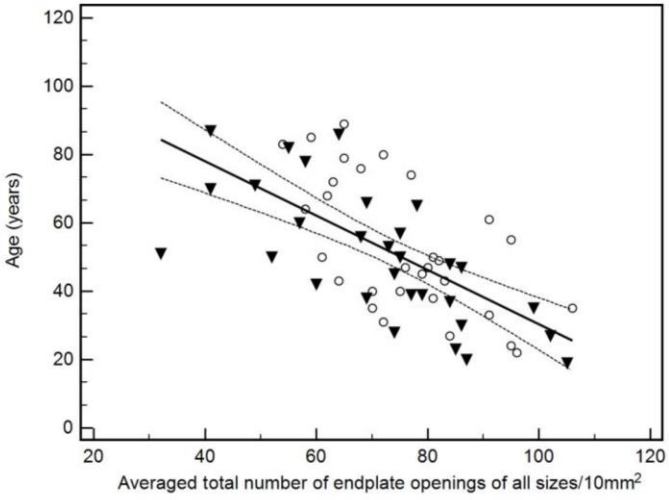
Age (years)
Averaged total number of endplate openings of all sizes/10mm2

E

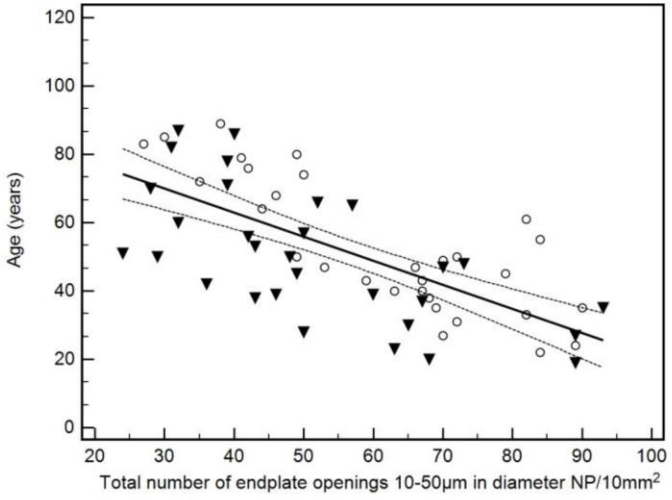
Age (years)
Total number of endplate openings 10-50μm in diameter NP/10mm2

F

Figure 4. The number of endplate openings grouped according to Thompson's grading.

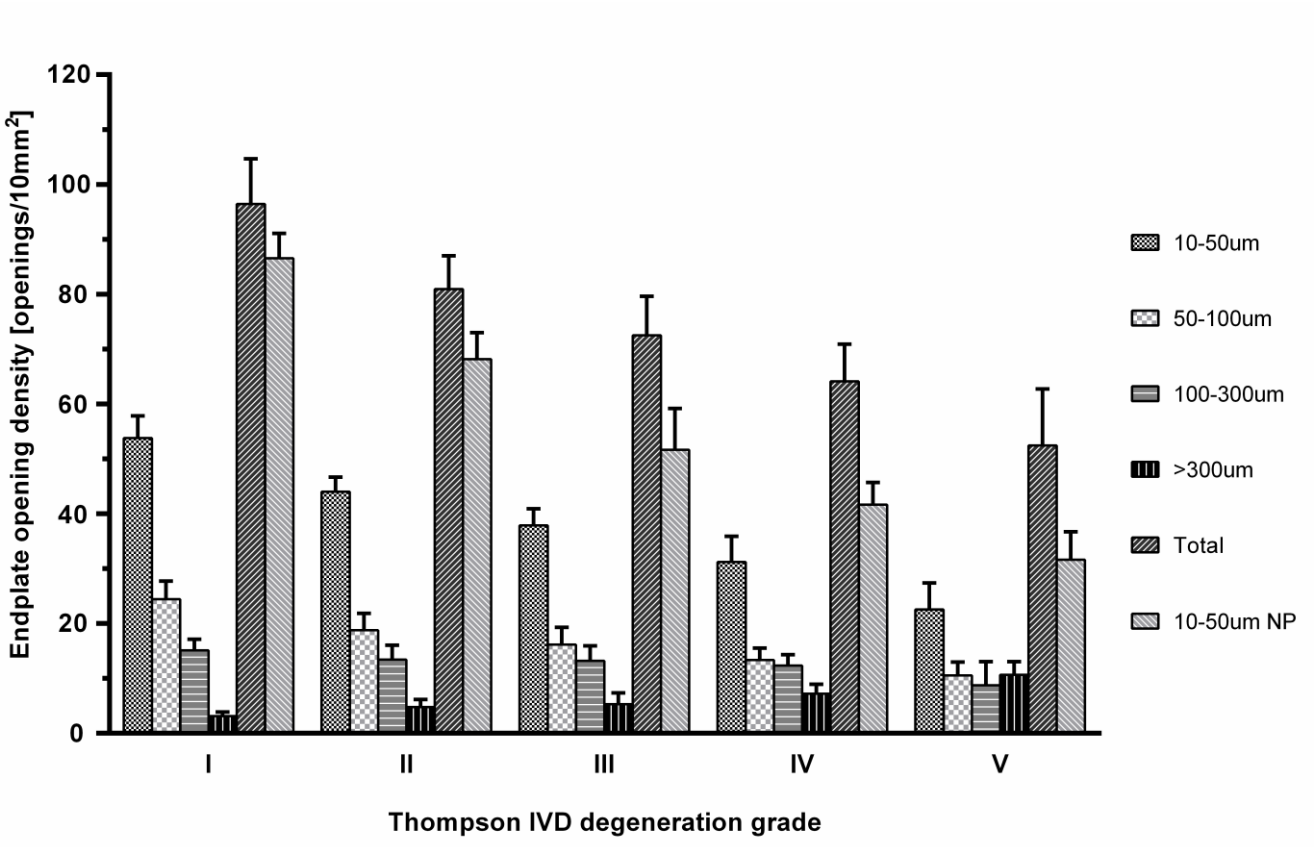

10-50 μm; 50-100 μm; 100-300 μm; >300 μm; Total - opening density per 10 mm^2 of endplate area, averaged from all endplate regions (sizes represent opening diameter). "Total" referring to the added number of endplate openings of all sizes, averaged from all endplate regions.

10-50 μm NP - opening density per 10 mm^2 of endplate area, number of openings given only for the endplate region underlying the nucleus pulposus (sizes represent opening diameter).

8. Potwierdzenia przyjęcia prac do druku

a) Tomaszewski KA, Saganiak K, Gładysz T, Walocha JA. The biology behind the human intervertebral disc and its endplates. Folia Morphologica 2014

[FM] Decyzja redaktora #39534

Od: Professor Janusz Moryś

Do: lek. Krzysztof Tomaszewski:

Uprzejmie informujemy, że została podjęta decyzja w sprawie manuskryptu pod tytułem "The biology behind the human intervertebral disc and its endplates" zgłoszonego do czasopisma Folia Morphologica.

Nasza decyzja to: Akceptacja bez poprawek

Professor Janusz Moryś

Medical University of Gdańsk

Telefon 4858 3491401

jmorys@gumed.edu.pl

Folia Morphologica

Department of Anatomy and Neurobiology

Medical University of Gdańsk

ul. Dębinki 1, 80-211 Gdańsk, Poland

jmorys@gumed.edu.pl

tel: +48 58 349 14 01 fax: + 48 58 349 14 21

b) Tomaszewski KA, Walocha JA, Mizia E, Gładysz T, Głowacki R, Tomaszewska R. Age- and degeneration-related variations in cell density and glycosaminoglycan content in the human cervical intervertebral disc and its endplates. Polish Journal of Pathology 2014

PJP-00471-2014-01

Age- and degeneration-related variations in cell density and glycosaminoglycan content in the human cervical intervertebral disc and its endplates

Dear Krzysztof Tomaszewski,

I am pleased to inform you that your manuscript, entitled: Age- and degeneration-related variations in cell density and glycosaminoglycan content in the human cervical intervertebral disc and its endplates, has been finally accepted for publication in our journal.

Thank you for submitting your work to us.

Kindest regards,

Janusz Ryś

Editor-in-Chief

Polish Journal of Pathology

c) Tomaszewski KA, Adamek D, Pasternak A, Głowacki R, Tomaszewska R, Walocha JA. Degeneration and calcification of the cervical endplate is connected with a decreased expression of ANK, ENPP-1, OPN and TGF-β1 in the intervertebral disc. Polish Journal of Pathology 2014;65(3):204-211

PJP-00401-2014-01

Degeneration and calcification of the cervical endplate is connected with a decreased expression of ANK, ENPP-1, OPN and TGF-β1 in the intervertebral disc

Dear Dr. Tomaszewski,

I am pleased to inform, that your manuscript, entitled: Degeneration and calcification of the cervical endplate is connected with a decreased expression of ANK, ENPP-1, OPN and TGF-β1 in the intervertebral disc, has been accepted for publication in our journal.

The paper should appear in the issue 3/2014.

Thank you for submitting your work to us.

Kindest regards,

Krzysztof Okoń

d) Tomaszewski KA, Adamek D, Konopka T, Tomaszewska R, Walocha JA. Endplate calcification and cervical intervertebral disc degeneration – the role of endplate marrow contact channel occlusion. Folia Morphologica 2014

Professor Janusz Moryś <czasopisma@viamedica.pl>

Do: lek. Krzysztof Tomaszewski:

Uprzejmie informujemy, że została podjęta decyzja w sprawie manuskryptu pod tytułem "Endplate calcification and cervical intervertebral disc degeneration – the role of endplate marrow contact channels occlusion" zgłoszonego do czasopisma Folia Morphologica.

Nasza decyzja to: Akceptacja bez poprawek

Wyniki recenzji dostępne są na stronie:

http://czasopisma.viamedica.pl/fm/author/submissionReview/38333

Professor Janusz Moryś

Medical University of Gdańsk

Telefon 4858 3491401

jmorys@gumed.edu.pl